An investigation into the synergistic action of cellulose-degrading enzymes on complex substrates

A thesis submitted in fulfilment of the requirements for the degree of

MASTER OF SCIENCE (Biochemistry)

at

RHODES UNIVERSITY

By

Mariska Thoresen

February 2015

Department of Biochemistry and Microbiology

Rhodes University, 2015

Grahamstown, South Africa

Dedication

I dedicate my work to the Lord Jesus Christ, in whom all things are possible. Only through His richest grace have I been able to complete this research.

Acknowledgements

The completion of this research study would not have been possible without the support and encouragement of several individuals. I would like to take this opportunity to acknowledge all of them.

First of all, I would like to express my utmost gratitude to my supervisor Professor Brett Pletschke for giving me the opportunity to carry out this research in his lab, and for providing me with the best possible scientific surroundings. I would also like to acknowledge my co-supervisor Dr. Susan van Dyk for all her selfless help, constructive comments and insightful discussions. She had a great influence on me and I could never have imagined a better mentor for my research. Without the guidance, patience and immense knowledge from my two supervisors, this study would not have been possible.

A special thanks to our collaborators Professor Emile van Zyl from Stellenbosch University and Dr. Riaan den Haan from the University of the Western Cape for providing the cellulases and paper sludge for this study. I am also grateful for the valuable advice given by Dr. Den Haan regarding some of the challenges I encountered in my study.

I want to thank the members of the Lignocellulose Synergy Research group for making the lab a happy and friendly environment. It was a privilege being a part of this research group. I would like to express my sincere gratitude and appreciation to Mr Samkelo Malgas for his friendship, continuous support and encouragement throughout my study. His passion and enthusiasm for research has had a great impact on my work. In addition, a special thanks to Dr. Abhishek Bhattacharya for providing the xylanase for this study as well as for his useful advice throughout my research. I would also like to thank Sagaran Abboo for his friendship and for the help with HPLC.

I wish to thank my parents, Ronnie and Ronel, for their wholehearted support throughout my life and for always believing in me, and to my sister Landi, for always being there to encourage me.

I am ever grateful to Dusty Zeisberger for his endless love, understanding and support; and my best friends Lauren Barnes and Melissa Mayo for their motivation when it was the most needed.

Thanks is given to National Research Foundation (NRF-RSES) for its financial support to conduct this study.

Contents

Abstract

The environmental issues associated with the rapid depletion of fossil fuels have encouraged the production of bioethanol from lignocellulosic biomass, the most abundant carbon resource on earth. However, the key obstacles to this process are the recalcitrant structure of biomass and low hydrolytic activities. Improvements to this process are ongoing, and some of the first commercial facilities producing cellulosic ethanol were opened in 2013 and 2014. However, there is an urgency to make the facilities more economically feasible. Enhancing cellulose hydrolysis through enzyme synergy is essential for achieving higher hydrolysis rates, and numerous research efforts have focused on trying to elucidate the enzyme mechanisms to design optimal enzyme cocktails.

Most of the work reported in literature has been conducted on model substrates, however it has been realised that model substrates may provide unrealistic insights into the interactions of the enzymes on natural lignocellulosic substrates. Therefore this study strived to obtain a better understanding of enzyme synergy using model and natural cellulosic substrates.

Firstly, the study assessed the biochemical properties of partially purified cellulases, which had been expressed in *Saccharomyces cerevisiae*. The physico-chemical and kinetic characteristics were also assessed to determine the factors that influenced their activities. The cellulases used in this study were cellobiohydrolases (CBHI from *Talaromyces emersonii* and CBHII from *Chrysosporium lucknowense*); endoglucanases (EGI from *Aspergillus terreus* and EGII from *Trichoderma reesei*); and β-glucosidase from *Saccharomycopsis fibuligera*. SDS-PAGE analysis showed that the enzymes were glycosylated, and the estimated sizes for CBHI, CBHII, EGI, EGII and BGL were 66, 67, 57, 56 and >116 kDa, respectively. The substrate specificities were Avicel, CMC and *p*NPG for CBHs, EGs and BGL, respectively. It was found that the enzymes exhibited maximal activity at pH 4.5 - 5.5 and at 60°C, with the exception of BGL, which exhibited maximal activity at 40°C, with stability studies showing that the cellulases maintained >80% activity for 96 hours at their optimum temperature. Kinetic data showed that all of the enzymes had low K_M values for their preferred substrates and that the EGs and BGL had high V_{max} values, while the CBHs had low V_{max} values.

Substrate characterisation was investigated prior to enzyme synergy. The three substrates that were chosen for this study were Avicel, which was a representative model microcrystalline substrate (>90% glucan); steam exploded bagasse (SEB), which was a representative of an

agricultural substrate and paper sludge (PS), which was a representative of a municipal substrate. Chemical compositional analysis showed that SEB was composed of 42% glucan, 7.2% xylan, 5.8% mannan and 2.3% arabinan, 40% insoluble lignin and ash, and 1.2% soluble phenolics, while PS was composed of 48% glucan, 2.7% xylan, 2.2% mannan, 3.9% galactan, 41.2% lignin and ash, and 1.2% soluble phenolics. During pretreatment, many compounds can be produced that may have an effect on enzyme activity. This was assessed, and it was found that compounds (currently unknown) present in SEB inhibited the activities of CBHI, CBHII, and BGL by 40, 20 and 80%, respectively, while the activities of EGI and EGII were activated by 5 and 50%, respectively. Compounds (unknown) in the PS activated the activities of CBHI, CBHII, EGI, EGII and BGL by 157, 158, 34, 72%, respectively. Adsorption studies showed that the enzymes were capable of binding to all three the substrates, but the most rapid adsorption was to Avicel, followed by SEB and then PS. It was suggested that this was attributable to the accessibility of the cellulosic surface area, and it would therefore have a direct impact on their efficiency to hydrolyse their different substrates.

Synergy studies using the different combinations of cellulases on the substrates were conducted. It was observed that the combined activities of various cellulase combinations enhanced the hydrolysis of the three substrates. The observed trend for all three substrates was that a combination of CBH and EG was required, and that CBH was required at a higher protein concentration than EG. The combination 75% CBHI: 25% EGII produced the highest quantity of reducing sugars for Avicel hydrolysis (0.88 mg/mL) after 24 hours, and the highest quantity of reducing sugars for PS hydrolysis (0.49mg/mL) after 72 hours, while the combination of 75% CBHI: 25% EGI produced the highest quantity of reducing sugars for SEB hydrolysis (0.75 mg/mL) after 72 hours.

Temporal studies on the optimal combinations were conducted to further investigate the established interactions between cellulases on the substrates. The results indicated that over time, different synergistic patterns were established for each substrate. Hydrolysis of Avicel showed that the DS was highest at the initial stages of hydrolysis; SEB hydrolysis showed that the DS varied throughout the course of hydrolysis, and the hydrolysis of PS showed that the DS was highest in the middle stages of hydrolysis. Different synergistic models were proposed for each observed trend and it was suggested that the major contributing factor for these results was the characteristics of the substrate, such as its composition, availability of binding sites and their 3D structures.

As the substrates contained small quantities of xylan (7.2 and 2.7% for SEB and PS, respectively), intermolecular synergy between the optimal cellulase combinations and a xylanase was investigated, to further assess whether this combination could boost the hydrolysis of the three substrates. Results revealed that no improvements occurred when the xylanase was added.

In conclusion, this study confirmed that cellulose hydrolysis can be enhanced by the activities of endo- and exo- acting enzymes. However, the characteristics of a particular substrate has a direct impact on their hydrolysis rates which, in turn, has an effect on synergistic interactions that are established between them.

List of abbreviations

°C	Degree(s) Celsius
µg	Microgram
µmol	Micromole
µL	Microlitre
AA	Auxillary activity
AA9	Auxillary activity family 9
AA10	Auxillary activity family 10
AA11	Auxillary activity family 11
AFM	Atomic force microscopy
APS	Ammonium Persulphate
BSA	Bovine Serum Albumin
BGL	β-glucosidase
BC	Bacterial cellulose
BMC	Bacterial microcrystalline cellulose
CAZy	Carbohydrate active enzyme database
CBHI	Cellobiohydrolase I
CBHII	Cellobiohydrolase II
CBM	Carbohydrate binding domain
CD	Catalytic domain
DNS	3,4 Dinitrosalicylic acid
DS	Degree of synergy
DP	Degree of polymerization
EC	Enzyme commission number

EGI	Endoglucanase I
EGII	Endoglucanase II
FPLC	Fast proten liquid chromatography
g	Gram
GH	Glycosyl hydrolase
h	Hours
HCl	Hydrochloric acid
HPLC	High performance liquid chromatography
k_{cat}	Turnover number
k_{cat}/K_m	Catalytic efficiency
kDa	KiloDalton
K_M	Michaelis constant
LiP	Lignin peroxidase
LPMO	Lytic polysaccharide mono-oxygenase
M	Molar
mg	Milligram
mg/mL	Milligram per millilitre
mL	Millilitre
mM	Millimolar
MnP	Manganese peroxidases
nm	Nanometre
NC-IUBMB	International Union of Biochemistry and Molecular Biology
NREL	National Renewable Energy Laboratory
pI	Isoelectric point

PS	Paper sludge
SCB	Sugarcane bagasse
SEB	Steam exploded bagasse
*p*NPG	*p*- nitrophenol-α-D-glucopyranoside.
SD	Standard deviation
SDS	Sodium dodecyl sulphate
SDS-PAGE	Sodium dodecyl sulphate polyacrylamide gel electrophoresis
SEM	Scanning electron microscopy
TEMED	N,N,N´N´-tetramethylethylenediamine
U/mg	Units per milligram
V_{max}	Maximum velocity
v/v	Volume per volume
w/v	Weight per volume
X	Xylanase

List of research outputs

a. Anticipated publications:

Malgas, S., Thoresen, M., Van Dyk, J. S. and Pletschke, B. I. (2015). The effect of time on the synergistic associations between various polysaccharide active enzymes on different lignocellulosic feedstocks. Article in preparation.

b. National conference proceedings:

Thoresen, M., Den Haan, R., Van Zyl, W.H., Van Dyk, J. S., Pletschke, B.I. An investigation into the synergistic action of exo-type and endo-type cellulases on the hydrolysis of complex substrates (Oral). 2nd Annual Energy Post Graduate Conference (EPC), Ithemba Labs, Cape Town, 11 - 14 August 2013.

Thoresen, M., Den Haan, R., Van Zyl, W.H., Van Dyk, J. S., Pletschke, B.I. An investigation into the synergistic action of exo-type and endo-type cellulases on the hydrolysis of complex substrates (Oral). 18th Annual Meeting of the SASM, Bela Bela, Limpopo, 24 - 27 November 2013.

Thoresen, M., Den Haan, R., Van Zyl, W.H., Van Dyk, J. S., Pletschke, B.I. An investigation into the synergistic action of cellulose degrading enzymes on the hydrolysis of complex substrates (Poster). 25th Annual CATSA Conference, Saint Georges Hotel and Conference Centre, Pretoria, 9-12 November 2014.

List of Figures

List of Tables

Chapter 1: Literature review

1.1 Introduction

Fossil fuels (coal, oil and natural gas) are being depleted at an enhanced rate, due to the continual growth in global population and industrialisation (Beukes and Pletschke, 2011). This has raised issues of great worldwide concern, specifically with regards to the negative impact it has on the environment, such as global climate change (Choi *et al.,* 2014; Khan *et al.,* 2013; Yadav *et al.,* 2014; Zabed *et al.,* 2014). Consequently, to create a sustainable environment, there is an urgency to replace non-renewable fossil fuels with renewable fuels (Babajide, 2013).

In particular, the transportation sector accounts for 20 - 25% of the world's energy consumption, and is still highly-dependent on conventional fossil fuels (Müller-Langer *et al.,* 2014; Rodrique, 2013). This has encouraged global initiatives to replace petroleum-based technologies with alternative, sustainable liquid transportation fuels (biofuels) (Banerjee *et al.,* 2010; Cockeril and Martin, 2008; Kumar *et al.,* 2013; Macrelli *et al.,* 2014). Some of the targets that have been put forward globally are: i) 25% of transportation fuels need to be replaced with biofuels by 2030 in Europe; ii) 30% of transportation fuels need to be replaced with biofuels by 2030 in USA, and iii) 44% of transportation fuels need to be derived from biofuels by 2021 in Thailand (Himmel *et al.,* 2007; Kumar *et al.,* 2013).

The vast majority of current biofuels are produced from sugar, starch and oils (first generation biofuels), but emphasis is increasingly being placed on advanced biofuels from plant biomass (Naik *et al.,* 2010; Sims *et al.,* 2010). Biomass has vast potential as a feedstock for biofuel production, due to its abundance, feasibility and high polysaccharide content (~75%) (Kumar and Wyman, 2009; Sweeney and Xu, 2012). Furthermore, it does not compromise food security, therefore, it has a distinct advantage over first generation biofuels (Naik *et al.,* 2010; Raman and Mohr, 2014; Sims *et al.,* 2010). Biomass can be derived from various sources, including: i) forest residues (hardwood and softwood); ii) agricultural residues (sugar cane bagasse and corn stover); iii) municipal residues (paper waste); iv) dedicated energy crops (*Miscanthus*, and switchgrass) and v) various grasses (Lee *et al.,* 2014; Van Dyk and Pletschke, 2012).

Although plant biomass presents a feasible solution for the sustainable production of transportation fuels, its recalcitrant structure presents a major challenge in achieving efficient biomass saccharification (Zhao *et al.,* 2012). Consequently, various lignocellulose-degrading enzymes are required to hydrolyse the different polysaccharides that constitute biomass into sugars (Banerjee *et al.,* 2010; Mohanram *et al.,* 2013). However, the high cost of enzymes and their low hydrolysis rates present additional barriers towards improving the economics of this process (Banerjee *et al.,* 2010; La Grange *et al.,* 2010). Enhancing cellulose hydrolysis through optimised enzyme synergy has gained significant attention in research with the aim of achieving higher conversion rates and yields (Den Haan *et al.,* 2013; Kim *et al.,* 2014). Despite the extensive research conducted on enzyme synergistic interactions, their exact mechanisms have not been elucidated (Kostylev and Wilson, 2012). Furthermore, enzyme and substrate characteristics play significant roles in enzyme synergy, and thus requires further research (Beukes and Pletschke, 2011; Yang *et al.,* 2011).

1.2 Lignocellulose chemistry: the structure of biomass

1.2.1 An overview of lignocellulose

Lignocellulose is the major structural component of plant biomass and is predominantly composed of a meshwork of cellulose, hemicellulose and lignin (Figure 1.1.) (Horn *et al.*, 2012; Lee *et al.*, 2014). Minor quantities of pectin, proteins and ash may also be present (Gandolfi *et al.*, 2013). Cellulose is the most abundant polysaccharide and provides the plant with strength and rigidity, whereas hemicellulose is the second most abundant polysaccharide, made up of varying amounts of xylan, mannan, galactan and arabinan (Shahzadi *et al.*, 2014). Lignin is a complex polyphenol that forms a protective sheath around the polysaccharides (Decker *et al.*, 2009). Depending on the type of biomass, their compositions may vary.

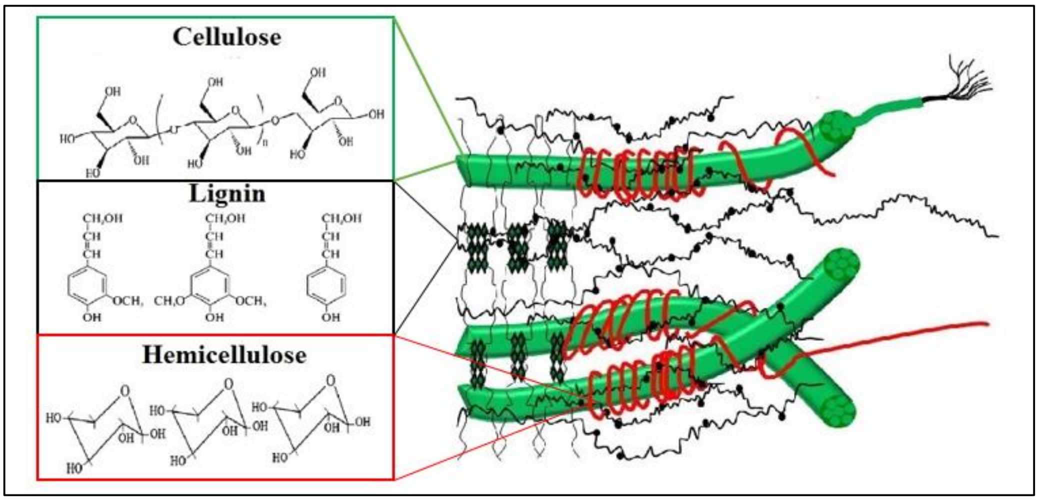

Figure 1.1. The three components that make up the general structure of lignocellulose (Adapted and modified from Tomme *et al.*, 1995).

1.2.2 The structure of cellulose

Cellulose is the major constituent of the plant cell wall, comprising approximately 40 - 50% of the total biomass (Peciulyte *et al.*, 2014; Vazana *et al.*, 2013). It is also considered to be the largest carbon resource on earth (Kumar and Murthy, 2013). Although it is predominantly found in plant cell walls, it can also be produced by some animals (tunicates) and microorganisms (fungi and bacteria) (Jalak *et al.*, 2012; Lynd *et al.*, 2002).

Cellulose is a homo-polysaccharide composed of unbranched β 1, 4-glycosidic linked glucose monomers (Bayer *et al.*, 1998; Howard *et al.*, 2003; Teeri, 1997). The number of glucose molecules per chain can range from 500 - 14000, with varied degrees of polymerization (DP) (Bayer *et al.*, 1998; Festucci-Buselli *et al.*, 2007; Lynd *et al.*, 2002). Through a high degree of strong intra and inter molecular hydrogen bonds, the cellulose fibrils pack tightly together to form microfibrils with cellobiose being the repeating unit on the chain (180° rotation of sugars) (Kim et al., 2014; Lynd *et al.*, 2002; Moon *et al.*, 2011). Approximately 36 microfibrils aggregate into larger fibrils to form the framework of the cellulose fiber (Figure 1.2) (Horn *et al.*, 2012).

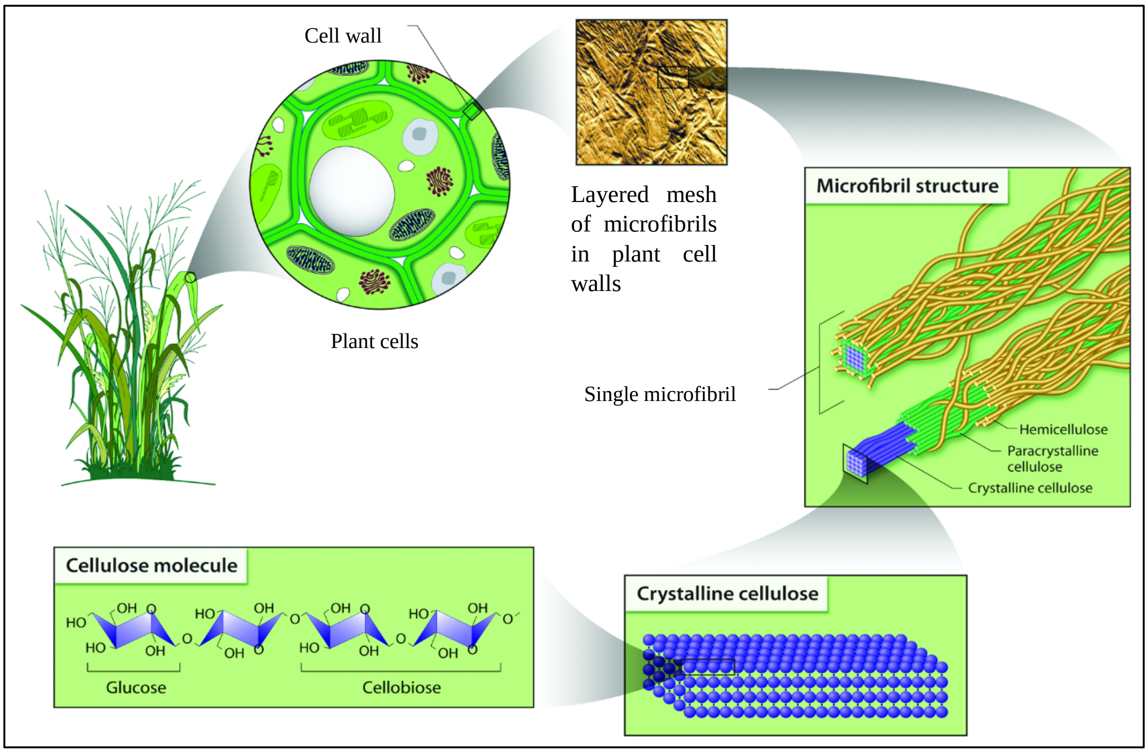

Figure 1.2. Structural overview of cellulose. Long chains of 1, 4-glycosidic linked glucose monomers pack in a parallel arrangement to form microfibrils. The microfibrils aggregate further to form macrofibrils, which form the framework for the cellulose fiber (Adapted from Quiroz-Castañeda and Folch-Mallol, 2013).

Cellulose is predominantly crystalline in nature, however, it also contains less ordered regions, which are interspersed within the cellulose chain (Horn *et al.,* 2012; Segato *et al.,* 2012). These regions are classified as the amorphous regions, thus making natural cellulose paracrystalline in nature (Ioelovich *et al.,* 2010; Park *et al.,* 2010).

Cellulose can be found in different crystalline forms (polymorphs), including polymorph I, II, III_I, III_{II}, IV_I and IV_{II} (Moon *et al.,* 2011; O'Sullivan, 1997). However, only cellulose I and II are found in nature, of which cellulose I is the dominant form (Horn *et al.*, 2012; Lavoine *et al.*, 2012; Lee *et al.,* 1997; O'Sullivan, 1997). Cellulose I is further subdivided into allomorphs I_a (less compact regions) which are composed of one cellulose chain per unit, and I_b (compact regions) which are composed of two cellulose chains per unit (Moon *et al.*, 2011). The ratio of I_a:I_b varies between cellulose sources and are contributing factors towards the efficiency of cellulose hydrolysis (Cui *et al.*, 2014; Horn *et al.*, 2012).

1.2.3 The structure of hemicellulose

Hemicellulose comprises approximately 25 - 35% of plant cell walls and is considered to be the second largest carbon resource on earth, after cellulose (Bastawde, 1992; Shahzadi *et al.,* 2014). It is closely associated with cellulose and lignin through hydrogen bonds, thus contributing to the overall recalcitrance of biomass (Moreira and Filho, 2008; Zhang *et al.,* 2011).

Hemicellulose is less crystalline than cellulose and it is composed of various branched building blocks, including pentoses (D-xylose, D-arabinose), hexoses (D-mannose, D-glucose) and sugar acids (α-D-glucuronic and α-4-*O*-methyl-D-glucuronic acids) (Figure 1.3A) (Horn *et al.*, 2012; Mohanram *et al.,* 2013; Van Dyk and Pletschke, 2012). Hemicellulose can generally be classified as xylans or mannans, according to the main sugar in its backbone (Moreira and Filho, 2008; Van den Brink and de Vries, 2011; Wagschal *et al.,* 2009). The distribution of hemicellulose varies between softwoods and hardwoods, whereby mannan and xylan are the most dominant hemicellulosic components found in each biomass, respectively (Moreira and Filho, 2008; Ramos, 2003; Yamabhai *et al*., 2014).

1.2.3.1 Xylan

Xylan is the most abundant hemicellulose in nature and is composed of branched β 1, 4- linked D-xylopyranosyl residues (Zhang *et al.,* 2011). The most dominant xylans in nature are the heteroxylans, which are modified by various substituents in their backbone (Zhao *et al.,* 2012). These substituted residues can either be 1, 2 linked α-D glucuronic acid or 4-*O*-methyl-α-D glucuronic acid, which are predominantly found in hardwoods; or 1, 2 and 1, 3 α-linked arabinose which are predominantly found in softwoods (Sunna and Antranikian, 1997; Wagschal *et al.,* 2009). Acetylation at the C-2 or C-3 position may also occur, but this is predominantly found in hardwoods (Zhang *et al.,* 2011).

1.2.3.2 Mannan

Mannan is a linear polysaccharide composed of β 1, 4 linked D-mannopyranose residues and is mainly found in softwoods and in endosperm seeds (Malgas *et al.,* 2015). Mannans may also exist as galactomannans, with the backbone composed of mannan residues; or glucomannans with the backbone composed of glucose and mannan residues to varying degrees (Moreira and Filho, 2008; Petkowicz *et al*., 2001). The chains may be substituted with α-D galactosyl residues, therefore glucomannans can in turn give rise to galactoglucomannans (Malgas *et al.,* 2015; Yamabhai *et al*., 2014).

1.2.4 Lignin

Lignin constitutes approximately 10 - 25% of plant cell walls, and is not considered a polysaccharide (Mohanram *et al.,* 2013; Shahzadi *et al.,* 2014). It is a hydrophobic, complex polyphenol that forms a protective sheath around the polysaccharides through various ester and ether linkages (Decker *et al.,* 2009; Horn *et al.,* 2012; Perez *et al.,* 2002). Thus, it provides mechanical strength to the plant, making it highly resistant to microbial degradation (Hendriks and Zeeman, 2009; Van Zyl *et al*., 2010; Yang *et al*, 2011). Furthermore, studies have reported that the presence of lignin may lead to non-productive binding of cellulases through hydrophobic interactions, thereby restricting the access of cellulases to the cellulose chain (Haven and Jørgensen, 2013; Rahikainen *et al.,* 2013).

Lignin is composed of various aromatic groups, depending on the degree of alcohol methoxylation, including i) phenylpropanoids *p*-hydroxyphenyl; ii) guaiacyl and iii) syringyl monolignols (Karp *et al.,* 2013; Ramos, 2003) (Figure 1.3B). Depending on the plant species, the relative composition of monolignols may vary (Ramos, 2003). Softwoods contain mostly guaiacyl lignin, whereas hardwoods contain a combination of both guaiacyl and syringyl lignin. All three monolignols are found in grasses (Horn *et al.,* 2012).

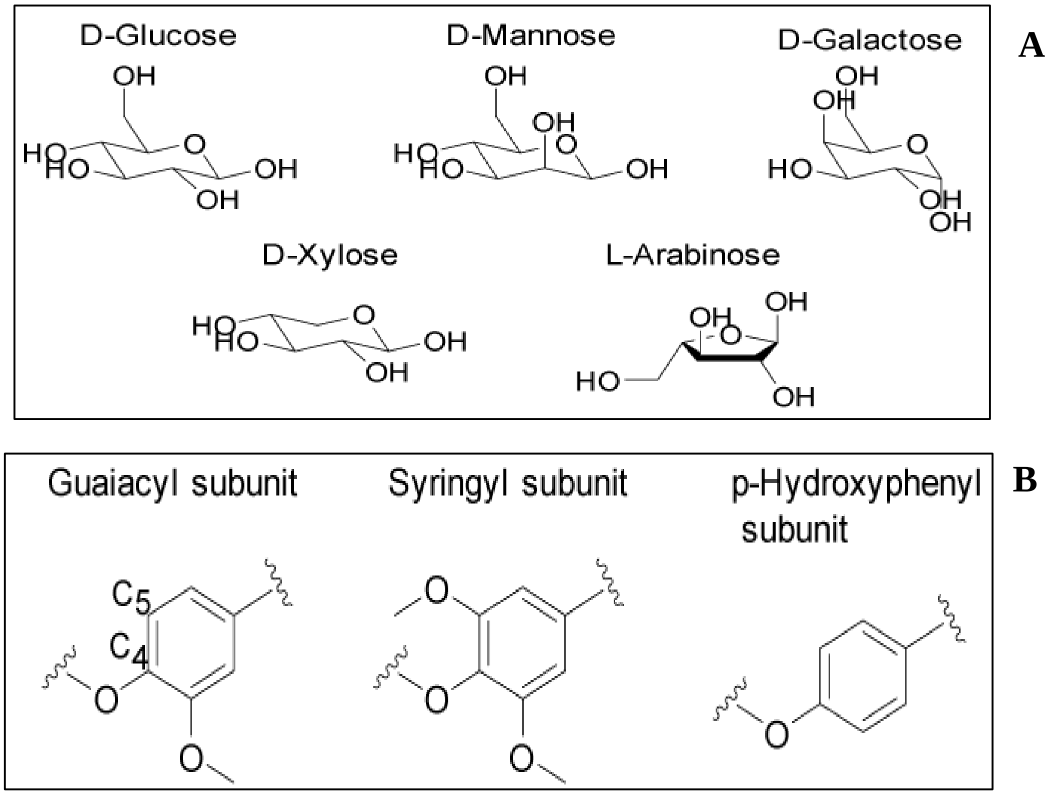

Figure 1.3. The chemical structures of (A): the different hexoses and pentoses of hemicellulose and (B): the different phenolic groups of lignin (Adapted from Pierson *et al.,* 2013).

1.3 Microbial biomass degradation

A consortium of lignocellulose degrading enzymes are required to efficiently degrade the polysaccharides (cellulose and hemicellulose) present in biomass (Peciulyte *et al.,* 2014; Van den Brink and de Vries, 2011). These enzymes (complexed or non-complexed systems) are mainly produced by microorganisms such as fungi and bacteria (Gusakov *et al.,* 2006; Mohanram *et al.,* 2013). Fungi are the most attractive candidates for producing enzymes required for cellulose degradation, as they are well-known agents of decomposition of organic matter, particularly cellulosic substrates (Gusakov *et al.,* 2006; Lynd *et al.,* 2002). Examples of well characterised fungi include *Humicola insolens, T. reesei, Phanerochaete chrysosporium and Penicillium pinophilum* (Bhat and Bhat, 1997). In contrast, bacteria are reported to be the best producers of enzymes required for hemicellulose degradation. The most characterised bacteria include *Bacillus, Erwinia, Cellulomonas* and *Clostridium* (Mohanram *et al.,* 2013).

1.3.1 Enzyme classification

The enzymes required to degrade polysaccharides are classified as glycosyl hydrolases (GH) (enzymes with the ability to hydrolyse glycosidic bonds between sugars) (Bayer, 1998; Peciulyte *et al.,* 2014). Enzymes are classified by the Nomenclature Committee of the International Union of Biochemistry and Molecular Biology (NC-IUBMB) which has assigned a four digit number (Enzyme classification (EC number)) to each enzyme. The EC number is based on their specificities for a particular substrate and does not provide any information regarding their structural characteristics (Aspenborg *et al.*, 2012). However, classification may be challenging, due to the broad substrate specificities exhibited by some hydrolases (Aspenborg *et al.,* 2012; Naumhoff, 2011). Consequently, Henrissat (1991) grouped GHs into different families, based on their evolutionary origins (similarities in sequence homology and folding characteristics). As of January 2015, GH's have been divided into 133 families on the online carbohydrate active enzyme (CAZy) database (http://www.cazy.org/). A summary of classifications for the major hydrolases are presented in Table 1.1.

Table 1.1 Classification of the major glycoside hydrolases (Information retrieved from CAZy)

Enzyme	**EC number**	**Family**	**Reaction mechanism**	**3D structure**
Cellobiohydrolase	3.2.1.91 3.2.1.176 3.2.1.176	6 7 48	Inverting Retaining Inverting	- β-jellyroll $(\alpha/\alpha)_6$
Endoglucanase	3.2.1.4	5 6 7 9 12 45	Retaining Inverting Retaining Inverting Retaining Inverting	$(\beta/\alpha)_8$ - β-jellyroll $(\alpha/\alpha)_6$ β-jellyroll -
B-glucosidase	3.2.1.21	1 3 5	Retaining Retaining Retaining	$(\beta/\alpha)_8$ - $(\beta/\alpha)_8$
Xylanases	3.2.1.8	10 11	Retaining Retaining	$(\beta/\alpha)_8$ β-jellyroll
Mannanases	3.2.1.25 3.2.1.78 3.2.1.78	5 26 113	Retaining Retaining Retaining	$(\beta/\alpha)_8$ $(\beta/\alpha)_8$ $(\beta/\alpha)_8$

The mechanism by which GHs cleave glycosidic bonds is based on a general acid base catalysis mechanism (carboxylate groups act as a proton donor or a nucleophile/base), leading to either: i) net retention (single displacement) or ii) net inversion (double displacement) of the anomeric carbon configuration (Figure 1.4) (Bayer *et al.,* 1998; Dashtban *et al*., 2009).

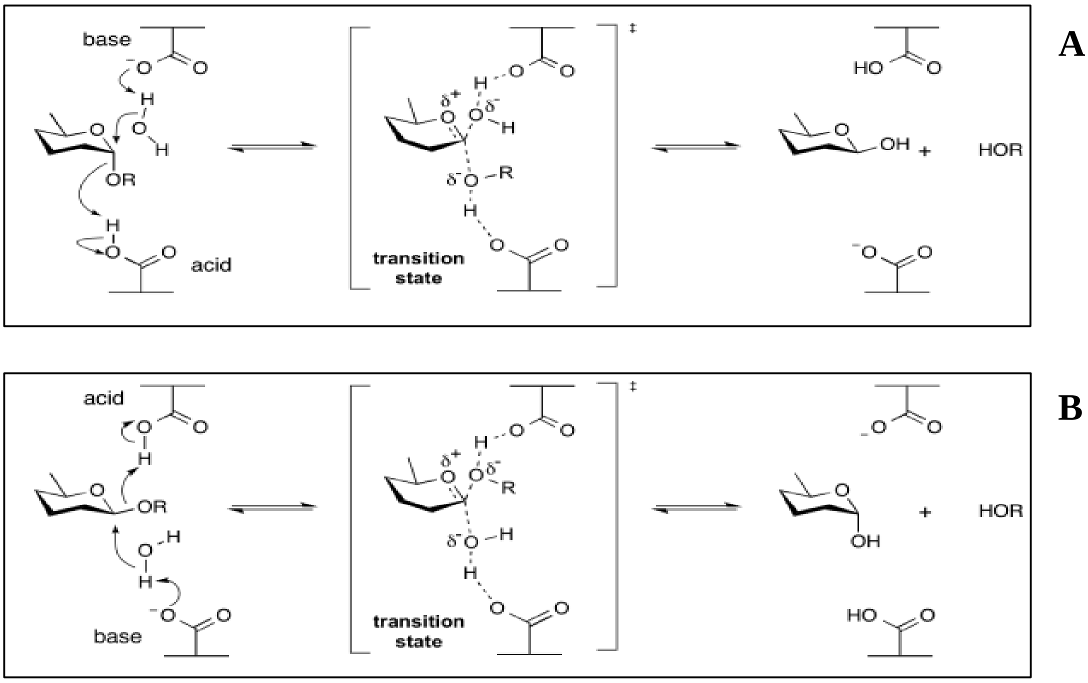

Figure 1.4. The general acid to base hydrolysis of a glycosidic bond with an (A): inversion mechanism and (B): retention mechanism (Adapted from McCarter and Withers, 1994).

1.3.2 Enzymes required to degrade cellulose

The degradation of cellulose requires the co-operative activities of multiple cellulolytic enzymes namely: i) cellobiohydrolases (CBH1, EC 3.2.1.176; CBHII, EC 3.2.1.91); ii) endoglucanases (EGI, 3.2.1.4; EGII, EC 3.2.1.4) and iii) β-glucosidases (EC 3.2.1.21) (Figure 1.5) (Ganner *et al.,* 2012; Horn *et al.,* 2012; Van den Brink and de Vries, 2011; Warden *et al.*, 2011; Zhou *et al.,* 2009).

1.3.2.1 Cellobiohydrolases (EC 3.2.1.91 and EC 3.2.1.176)

Fungal CBHs are grouped into GH families 6, 7 and 48 (Imai *et al.,* 1998). They are the most abundant enzymes produced by cellulolytic fungi (50 - 70%), and are the major cellulases responsible for degrading highly crystalline cellulose (Boisset *et al.,* 2000; Den Haan *et al.*, 2013, Imai *et al.,* 1998). CBHs act processively from the chain ends, liberating cellobiose from either the reducing ends (CBHI) or non-reducing ends (CBHII) (Dashtban *et al.,* 2009; Horn *et al.* 2012; Nutt *et al.,* 1998). However, it has been reported that CBHII can also degrade amorphous regions, therefore, it has been classified as a bi-functional enzyme (Ganner *et al.,* 2012; Teleman *et al*., 1998). Due to their specificities for opposite ends of the cellulose chain, the combined activities of CBHI and CBHII may enhance the overall degradation of cellulose (Barr *et al.,* 1996; Nutt *et al.,* 1998; Wood and Mcrae 1979).

CBHs are modular enzymes that possess enclosed tunnel-like active sites which allow them to initiate a processive mode of action from the chain ends (Granum *et al.*, 2014). The active sites are connected to a catalytic domain (CD) and a carbohydrate-binding module (CBM) through a flexible linker peptide (Eriksson *et al.,* 2002; Grassick *et al.*, 2004; Segato *et al.*, 2012). The presence of CBMs are essential for CBH activity as they are believed to bring the enzyme and substrate in close proximity to each other, leading to increased enzyme activity (Igarashi *et al.*, 2009; Jalak *et al.*, 2012; Teeri, 1997).

1.3.2.2 Endoglucanases (EC 3.2.1.4)

Fungal EGs belong to GH families 5, 6, 7, 9, 12 and 45 (Okada *et al.*, 1998; Vlasenko *et al.*, 2010). Endoglucanases are responsible for cleaving random sites in the amorphous regions of the cellulose chain, thus decreasing the DP of the substrate (Beldman *et al.*, 1988; Ganner *et al.,* 2012; Lee, 1997; Nidetzky *et al.*, 1994). The ability of the EGs to bind internally to the cellulose chain is linked to its open active site, which is in the shape of a cleft or a groove (Eriksson *et al.*, 2002; Teeri, 1997). Conversely, some studies have shown that EGs may possess a modular architecture similar to that of the CBHs, thus allowing them to act in a processive manner (Teeri, 1997; Zhang and Zhang, 2013). There has been evidence that GH families 5, 7, 9, 12 and 45 lack CBMs, whereas GH family 6 has been found to carry a CBM (Forseberg *et al.,* 2014).

1.3.2.3 β-glucosidases (EC 3.2.1.21)

Fungal BGLs are grouped into GH families 1, 3 and 5 (Nijikken *et al.*, 2007, Singhania *et al.*, 2013). They are the key enzymes accountable for catalysing the complete hydrolysis of cellulose (Lima *et al.*, 2013; Singhania *et al.*, 2013). They do not show any activity on crystalline cellulose, but are responsible for converting cello-oligosaccharides and cellobiose into glucose monomers, which results in reduced product inhibition of upstream enzymes (Kostylev and Wilson, 2012; Sørensen *et al.*, 2013). The crystal structure of BGL has not been documented sufficiently; however, it has been proposed that BGLs contain pocket-like active sites, allowing them to bind to cellobiose which is converted into glucose (Zhang and Zhang, 2013).

1.3.2.4 Other enzymes required for cellulose degradation

Although the key enzymes required for cellulose degradation are CBHs, EGs and BGLs, other proteins have been shown to contribute to the overall degradation of cellulose by increasing cellulose accessibility (Arfi *et al.*, 2014; Horn *et al.*, 2012; Peciulyte *et al.*, 2014). In doing so, they offer great potential for reducing overall enzyme production costs (Wu *et al.,* 2013). These proteins are:

1.2.3.4.1 Lytic polysaccharide monooxygenases (LPMOs)

LPMO's are newly discovered oxidative enzymes which have been found to enhanc cellulose degradation (Arfi *et al.,* 2014; Book *et al.,* 2014; Horn *et al.,* 2012; Morgenstern *et al.,* 2014). These enzymes were previously classified as GHs (previously thought to have endoglucanase activity), but further investigations revealed that these enzymes could not hydrolyse lignocellulosic substrates and were therefore classified as auxillary activities (AA) (Langston *et al.,* 2011). LPMO's cause disruptions in the cellulose chain through the oxidation of a glucose molecule at the C-1 and C-4 positions, resulting in the formation of an aldic acid and a keto-aldose moiety, respectively (Arfi *et al.,* 2014; Wu *et al.,* 2013). Some LPMO's have also shown to oxidise glucose molecules at position C-6. According to Forseberg *et al.* (2014), oxygen boosts the activities of fungal enzymes on the cellulose chain. The activities of LPMOs are dependent on a metal (copper) catalytic site and the presence of reducing agents (cellobiose dehydrogenase, gallate and ascorbate) or non-carbohydrate species in the lignocellulosic biomass (Wu *et al.,* 2013).

LPMO's have been classified into 3 families - the fungal AA9 (GH61) and the bacterial AA10 (CBM33) are the two most common families. Family AA11 has only recently been characterised but shows similar structural characteristics to the AA9 and AA10 families (Forseberg *et al.,* 2014; Morgenstern *et al.,* 2014). Their ability to bind to the cellulose surface is linked to their flat binding sites, which aligns with the cellulose microfibrils (Forseberg *et al.,* 2014; Wu *et al.,* 2013).

1.2.3.4.2 Carbohydrate binding modules (CBMs)

CBMs are modular accessory domains (consisting of amino acid sequences) that are attached to cellulases through a linker peptide (Eriksson *et al.,* 2002; Grassick *et al.,* 2004). Currently, CBMs are classified into 67 families, and the CBMs from family 1 are the most commonly found (Chen *et al.,* 2014). Their proposed functions include: i) directing the cellulases to their specific substrate binding sites; ii) increasing the concentrations of enzyme onto the cellulose surface, and iii) loosening the substrate by disrupting the tightly packed cellulose chains **(**Kim *et al.,* 2014). Similar to LMPO's, they contain flat binding sites and their association with cellulose is as a result of hydrophobic interactions.

1.2.3.4.3 Swollenins and expansins

These proteins are responsible for loosening and disrupting the substrate to increase the accessibility of cellulases to cellulose (Arantes and Saddler, 2010). It has been proposed that the hydrogen bonds between microfibrils are disrupted in the presence of these proteins (Kang *et al.*, 2013; Saloheimo *et al.*, 1988).

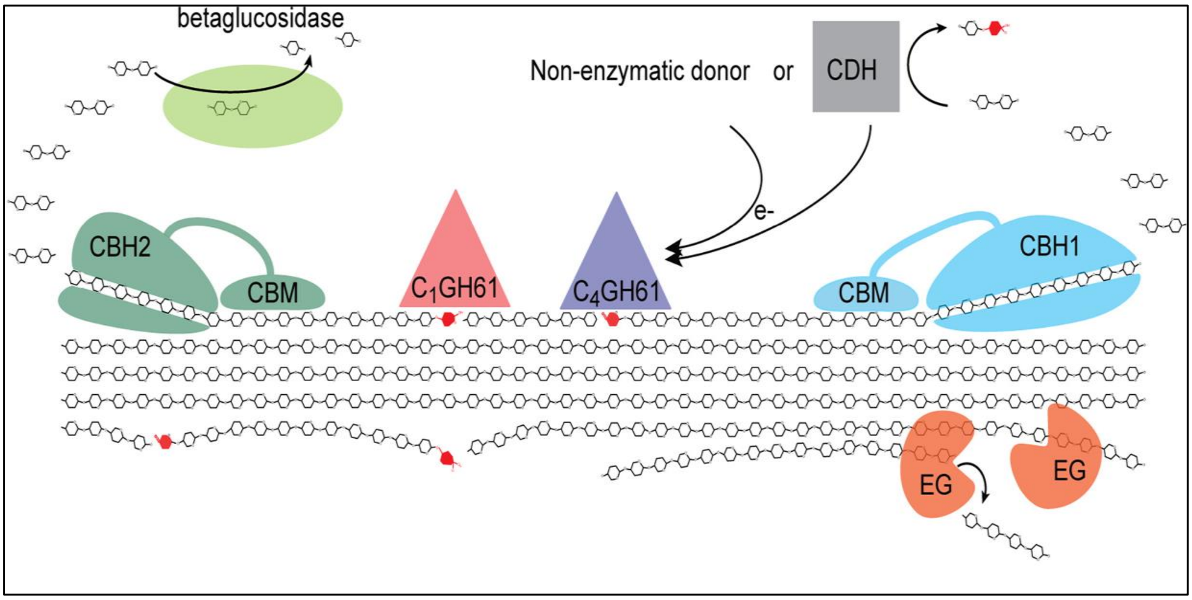

Figure 1.5. Enzymes required for cellulose degradation. CBHs degrade crystalline cellulose, whereas the EGs degrade the amorphous regions. BGLs convert cellobiose to glucose, alleviating product inhibition. Accessory enzymes contribute to the overall degradation of the substrate (Adapted from Horn *et al.*, 2012).

1.3.3 Enzymes required to degrade hemicellulose

1.3.3.1 Xylanases (EC 3.2.1.8)

The degradation of xylan requires the co-operative activities of multiple xylanases (Hu *et al.*, 2011; Zhang *et al.*, 2011). Bacterial xylanases are grouped into families 10 and 11, based on their secondary structures, molecular weights and isoelectric points (pI) (Wong *et al.*, 1988). The key xylanases are: i) endo-1, 4-*β*-D-xylanases (EC 3.2.1.8) which are responsible for cleaving the xylan backbone to give rise to shorter oligosaccharides, and ii) 1, 4-*β*-D-xylosidases (EC 3.2.1.37) which are responsible for hydrolysing xylo-oligosaccharides to D-xylose from the non-reducing end of the xylose chain (Sunna and Antranikian, 1997; Van Dyk and Pletschke, 2012). Additional enzymes such as arabinofuranosidases (EC 3.2.1.55), α-D-glucuronidases (EC 3.2.1.131) and phenolic esterases (EC 3.1.1.73) are required to liberate the substituted residues from the xylan backbone, thereby contributing to the overall degradation of xylan (Meyer *et al.*, 2009; Sweeney and Xu, 2012).

1.3.3.2 Mannanases (EC 3.2.1.25 and EC 3.2.1.78)

The degradation of mannan requires the co-operative activities of multiple mannanases which are grouped into families 5, 26 and 113 (Malgas *et al.*, 2015; Van Zyl *et al*, 2010). The key mannanases are: i) β-mannanases (EC 3.2.1.78) which are responsible for cleaving the mannan backbone to give rise to shorter oligosaccharides; ii) β-mannosidases (EC 3.2.1.25) which are responsible for hydrolysing the manno-oligosaccharides into mannose monomers from the non-reducing end of the mannan chain, and iii) β-glucosidases which are responsible for hydrolysing the oligosaccharides into glucose monomers (Shallom and Shoham, 2003). Additional enzymes such as galactosidases (EC 3.2.1.22) and acetyl-mannan esterases (EC 3.1.1.6) are required to liberate the substituted residues from the mannan backbone, thereby contributing to the overall degradation of mannan (Moreira and Filho, 2008; Yamabhai *et al*., 2014).

1.3.4 Enzymes required to degrade lignin

The degradation of lignin requires enzymes such as such as manganese peroxidase (MnP) (EC 1.11.1.13), lignin peroxidase (LiP) (EC 1.11.1.14) and laccase (EC 1.10.3.2) (Lee, 1997). These enzymes are responsible for catalysing the oxidation of phenolic compounds (Chen *et al.*, 2012; Howard *et al.*, 2003).

A summary of the key enzymes required for lignocellulose degradation is presented below (Table 1.2).

Table 1.2 Key enzymes required for biomass degradation (Modified from Lima *et al.*, 2001)

Constituent	**Chain residue**	**Branch residue**	**Enzymes**
Cellulose	Glucose		CBHI; CBHII, BGL; LPMO's; expansins swollenins; CBMs
Xylan	Xylose		Endo-β xylanase; β- xylosidase
		Arabinose	Arabinofuranosidase
		Glucoronic acid	Glucuronosidase
		Acetyl esterase	Phenolic esterases
Mannan	Mannose		Endo-β mannanase; β- mannosidases
Galactomannan	Mannose	Galactose	Endo-β mannanase; β-mannosidase; α-galactosidase; esterases
Glucomannan	Glucose + Mannose	Galactose	Endo-β mannanase; β-mannosidases; β-glucosidases; esterases
Lignin			MnP, LiP and laccases

1.4 Enzyme synergy

Lignocellulose is a complex substrate that requires a consortium of lignocellulose degrading enzymes for its degradation into monomeric sugars (Banerjee *et al.,* 2010; Mohanram *et al.,* 2013). When the combined activities of two or more enzymes increase the overall rate of substrate hydrolysis, as opposed to the theoretical sum of their activities when acting independently on a substrate, they are said to be acting in synergism (Lynd *et al.*, 2002; Olver *et al.*, 2011; Van Dyk and Pletschke, 2012; Zhou *et al.*, 2009).

1.4.1 Degree(s) of synergy

The degree of synergy (DS) is a quantitative measure used to determine whether enzymes interact synergistically to enhance the overall hydrolysis of a particular substrate (Jalak *et al.*, 2012; Van Dyk and Pletschke, 2012). The DS is calculated by dividing the amount of reducing sugars produced by an enzyme cocktail by the theoretical sum of reducing sugars produced by their independent activities (Andersen *et al.*, 2008; Van Dyk and Pletschke, 2012). The three outcomes for DS are: i) DS > 1 when enzymes act synergistically to degrade a substrate; ii) DS = 1 when the activity of one enzyme does not facilitate the activity of another enzyme: ie no synergy, and iii) DS < 1 when enzymes do not interact synergistically, but could be a result of competitive behaviour (enzymes competing for the same binding sites) (Hu *et al.*, 2011; Van Dyk and Pletschke, 2012). The DS can be influenced by factors such as enzyme characteristics (ratios of enzyme in a mix) and substrate characteristics (recalcitrance, DP and chemical composition) (Hu *et al.*, 2015; Jalak *et al*., 2012).

1.4.3 Synergistic interactions

Investigating the synergistic interactions between lignocellulose degrading enzymes has been the subject of extensive research in an attempt to improve biomass hydrolysis and alleviate high enzyme costs (Kallioinen *et al.*, 2014; Olver *et al.*, 2011). The most widely documented phenomenon is the synergy that occurs between cellulases (Boisset *et al.*, 2000; Moraïs *et al.*, 2010; Olver *et al.*, 2011; Teeri, 1997; Woodward, 1991). Intermolecular synergy between cellulases and xylanases has also been reported, however, this type of synergy is not as extensively studied as the synergy between cellulases (Bura *et al.*, 2009; Hu *et al.*, 2011).

1.4.3.1 Intra- molecular synergy between cellulases

Numerous types of synergy between the various classes of cellulose-degrading enzymes have been investigated and proposed (Table 1.3). In particular, the most characterised cellulase synergism systems are: i) endo-exo synergism, whereby CBHs act on the new chain ends generated by the activities of the EGs, and ii) exo–exo synergism, whereby CBHs degrade cellulose chains at opposite ends (Henrissat *et al.,* 1985; Tomme *et al.,* 1990; Väljamäe *et al.*, 1999). Furthermore, the addition of a β-glucosidase is believed to prevent product inhibition of upstream enzymes by converting cellobiose into glucose, thus contributing to the overall degradation of cellulose (Kostylev and Wilson, 2012). Other types of synergism that have been reported include endo-endo synergism (endoglucanases attacking different sites on the chain) and intramolecular synergy between catalytic domains and CBMs (Din *et al*., 1994; Lamed *et al*., 1991; Woodward, 1991). For the past few decades, various hypotheses have been proposed to explain these synergistic interactions, however, the most widely accepted enzyme synergy model is based on the hypothesis that enzymes work on different regions on the substrate (crystalline or amorphous regions or reducing and non-reducing sides), thus exposing or creating new sites to facilitate the action of another enzyme (Kosytlev and Wilson, 2014; Wood and Mcrae, 1994). It has been reported that this is an over-simplification of a far more complex process (Hu *et al.,* 2015; Jalak *et al.,* 2012; Kostylev and Wilson, 2012). New paradigms for enzyme synergy have been proposed in literature, including:

1.4.3.1.1 Surface erosion model

Väljamäe *et al.* (1998) studied the hydrolysis of bacterial cellulose (BC) using two cellulases. They proposed a surface erosion model for enzyme synergy, which is complementary to the endo-exo synergism model. This model is based on the hypothesis that the processive action of the one enzyme (CBHI) alters the substrate structure, thereby creating obstacles that hinders its own activity (can no longer bind to the substrate). However, the eroded substrate is made more accessible for the activity of another enzyme (CBHII or EG), thus cellulose degradation is enhanced. Kostylev and Wilson (2014) similarly proposed this synergism model, however, they hypothesised that the roles of the enzymes were reversed (EG erodes the surface, making the substrate more hydrolysable for CBH).

1.4.3.1.2 "Traffic jam" effect

Igarashi *et al.* (2011) used Atomic Force Microscopy (AFM) to study the action of cellulases, and proposed that synergy was a result of a traffic jam effect. It was proposed that obstacles present in the cellulose chain impedes the activity of a particular enzyme. Other enzymes facilitate the action of the blocked enzyme to overcome the obstruction in the cellulose chain. This causes cellulose "peeling", which increases the accessibility of cellulases to the substrate, thus increasing overall cellulose hydrolysis.

1.4.3.1.3 "Substrate polishing" effect

Ganner *et al.* (2012) studied the mechanistic actions of CBHI, CBHII and EG on a polymorphic cellulosic substrate, using AFM. Their studies interestingly found CBHII to display EG activity, due to its ability to degrade amorphous cellulose. It was therefore put forward that CBHII was a bi-functional enzyme. Furthermore, their results indicated that crystalline cellulose is covered by amorphous cellulose and that CBHII and EG are required to remove the amorphous regions. In doing so, they polish (expose) the crystalline regions in the cellulose chain, which ultimately requires the activity of CBHI for its hydrolysis.

1.4.3.2 Inter-molecular synergy between cellulases and xylanases

Some studies have been reported that cellulose hydrolysis may be enhanced by the synergistic interactions between cellulases and xylanases (Table 1.4) (Hu *et al.*, 2011; Kumar and Wyman, 2009). Cellulose and hemicellulose are closely associated with each other through various covalent bonds (Moreira and Filho, 2008; Zhang *et al.*, 2011). Therefore, xylanases may contribute to the overall hydrolysis of cellulose by removing the hemicellulosic component (xylan) in biomass that restricts the accessibility of cellulases to cellulose (Hu *et al.*, 2011; Kumar and Wyman, 2009; Zhang *et al.*, 2011).

1.5 Biomass pre-treatment

The major bottleneck in achieving efficient biomass saccharification is overcoming the recalcitrant structure of plant biomass. This necessitates that a pre-treatment step to be conducted on the substrate to break the bonds between the lignin-polysaccharide complex, thus opening up the substrate to allow enzymes more accessibility to the polysaccharides (Karp *et al.*, 2013; Van Dyk and Pletschke, 2012). Various pre-treatment methods been reported in literature, including acid pre-treatment (Chandel *et al.*, 2007), alkaline pre-treatment (Rabelo *et al.*, 2011), ammonia fibre explosion (Krishnan *et al.*, 2010), biological pre-treatment (Camassola and Dillon, 2009), liquid hot water pre-treatment (Allen *et al.*, 1996), organic solvent pre-treatment (Pasquini *et al.*, 2005), steam explosion (Rocha *et al.*, 2012) and wet oxidation pre-treatment (Martín *et al.*, 2008).

Table 1.3 Synergy studies between cellulases on various cellulosic substrates reported in literature (Intra-molecular synergy)

Substrate	Organism	Enzymes	Reference
Phosphoric acid	*H. insolens*	Cel6A (CBHII); Cel45A (EGV)[a]	Andersen *et al.*, 2008
Bacterial ribbons	*H. insolens*	Cel6A (CBHI); Cel7A (CBHII); Cel45A (EG)[a]	Boisset *et al.*, 2000
Avicel	*T. reesei* *Thermomonospora fusca*	CBHI EGII/EGIII	Bothwell *et al.*, 1993
Avicel	*C. lucknowense* *T. reesei*	Cel7A (CBHI); Cel5A (EGII)[a]	Den Haan *et al.*, 2013
Avicel and Whatman paper	*T. reesei*	CBHI CBHII	Fägerstam and Pettersson,1980
PASC	*T. reesei*	CBHII EGII[a]	Fujita *et al.*, 2004
Cotton cellulose	*C. lucknowense*	Cel7B (CBH I); Cel6B (CBH II)[a]	Gusakov *et al.*, 2006
Pre-treated lodgewood pine and corn stover	*T. reesei*	Cel6A CelA Cel7B Cel5B[a]	Hu *et al.*, 2015
Filter paper	*T. reesei*	CBHI CBHII[a]	Irwin *et al.*, 1993
Steam pre-treated wheat straw	*T. reesei*	Cel7A (CBHI); Cel6A (CBHII); Cel5A (EGII)[a]	Kallioinen *et al.*, 2014
Cotton cellulose	*T. reesei*	CBHII EGII[a]	Kleman-Leyer *et al.*, 1996
Avicel	*T. reesei*	CBHI; EGII	Medve *et al.*, 1998
Filter paper	*T. reesei*	CBHI; CBHII[a]	Nidetzky *et al.*, 1994
Avicel	*Humicola grisea*	CBHI EGIII	Takashima *et al.*, 1998
Avicel	*Neurospora crassa*	CBHI; Cel6A (CBHII); CEL5A (EGI)[a]	Phillips, 2011
Avicel	*T. reesei*	CBHI; CBHII EGII[a]	Woodward *et al.*, 1988
Bacterial cellulose	*T. reesei*	CBHI; EGI[a]	Väljamäe *et al.*, 1999
Filter paper	*Phialophora*	Cel6A (CBHII); Cel45A (EG)	Zhang *et al.*, 2012
Steam exploded cornstover	*Trichoderma viride*	Cel6A (CBHI); Cel7A (CBHII); Cel7B[a]	Zhou *et al*, 2009

[a]β-glucosidase supplementation

Table 1.4. Synergy studies between cellulases and xylanase on various cellulosic substrates reported in literature (Inter-molecular synergy)

Substrate	Organism	Enzymes	Reference
Steam pre-treated wheat straw		Accelerase 1500 XynC[a]	Alvira *et al.*, 2011
Wet oxidized corn stover	*T. reesei*	Cel7A (CBHI); CeL6A (CBHII); Cel5A (EGII); Cel74A (Xyn)[a]	Benko *et al.*, 2008
Steam pre-treated corn stover		Celluclast Multifect Xylanase[a]	Bura *et al.*, 2009
Steam pre-treated rice straw	*Aspergillus awamori*	Xyn; Cellulase[a]	Choudhary *et al.*, 2014
AFEX pre-treated corn stover	*T. reesei* *Clostridium thermocellum, Geobacillus thermodenitrificans*	CBHI; CBHII; EGII; Xyn10; Xyn11[a]	Gao *et al.*, 2011
Steam pre-treated barley straw		Celluclast; Shearzyme[a]	García-Aparicio *et al.*, 2007
Steam pre-treated corn stover	*T. reesei*	Celluclast Multifect Xylanase[a]	Hu *et al.*, 2011
Pre-treated wheat straw	*T. reesei*	Cel7A (CBHI); Cel6A (CBHII); Cel7B (EGI); Cel5A (EGII); Xyn11A[a]	Kallioinen *et al.*, 2014
AFEX pre-treated poplar		Spezyme cellulase; Multifect Xylanase[a]	Kumar and Wyman, 2009
Superfine ground sugarcane bagasse	*T. reesei* *Trichoderma longibrachiatum*	Celluclast; Xyn[a]	Li *et al.*, 2014
Pre-treated corn stover	*T. reesei* *Thermomyces lanuginosus*	Cel7A(CBHI) XynA	Selig *et al*, 2008
Steam pre-treated rice straw; giant reed	*T. reesei* *Thermoascus aurantiacus*	CeL7A (CBHI); CeL6A (CBHII); CeL5A (EGII); Xyn10[a]	Zhang *et al.*, 2013
Hydrothermally pre-treated corn stover	*T. aurantiacus*	CBHI; EGII; Xyn[a]	Zhang and Viikari, 2014

[a]β-glucosidase supplementation

1.6 Problem statement

The large percentage of underutilised cellulose (glucan) in lignocellulosic biomass makes it one of the most promising feedstocks for the production of sustainable liquid transportation fuels (Kumar and Wyman, 2009; Sweeney and Xu, 2012). It is well documented that cellulases can efficiently degrade its recalcitrant structure, thus advancements in the commercialisation of cellulosic fuels are ongoing. However, the low enzyme activities on a substrate associated with high enzyme costs, necessitates the urgency to improve these facilities to make them more economically feasible (Limayem and Ricke, 2012; Zhao *et al.*, 2012).

Enhancing cellulose hydrolysis through enzyme synergy shows potential for achieving higher conversion rates and yields from complex substrates. However, the mechanisms behind their interactions have not been elucidated completely, and due to the contradictions reported in literature, there are still major gaps in our understanding of enzyme synergy (Ganner *et al.*, 2012; Kostylev and Wilson, 2012). It has been proposed that enzyme and substrate characteristics are the major contributing factors that influence enzyme synergy (Hu *et al.*, 2014; Van Dyk and Pletschke, 2012). Investigating the synergistic interactions between enzymes on various substrates, including model and natural substrates, could potentially provide useful insights into obtaining a better comprehension of enzyme mexhanisms. This could ultimately provide a platform for the development of better enzyme cocktails for improved cellulose hydrolysis.

1.7 Hypothesis

Exo- and endo-type cellulases can act synergistically to degrade complex cellulosic substrates, and the characteristics of a particular substrate directly influences cellulase synergism; thus an understanding of enzyme and substrate characteristics can assist in elucidating enzyme synergy.

1.8 Aims and Objectives

1. To characterise pure fungal cellulolytic enzymes (CBHI; CBHII; EGI; EGII and BGL) and determine the conditions required for optimal cellulase activity;
2. To characterise three cellulosic substrates (Avicel; steam exploded bagasse and paper sludge) and elucidate substrate-enzyme interactions;

3. To establish the synergistic interactions between various combinations of cellulases on cellulosic substrates and determine the combinations required for optimal cellulose hydrolysis (intra-molecular synergy);
4. To establish the synergistic interactions between cellulases and a xylanase, and determine whether their interactions can lead to enhanced cellulose degradation (inter-molecular synergy).

1.9 Overview of thesis

The fungal cellulases (expressed in *Saccharomyces cerevisiae*) were kindly provided by Prof. W.H van Zyl (Stellenbosch University). The enzymes were fully characterised based on their substrate specificities, physicochemical characteristics and kinetic parameters (Chapter 2). The conditions required for optimal enzyme activity were obtained. The characteristics of three substrates, namely a model microcrystalline substrate, Avicel and two natural substrates, namely steam exploded bagasse and paper sludge were determined (Chapter 3). These studies focused on determining the chemical composition of each substrate, performing histochemical assays for lignin, determining the presence of potential inhibitors present in the substrates as well as investigating substrate-enzyme interactions by simple binding assays. In Chapter 4, the synergistic interactions between the cellulases were investigated and the optimal binary-synergy combination for each substrate was established. The effect of time on synergy was also investigated. Furthermore, inter-molecular synergy between the optimal binary cellulase combination and a xylanase was investigated. A general discussion and future recommendations is provided in Chapter 5.

Chapter 2: Enzyme characterisation

2.1 Introduction

Cellulose offers great potential as an alternative primary energy source for the production of sustainable liquid transportation fuels (Jorgensen *et al.,* 2007; Van Hanh *et al*., 2009). Efficient cellulose hydrolysis can be achieved by the activities of cellulases from microbial systems, due to their ability to hydrolyse the β-1, 4 glycosidic bonds between glucose molecules (Bayer *et al*, 1998; Ganner *et al.,* 2012). The major challenges associated with cellulases are their low hydrolytic activities and their high costs. Consequently, there is ongoing research to improve these activities (Banerjee *et al.,* 2010; La Grange *et al.,* 2010). Investigating the factors that influence enzyme activity, specifically their biochemical, physico-chemical and kinetic characteristics, could provide a platform for a better understanding of the conditions required for optimal enzyme activity (Nguyen and Quyen, 2010; Turon *et al.*, 2008).

The major cellulases involved in cellulose hydrolysis include cellobiohydrolases, endoglucanases and β-glucosidases (Ganner *et al.,* 2012; Horn *et al.*, 2012; Zhou *et al.,* 2009). These enzymes are classified as GHs, however, their affinities for a particular substrate is dependent on the 3D structure of their active sites (Vlasenko *et al.,* 2010). CBHs have a strong affinity for crystalline cellulose such as Avicel, due to its tunnel-like active site which allows it to act processively along the cellulose chain, whereas EGs have a strong affinity for amorphous cellulose such as carboxymethyl cellulose (CMC), due to its open active site (cleft-shaped) (Beldman *et al.,* 1988; Ganner *et al.,* 2012; Granum *et al.,* 2014). β-glucosidases convert cellobiose to glucose, and thus have a high affinity for substrates such as *p*-nitrophenyl β-D glucopyranoside (*p*NPG), which is a chromogenic analog of cellobiose (Van Rooyen *et al.,* 2005). Furthermore, some cellulases may exhibit activity on more than one substrate. Understanding their specificities for particular substrates is important to unravel information regarding their synergistic behaviours (Aspenborg *et al.,* 2012; Naumhoff, 2011).

The kinetic characteristics of an enzyme can provide a better understanding of how it functions (Berg *et al.,* 2002). "The rate at which an enzyme initiates catalysis is determined by the number of moles of product produced per unit of time" (Berg *et al.,* 2002; Pérez-Rodríguez *et al.,* 2013; Trayser and Seligson, 1969). This is variable with the concentration of the substrate, whereby the rate of reaction increases with an increase in substrate concentration, but reaches a saturation point at a high substrate concentration (Berg *et al.,* 2002; Gunawardena, 2012). The K_M (Michaelis constant) and V_{max} (maximum velocity) can be determined from the rate of catalysis by plotting a double reciprocal plot (Lineweaver - Burk plot) or a linear regression plot (Mason and Lai, 2000; Sjögren *et al.,* 2012). These kinetic parameters are useful for determining the amount of substrate required to achieve efficient catalysis (K_M), and the fastest rate at which an enzyme can convert substrate molecules into product, per unit of time (V_{max}) (Gunawardena, 2012; Sjögren *et al.,* 2012).

Enzyme activities are governed by physico-chemical factors such as temperature and pH (Turon *et al.,* 2008; El-Hefnawy *et al.,* 2014). Most enzymes display optimum activity at a characteristic pH and temperature, thus determining the effect of these two factors on enzyme activity could provide useful information of the conditions required for optimal enzyme activity (Jahangeer *et al.,* 2005). Furthermore, investigating the thermal stability of an enzyme is essential, especially for their potential in industrial applications (Thomas and Scopes, 1998). Although enzymes display optimum activity at a specific temperature, enzyme denaturation may occur at high temperatures, resulting in a loss of activity over time (Daniel *et al.*, 2008; Thomas and Scopes, 1998). Glycosylated enzymes have been reported to be more stable than un-glycosylated enzymes, since glyco-proteins are believed to reduce the structural dynamics of an enzyme (Beckham *et al.*, 2012).

Since enzyme activities are governed by various factors, it was important to characterise the enzymes used in this study to understand the factors that influenced their activities, thus assisting in the design of an ideal environment for future experiments. The enzymes characterised in this study were CBHI, CBHII, EGI, EGII and BGL from various fungal sources.

2.2 Aims and Objectives:

2.2.1 Aims

- To characterise five fungal cellulases that have the potential to degrade complex cellulosic substrates;
- To determine the conditions for optimal cellulase activity.

2.2.2 Objectives

- To carry out bioinformatic characterisation of cellulolytic enzymes (ProtParam);
- To assess sizes of the cellulolytic enzymes by sodium dodecyl sulphate polyacrylamide gel electrophoresis (SDS-PAGE);
- To determine the substrate specificities of the cellulolytic enzymes;
- To determine the conditions (temperature and pH) for optimal cellulase activity;

- To determine the kinetic parameters of the cellulolytic enzymes (V_{max}, K_M, k_{cat}, k_{cat}/K_M).

2.3 Methods

2.3.1 Chemicals

Chemicals used for the preparation of solutions were of analytical grade and were purchased from chemical companies. (Appendix 1).

2.3.2 Enzyme source

Five partially purified fungal cellulase preparations, namely cellobiohydrolases Cel7A (CBH1, EC 3.2.1.176 from *Talaromyces emersonii* with C-terminally-fused CBM from *Trichoderma reesei*) and Cel6A (CBHII, EC 3.2.1.91 from *Chrysosporium lucknowense*), endoglucanases Cel7B (EGI, EC 3.2.1.4 from *Aspergillus terreus*) and Cel5A (EGII, EC 3.2.1.4 from *Trichoderma reesei*) and β-glucosidase (Cel3A, EC 3.2.1.21 from *Saccharomycopsis fibuligera* were kindly provided by Prof. W.H Van Zyl (Stellenbosch University) and used for this study. All enzymes were expressed in *S. cerevisiae*, and the fermentation broths were used for the study (Den Haan[b] *et al.*, 2013). These enzymes were selected due their ability to be produced at relatively high levels in *S.cerevisiae* at optimum conditions required for yeast growth.

2.3.3 Substrates

A selection of cellulosic substrates were chosen for this study, including commercial cellulosic substrates (Avicel, carboxymethyl cellulose (CMC) and *p*NPG) and two natural lignocellulosic substrates (steam exploded bagasse (SEB) and paper sludge (PS)). Avicel, CMC and *p*NPG were purchased from Sigma (South Africa), the PS was kindly provided by Prof. W.H Van Zyl (Stellenbosch University) and the steam exploded bagasse was pre-treated at the University of the Western Cape. All substrates were prepared to a 2% final concentration in sodium citrate buffer (pH 5.0; 0.05 M).

2.3.4 Bioinformatic characterisation of cellulolytic enzymes

The protein sequences for the cellulases were retrieved from the Carbohydrate-Active Enzyme (CAZy) database and their physical and chemical properties were determined using the ProtParam tool in the ExPASy Bioinformatics Resource Portal (http://expasy.org/cgi-bin/protparam).

2.3.5 Protein determination

Protein concentrations were estimated using a modified Bradford method and bovine serum albumin (BSA) was used as the protein standard (Bradford, 1976). A standard curve was prepared using concentrations ranging from 0 to 1 mg/mL (Appendix 2A). Protein sample (25 µL) was added to Bradford reagent to (230 µL) and incubated for 10 minutes at room temperature. Absorbance readings were measured at 595 nm on a microtitre plate reader (PowerWaveX reader)

2.3.6 Enzyme activity assays

2.3.6.1 Avicelase activity

Cellobiohydrolase activity was measured against Avicel. Appropriately diluted enzyme (100 µL of a 0.1mg/mL stock solution)) was mixed with 300 µL of Avicel (2% final concentration) in sodium citrate buffer (pH 5.0; 0.05 M). The reaction was carried out at 50°C for 24 hours after which the sample was centrifuged for 5 minutes (16, 060 x *g*). The supernatant was used to measure the amount of reducing sugars released (as glucose equivalents) using a modified 3, 4 dinitrosalicylic acid (DNS) protocol (Miller, 1959). The supernatant (150 µL) was added to DNS solution (300 µL) (Appendix 2B) and incubated at 100ºC (Labnet AccuBlock digital dry bath) for 7 minutes, followed by cooling the samples on ice for 10 minutes. The DNS solution (250 µL) was pipetted into a microtitre plate and the absorbance was measured at 540 nm using the PowerWaveX reader. The reducing sugars released were determined from a glucose standard curve (Appendix 2B). All the activities were expressed in International Units. One unit of enzyme activity was defined as the amount of enzyme required to liberate 1 µmol of glucose per minute under the specified assay conditions.

2.3.6.2 CMCase activity

Endoglucanase activity was measured using CMC as a substrate. Appropriately diluted enzyme (100 µL of a 0.1mg/mL stock solution) was mixed with 300 µl of CMC (2% final concentration) in sodium citrate buffer (pH 5.0; 0.05 M). The reaction was carried out at 50ºC for 20 minutes after which the sample was centrifuged for 5 minutes (16, 060 x *g*). The release in reducing sugars was measured using the protocol as described in 2.3.6.1. One unit of enzyme activity was defined as the amount of enzyme required to liberate 1 µmol of glucose per minute under the specified assay conditions.

2.3.6.3 Glucosidase activity

β-glucosidase activity was measured using *p*NPG as a substrate. Appropriately diluted enzyme (50 µL of a 0.1mg/mL stock solution) was mixed with 450 µL *p*NPG (2.25 mM final concentration) in sodium citrate buffer (pH 5.0; 0.05 M). The reaction was carried out at 50ºC for 20 minutes after which the reaction was stopped by the addition of 500 µL sodium carbonate

(2 M). The *p*NPG solution (250 µL) was pipetted into a microtitre plate and the amount of *p*-nitrophenyl product was measured at 405 nm using the PowerWaveX reader. The activity was determined from a *p*-nitrophenyl standard curve (Appendix 2C). One unit of enzyme activity was defined as the amount of enzyme required to liberate 1 µmol of glucose per minute under the specified assay conditions.

2.3.7 SDS-PAGE analysis

The sizes of the cellulases were analysed by SDS-PAGE using a 10% (w/v) resolving gel and a 4% (w/v) stacking gel according to the standard protocol (Laemmli, 1970). Protein (20 µL) was mixed with sodium dodecyl sulfate (SDS) reducing buffer (5 µL) and incubated at 95ºC for 5 minutes (Labnet AccuBlock digital dry bath). 18 µL (0.1mg/mL) enzyme sample were loaded in the wells and electrophoresis was performed at 100 V for 2 hours using a Mini-Protean® (BioRad) cell tank, after which the gel was stained with Coomassie Brilliant Blue. The molecular sizes of the enzymes were estimated by comparison to a pre-stained protein ladder (Thermo-scientific, 14-116 kDa). See Appendix 3 for the preparation of gels and solutions.

2.3.8 Substrate specificity assay

The substrate specificities of the cellulases were determined using Avicel, CMC, *p*NPG, SEB and PS as substrates. The amount of reducing sugar released was determined by the DNS method as described previously (section 2.3.6.1).

2.3.9 Temperature optimum studies

To determine the temperature optimum for the cellulolytic enzymes, the cellulases were incubated with their appropriate substrates in citrate buffer (pH 5.0; 0.05 M) at different temperatures (20ºC – 70ºC) (Labnet AccuBlock digital dry bath). The release in reducing sugars was measured using the DNS method as described in section 2.3.6.1.

2.3.10 Thermal stability studies

The thermal stability profiles for the cellulolytic enzymes were measured by incubating the enzymes at their optimum temperature for 96 hours. The release in reducing sugars was measured using the DNS method as described in section 2.3.6.1.

2.3.11 pH optimum studies

To determine the pH optimum of the cellulolytic enzymes, the cellulases were incubated with their appropriate substrates at different pH's (pH 3.0 - 8.0) in sodium citrate buffer (pH 3.0 –

6.0; 0.05 M) and phosphate buffer (pH 6.0 - 8.0; 0.5 M). The release of reducing sugars was measured using the DNS method as described in section 2.3.6.1.

2.3.12 Kinetic characterisation

The values of the Michaelis constant (K_M), maximum velocity (V_{max}), turnover number (k_{cat}), and catalytic efficiencies (k_{cat}/K_M) of the cellulolytic enzymes were determined at 50ºC in sodium citrate buffer (pH 5.0; 0.05 M). The concentrations for Avicel and CMC ranged from 0.5 mg/mL - 30 mg/mL and the concentrations for *p*NPG ranged from 0.125 mM - 3 mM. The kinetic data were analysed using Lineweaver - Burk plots.

2.4 Results

2.4.1 Bioinformatic characterisation of cellulolytic enzymes

Various physical and chemical parameters, such as sequence length, molecular mass, theoretical isoelectric point, binding and active sites and the presence of CBMs and glycosylated sites of the enzymes were determined using bioinformatics tools (Table 2.1) (ProtPoram tool in the ExPASy Bioinformatics Resource Portal) (Gasteiger *et al.,* 2005). The protein sequences were retrieved from CAZy.

Table 2.1 showed that CBHII (Cel7A) from *T. emersonii* has a polypeptide chain of 437 amino acids, a molecular mass of 46.84 kDa and a pI of 4.09. It also contains glycosylated sites. CBHII (Cel6A) from *C. lucknowense* has a polypeptide chain of 395 amino acids, a molecular mass of 42.23 kDa and a pI of 4.7. EGI (Cel7B) from *A. terreus* has a sequence length of 471 amino acids, a molecular mass of 49.33 kDa, a pI of 5.24 and contains a CBM from GH family 1. EGII from *T. reesei* (Cel5A) has a 418 amino acid polypeptide chain, a molecular mass of 44.28 kDa, and a pI of 4.97. The results also indicated that EGII has two active sites, contains glycosylated sites, and a CBM from GH family 1. BGL (Cel3A) from *S. fibuligera* has a sequence length of 876 amino acids, a molecular mass of 96.23 kDa and a pI of 5.24. It also contains one active site and has many glycosylated sites.

Table 2.1. Physical and chemical parameters of the cellulolytic enzymes as predicted from UniProt and ProtPoram

Protein name (UniProt ID)	CellobiohydrolaseI	CellobiohydrolaseII (AAQ38151.1)	Endoglucanase I (E5Q901)	Endoglucanase II (P07982)	Beta glucosidase (P22506)
Organism	*T. emersonii*	*C. lucknowense*	*A. terreus*	*T. reesei*	*S. fibuligera*
Sequence Length	437	395	471	418	18; 859; 876
Mass (kDa)	46.84	42.23	49.33	44.28	96.23
pI	4.09	4.7	5.24	4.97	4.79
Binding sites	-	-	-	-	-
Active sites	-	-	-	-239 (Proton donor) -350 (Nucleophile)	295
Glycosylated sites	285; 449	-	-	124	22; 75; 224; 267 332; 339; 37; 389; 426; 544; 585; 639; 780; 790
CBM		-	CBM1	CBM1	

Any annotated post-translational modifications were not taken into account

2.4.2 SDS-PAGE analysis

The sizes of the cellulases were confirmed by SDS-PAGE analysis as described in section 2.3.7. All the enzymes were determined to be monomeric, as evident by the single bands produced by each enzyme on the SDS-PAGE gel (Figure 2.1). SDS-PAGE analysis showed that that CBHI, CBHII, EGI, EGII and BGL had approximate molecular masses of 66 kDa; 67 kDa; 57 kDa; 56 kDa and >116 kDa, respectively. Minor contaminants were also present at lower molecular masses (35- 55 kDa), which may have been attributable *S. cerevisiae* and/or media components.

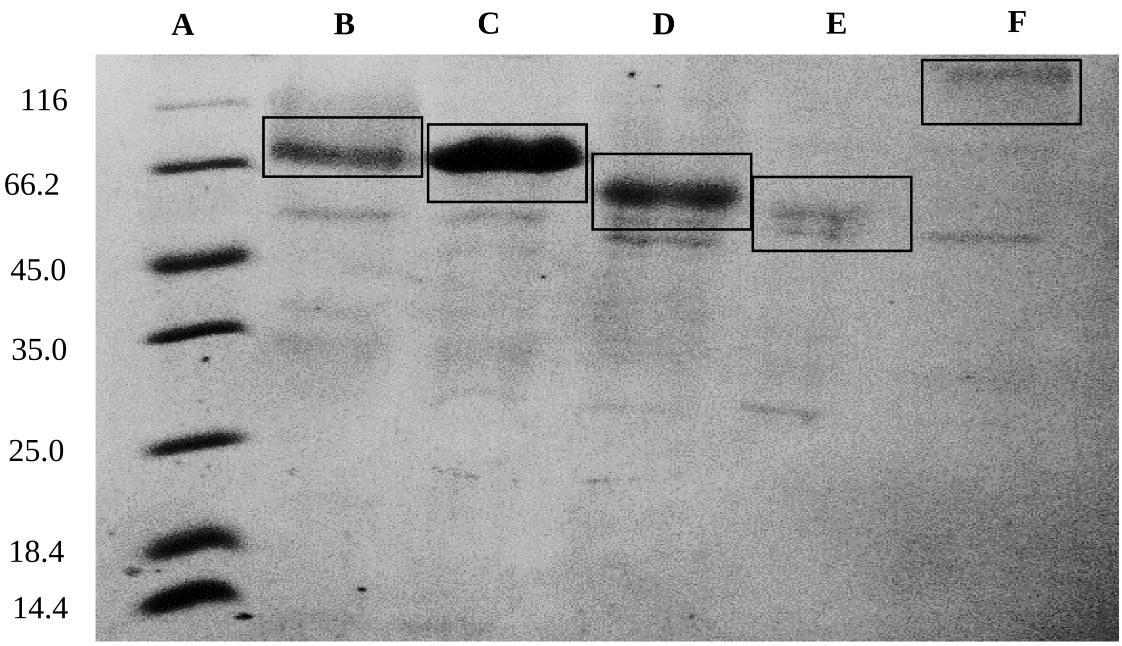

Figure 2.1. SDS-PAGE analysis of the cellulolytic enzymes. 15 µl (0.1 mg/mL) of each cellullase and 5 µl of prestained marker were loaded onto a 10% (w/v) SDS-PAGE gel and proteins were stained with Coomassie Blue. Lane (A): Prestained molecular marker; lane (B): CBHI; lane (C): CBHII; lane (D): EG1; lane (E): EGII and lane (F): BGL. Molecular masses (kDa) of marker proteins are shown on the left.

2.4.3 Specific activities of the cellulolytic enzymes

The specific activities of the enzymes were determined on various substrates. Enzyme activities were measured under standard assay conditions as described in 2.3.6. The substrates included the preferred substrates for the enzymes: Avicel, CMC, *p*NPG, as well as two natural cellulosic substrates: SEB and PS. CBHI and CBHII exhibited highest activity towards Avicel (0.06 U/mg for both enzymes), followed by SEB (0.04 and 0.03 U/mg) (Table 2.2). CBHI exhibited activity on PS (0.02 U/mg) whereas CBHII exhibited no activity on PS. As expected, EGI and

EGII exhibited the highest activity towards CMC (74 and 56 U/mg, respectively). EGI and EGII exhibited activity on Avicel (0.038 and 0.4 U/mg, respectively), and exhibited activity on SEB (0.05 and 0.07 U/mg, respectively). These enzymes did not display any activity on PS or *p*NPG. BGL only exhibited activity on *p*NPG (462 U/mg).

Table 2.2. The specific activities of the cellulases on Avicel, CMC, *p*NPG SEB and PS

Substrate	CBHI (U/mg)	CBHII (U/mg)	EGI (U/mg)	EGII (U/mg)	BGL (U/mg)
Avicel	0.06	0.06	0.038	0.04	-
CMC	-	-	74	56	-
*p*NPG	-	-	-	-	462
SEB	0.04	0.03	0.05	0.07	-
PS	0.02	-	-	-	-

Values are presented as mean values (SD < 5%)

2.4.3 Optimum conditions for cellulase activity

A) Temperature optimum

The activities of the cellulases were assayed at different temperatures ranging from 20 - 70ºC in sodium citrate buffer (pH 5.0; 0.05 M). Enzyme activities were measured under standard assay conditions as described in 2.3.6. CBHI displayed maximal activity at 60ºC and showed 50% ≤ activity at 40, 50 and 70ºC; however it exhibited no activity at 20 and 30ºC (Figure 2.2A). CBHII exhibited maximal activity at 60ºC and displayed ≥40% activity between 20 - 70ºC (Figure 2.2B). EGI had a temperature optimum of 60ºC and displayed ≥80% activity over a broad temperature range (20 - 70ºC) (Figure 2.2C). EGII was optimally active at 60ºC and displayed more than 45% activity between 20 - 70ºC (Figure 2.2D). BGL exhibited maximum activity at 40ºC and rapidly lost activity (>65%) at higher temperatures of 60 and 70ºC (Figure 2.2E).

B) Thermal stability

Thermal stability was investigated by incubating the enzymes at their optimum temperature over a period of 96 hours in sodium citrate buffer (pH 5.0; 0.05 M). The enzymes were found to be stable (Figure 2.3). CBHI was stable at its optimum temperature for 96 hours, however, an unexpected 53% increase in activity was observed between 24 - 96 hours (Figure 2.3A). CBHII displayed high stability at its optimum temperature and retained more than 80% residual activity over 96 hours (Figure 2.3B). EGI was relatively stable for 96 hours at its optimum temperature, however, there was a 20% decrease in activity between 24 - 48 hours (Figure 2.3C). EGII showed stability for 96 hours at its optimum temperature, however, an unexpected 50% increase in activity was observed between 24 - 96 hours (Figure 2.3D). BGL was highly stable and maintained ~90% activity for 96 hours at its optimum temperature (Figure 2.3E).

C) pH optimum

The activity pH profiles of the cellulases were determined by incubating the enzymes in sodium citrate buffer (pH 3.0 - 6.0) and phosphate buffer (pH 6.0 – 8.0) at 50ºC (Figure 2.4). Enzyme activities were measured under standard assay conditions as described in 2.3.7. The results showed that CBHI displayed a pH optimum of 4.5 and displayed ≥50% activity between pH 4.0- 6.5 (Figure 2.4A). There was a rapid loss in activity between pH 6.5 - 7.0 and the cellulase exhibited 0% activity at pH 7.0 - 8.0. CBHII had a pH optimum of 4.5 and displayed ≥60% activity between pH 4.5 - 7.0 (Figure 2.4B). EGI displayed a pH optimum of 5.5 and displayed ≥ 80% activity between pH 5.0 - 6.5 (Figure 2.4C). Figure 2.4D showed that EGII was optimally active at pH 4.5 and displayed ≥60% activity between pH 4.0 - 6.5. BGL was active over a broad pH range and exhibited maximal activity at pH 5.5 (Figure 2.4E). BGL displayed ≥50% activity at pH 4.0 – 6.0.

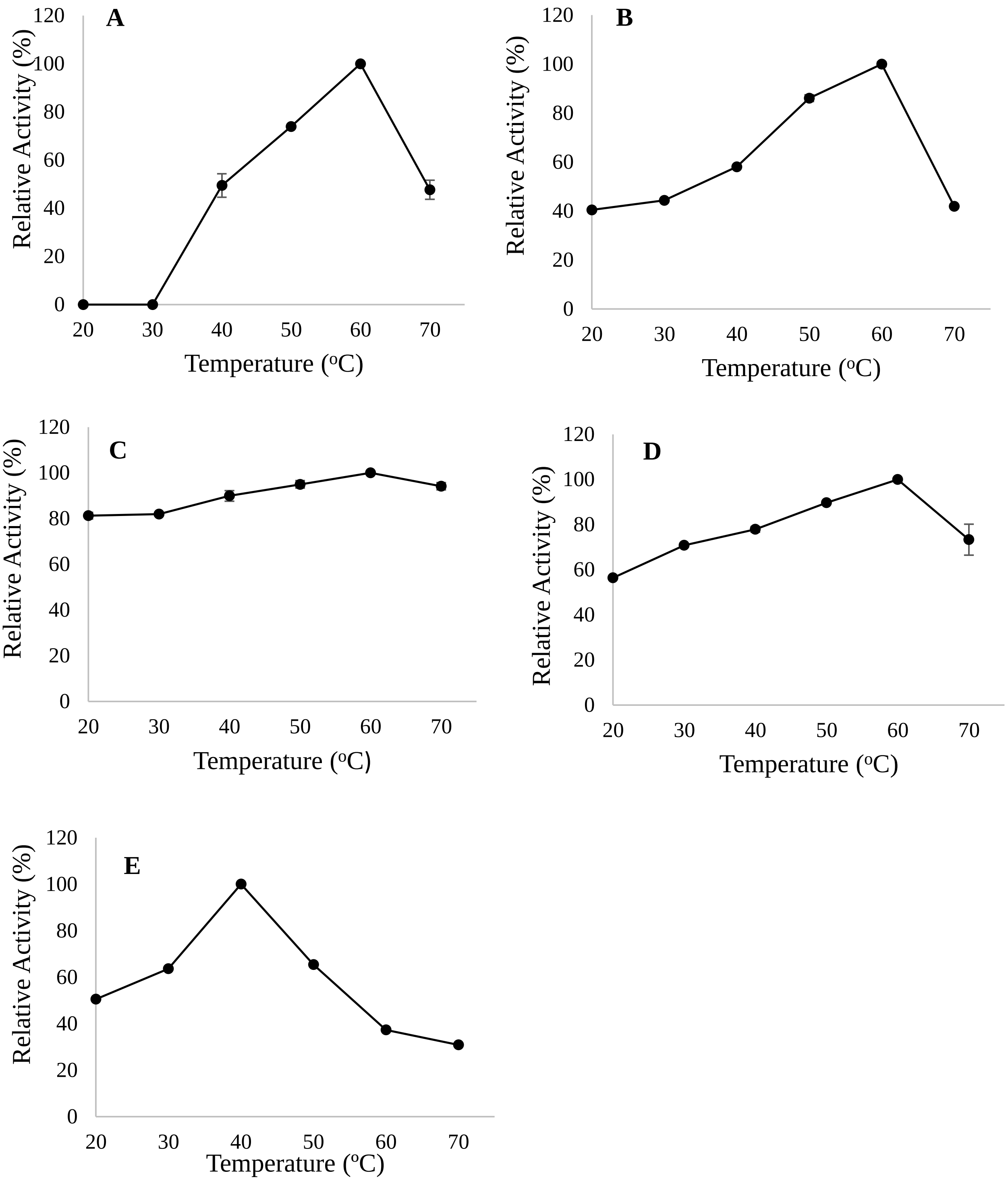

Figure 2.2. The effect of varying temperature on the activities of the cellulolytic enzymes. Activities were measured against their respective substrates in sodium citrate buffer (pH 5.0; 0.05 M). (A): CBHI; (B): CBHII; (C): EGI; (D): EGII; (E): BGL. Values are represented as mean values ± SD (n=3).

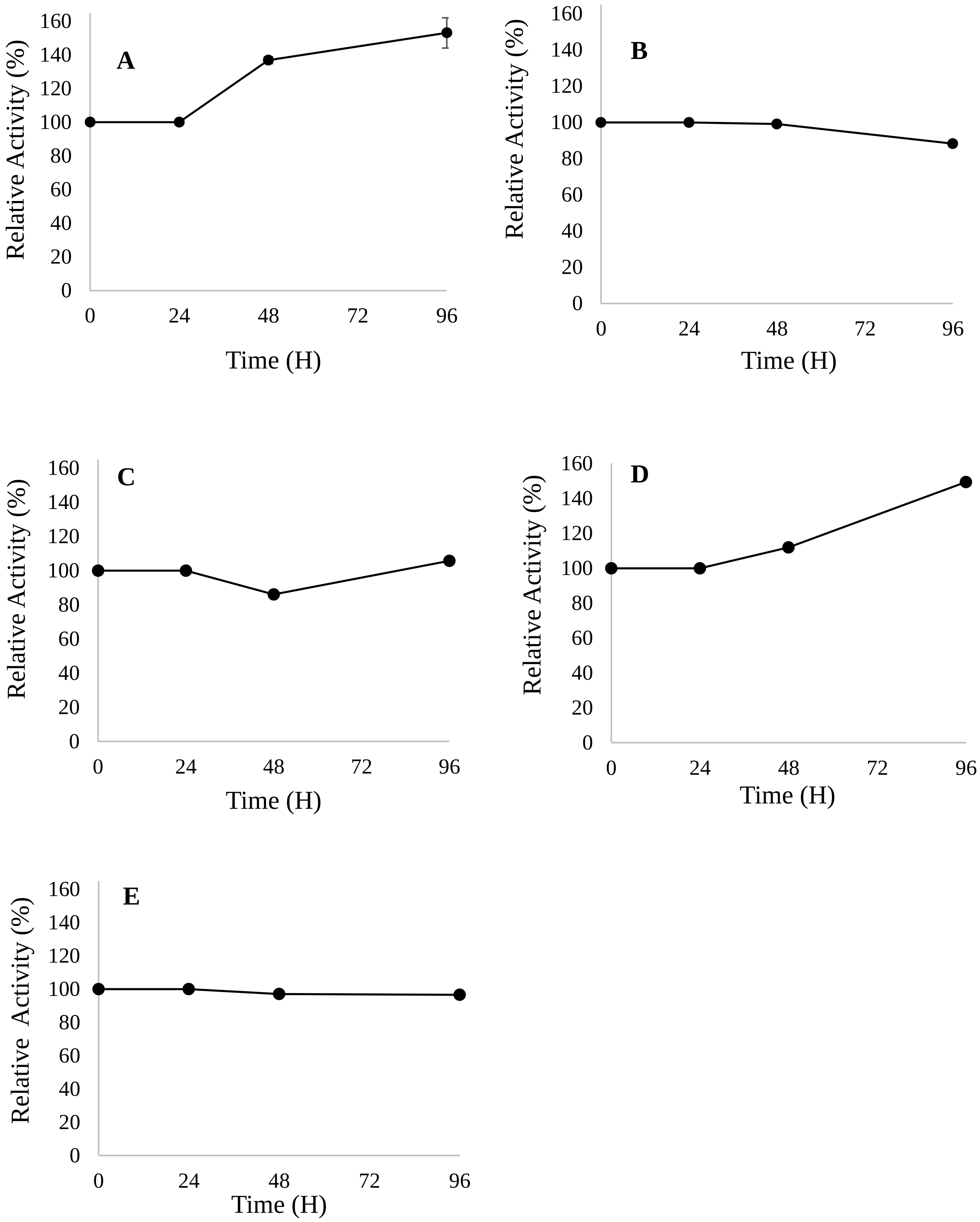

Figure 2.3. Thermal stability of the cellulolytic enzymes. Activities were measured against their respective substrates in sodium citrate buffer (pH 5.0; 0.05 M) at their temperature optima. (A): CBHI; (B): CBHII; (C): EGI; (D): EGII; (E): BGL. Values are represented as mean values ± SD (n=3).

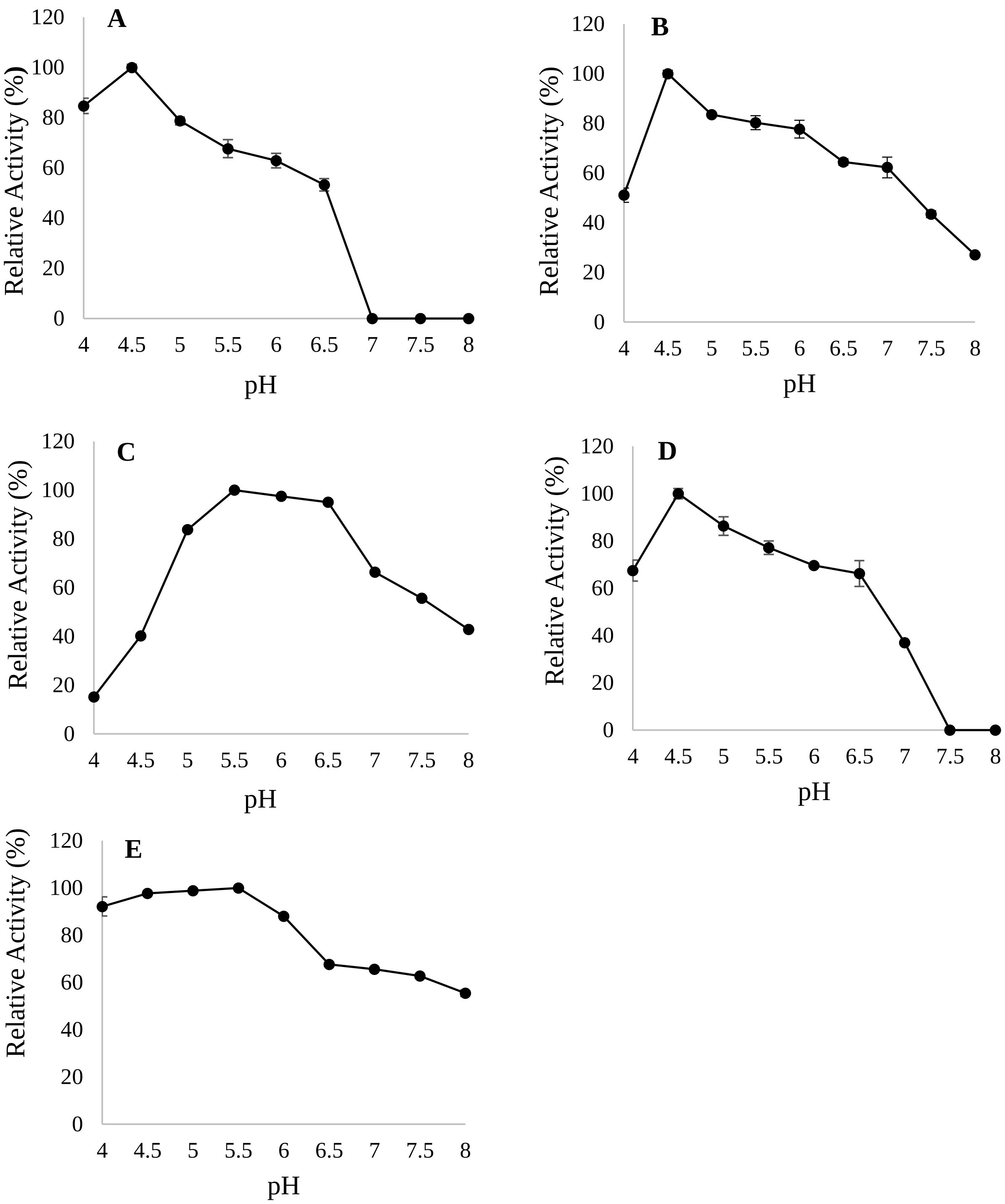

Figure 2.4. The effect of varying pH values on the activities of the cellulolytic enzymes. Activities were measured against their respective substrates in sodium citrate buffer (pH 3.0 - 6.0; 0.05 M) and phosphate buffer (pH 6.0 - 8.0) at 50ºC. (A): CBHI; (B): CBHII; (C): EGI; (D): EGII; (E): BGL. Data points are presented as mean values ± SD (n=3).

2.4.4 Kinetic characterisation of the cellulolytic enzymes

The kinetic parameters for the cellulolytic enzymes (K_M, V_{max}, k_{cat} and k_{cat}/K_M) were analysed using double reciprocal Lineweaver-Burk plots and are listed in Table 2.3. The concentration of Avicel and CMC ranged from 0.5 – 30 mg/mL and the concentration of *p*NPG ranged from 0.125 mM- 3.0 mM. Enzyme activities were measured under standard assay conditions as described in 2.3.6.

Table 2.3. Kinetic parameters estimated for CBH I, CBH II and EGI, EGII and BGL with Avicel, CMC and *p*NPG as their respective substrates

Enzyme	V_{max} (µmol/min)	K_M (mg/mL)	k_{cat} (min^{-1})	k_{cat}/K_M ($min^{-1}mg^{-1}$ mL)
CBHI	0.23	1.36	23	16.9
CBHII	0.40	3.3	40	12.12
EGI	149	2.1	59600	28380
EGII	85.47	1.55	34188	22056
Enzyme	V_{max} (µmol/min)	K_M (mM)	k_{cat} (min^{-1})	k_{cat}/K_M ($min^{-1}mM^{-1}$)
BGL	63.29	1.46	63290	43349

Characterisation of the cellulases used in this study allowed for a better understanding of the conditions required for optimal enzyme activities. The results are summarised below in Table 2.4.

Table 2.4. Summary of the characteristics displayed by various fungal cellulases

	CBHI	CBHII	EGI	EGII	BGL
Molecular mass (kDa)	66	67	57	56	45
Substrate preference	Avicel	Avicel	CMC	CMC	*p*NPG
Temperature optimum (ºC)	60	60	60	60	50
Temperature stability	+	+	+	+	+
pH optimum	4.5	4.5	5.5	4.5	5.5
K_M on preferred substrate	-	-	-	-	-
V_{max} on preferred substrate	-	-	+	+	+

+ represents high values and – represents low value (compared to previously reported data

2.5 Discussion

Biochemical, physico-chemical and kinetic paramaters govern the activities displayed by cellulases (Turon *et al.,* 2008). It was therefore essential to investigate these factors to understand the conditions required for optimal activity of the cellulases used in this study.

SDS-PAGE analysis

Figure 2.1 (lane B) showed that the size of the expressed protein, CBHI (Cel7A) from *T. emersonii* (66 kDa) was higher than the theoretical size of the native protein (46.84 kDa) (Grassick *et al.,* 2004). The inferred molecular mass discrepancies may have been a result of hyperglycosylation and/or the fusion of the CBM. To accurately determine whether the size increase was due to glycosylation, deglycosylation enzymes could have been used, followed by MALDI-TOF-MS and SDS-PAGE could have been carried out. (Voutilainen *et al.,* 2009). The size of the protein in this study was in agreement with Tuohy *et al.* (2002) and Voutilainen *et al.* (2010), who both found Cel7A (fused with a CBM) from *T. emersonii* to have a molecular mass of 66 kDa. The molecular mass reported in this study was similar to that which has been reported for CBHs (GH family 7), which was characterised from different fungal species, i.e. 65 kDa for *C. lucknowense*, 66 kDa for *Penicillium verruculosum* and 70 kDa for *T. reesei* (Bukhtojarov *et al.,* 2004; Morozova *et al.,* 2010; Xu *et al* 2014).

CBHII (Cel6A) was observed to be a monomeric protein with a molecular mass of approximately 67 kDa as evident by a defined protein band present on the SDS-PAGE gel (Figure 2.1, lane C). Minor contaminants were also present at lower molecular masses (30 -55 kDa). The molecular mass of CBHII was higher than what was determined by Bukhtojarov *et al.* (2004), but similar to Den Haan[b] *et al.* (2013), who determined *C. lucknowense* CBHII (Cel6A) to be 43 kDa and 75 kDa in size, respectively. The difference in the theoretical size and the expressed protein size (42.23 kDa) may have been caused by hyperglycosylation; however, further analysis such as using deglycosylation enzymes and MALDI-TOF MS would be required to confirm whether this was the case (Den Haan *et al.,* 2013; Wei *et al.,* 2014). The molecular masses of CBHIIs (GH family 6) from other fungal sources have been reported in literature and were similar to what was found in this study (67 kDa). These were 60 kDa and 83 kDa for *P. verruculosum* and *H. insolens,* respectively (Morozova *et al.,* 2010; Varrot and Davies, 1999).

EGI (Cel5B) produced a prominent single band at an approximate molecular mass of 57 kDa (Figure 2.1, lane D). Minor contaminants were also present on the gel (30 - 55 kDa). It was assumed that EGI was partially glycosylated, as the molecular mass was higher than the expected theoretical size (49.33 kDa) (Wei *et al.,* 2014). To the best of our knowledge, there have been no reports of the molecular mass of recombinant EG1 produced by *A. terreus* belonging to GH family 7; however, studies have documented the molecular masses for this fungus belonging to GH family 12. Gao *et al.* (2008) and Narra *et al.* (2012) determined the molecular masses of EGI from *A. terreus* to be 25 kDa and 29 kDa, respectively, which was considerably lower than what was found in this study (57 kDa). Nazir *et al*. (2009), however, determined the molecular mass to be 78 kDa. The molecular masses of EGIs (GH family 7), characterised from different fungal sources were found to be similar to that of *A. terreus* used in this study (57 kDa). These were 55 kDa for *T. reesei,* 55 - 70 kDa for *P. verruculosum* and 79 kDa for *Penicillium decumbens* (Herpoël-Gimbert *et al.,* 2008; Morozova *et al*., 2010; Xiao-Min *et al*., 2010).

Figure 2.1 (lane E) showed that EGII is a monomeric protein corresponding to an approximate molecular mass of 56 kDa with a minor contaminant at 25 kDa. This was in agreement with Den Haan *et al.* (2013), Qin *et al.* (2008) and Samanta *et al.* (2012) who determined the expressed *T. reesei* EGII (Cel5A) to be 54 kDa, 57 kDa and 53 kDa, respectively. The recombinant EGII had a higher molecular mass than the native EGII (44.28 kDa), which may be attributed to the different degrees of asparagine-linked glycosylation (Qin *et al.,* 2008; Samanta *et al*., 2012). Using de-glycosylation enzymes and MALDI-TOF MS could have been carried out to determine whether the size increase was attributable to glycosylation. The size of EGII in this study was in agreement with previous reports (Den Haan *et al*., 2013; Ilmén *et al.,* 2011). The molecular mass of *T. reesei* EGII in this study was similar to those reported in literature from various fungal EGIIs (GH family 5). These were 56 kDa for *Piromyces equi;* 51 kDa for *C. lucknowense*; 39 kDa for *P. verruculosum*, 50 kDa for *Postia placenta* and 70 kDa for *P. decumbens,* (Eberhardt *et al*., 2000; Gusakov *et al*., 2006; Morozova *et al*., 2010; Ryu *et al.,* 2011; Xiao-Min *et al*., 2010).

Figure 2.1 (lane F) showed that a band larger than 116 kDa was observed on the SDS-PAGE gel. It can therefore be stated that its molecular mass was greater than 116 kDa. A study performed by Machida *et al.* (1988) found the expressed BGL to be approximately 200 kDa on a SDS-PAGE gel. However, they stated that this was a result of glycosylation since the BGL contains 12-16 glycosylation sites and should have an approximate molecular mass of 96 kDa. To determine whether the size of BGL was bigger than 116 kDa, a molecular marker with a higher kDa range would be required. Fast protein liquid chromatography (FPLC) could also have been conducted for accurate molecular weight confirmation. Noteworthy, a band at an approximate molecular weight of 50 kDa was also observed. This may be a result of protein degradation or a minor contamination. The molecular masses of BGLs (Cel3A) from other recombinant cellulolytic fungi have been documented. These were 70 kDa, 85.1 kDa, 95 kDa, 93.5 kDa, 110 kDa and 130kDa for *T. reesei, Neocallimastix patriciarum, Volvariella volvacea, T. aurantiacus, Penicillium purpurogenum* and *T. emersonii,* respectively (Chen *et al*., 2012; Ding *et al*., 2007; Hong *et al*., 2007; Lee *et al.,* 2011; Murray *et al*., 2004; Shahbazi *et al.,* 2014).

Specific activities

Specific activities of the fungal cellulases towards different substrates are given in Table 2.2. CBHI (Cel7A) hydrolysed Avicel (0.06 U/mg), SEB (0.04 U/mg) and PS (0.02 U/mg), but was however, inactive against CMC and *p*NPG. This was expected since Avicel (model semi-crystalline substrate), SEB and PS contain crystalline regions on which CBHIs are known to initiate their mode of action (Imai *et al.,* 1998; Den Haan *et al*., 2013). Their ability to degrade only crystalline cellulose is linked to their tunnel-like active sites, which forms loops around the cellulose chain, allowing the enzyme to degrade the chain in a processive manner (Ganner *et al.,* 2012; Granum *et al.,* 2014). However, since crystalline cellulose is difficult to degrade (highly recalcitrant), the expected activity on the substrate would be low. The results were similar to what was found by Tuohy *et al*. (2002), who determined CBHI (Cel7A) from *T. emersonii* to be active against Avicel (0.41 U/mg) and inactive against CMC and *p*NPG. CBHIs (Cel7A) produced by other fungi, such as, *C. lucknowense* and *T. viride* also showed preference for Avicel with minimal to no activity on CMC and *p*NPG (Gusakov *et al*., 2005; Zhou *et al*., 2008). There have been no reports on the specific activities of CBHI (Cel7A) towards SEB and PS.

CBHII (Cel6A) hydrolysed Avicel (0.6 U/mg) and SEB (0.03 U/mg) but exhibited no activity against CMC, *p*NPG and PS. Since hydrolysis of crystalline cellulose is an identified characteristic of CBHs, activity on the crystalline cellulose was expected (Imai *et al.,* 1998; Den Haan *et al*., 2013). Furthermore, studies have reported that CBHII (Cel6A) from *C. lucknowense* have high preference for Avicel (0.2 - 0.24 U/mg), with no detectable activity against *p*NPG (Bukhtojarov *et al.,* 2004; Morozova *et al* 2010). Their studies did, however, show that CBHII exhibited some activity on CMC (1.1 U/mg - 2.0 U/mg). This could be linked to CBHII displaying bi-functional activity, thus having the ability to initiate its action on both crystalline and amorphous regions of the cellulose chain (Ganner *et al.,* 2012). Similarly, CBHII (Cel6A) produced by *Magnaporthe grisea* displayed the highest activity on Avicel and no activity against CMC (Takahashi *et al.,* 2010). There have been no reports on the specific activities of CBHII (Cel6A) towards SEB and PS

EGI (Cel7B) showed high specific activity towards CMC (74 U/Mg) and lower specific activity towards Avicel (0.038 U/mg) and SEB (0.053 U/mg). No activity was observed towards *p*NPG and PS. This is in agreement with literature, as EGs are known to be highly active on the amorphous region of cellulose (Karmakar and Ray, 2011). This is linked to their open active sites, allowing them to hydrolyse the cellulose chain at random positions (Beldman *et al.,* 1988). Amorphous cellulose is easier to degrade than crystalline cellulose, thus the specific activities of EG is higher on amorphous substrates than crystalline substrates, such as Avicel. To the best of our knowledge, EGI (Cel7B) produced by *A. terreus* from family 7 has not yet been characterised; however, the substrate specificities of this fungus belonging to GH family 12 have been reported. These studies showed that it was most active towards CMC (60 U/mg) and had no activity on Avicel (Narra *et al.,* 2012). Studies have previously reported the specific activities of EGIs (Cel7B) produced by other fungi, such as *P. verruculosom, T. reesei* and *P. decumbens*, which showed high specificity for CMC, minimal specificity towards *p*NPG and no activity towards Avicel (Morozova *et al.,* 2010; Nakazawa *et al*., 2008; Xiao-Min *et al*., 2010).

The substrate preference for EGII (Cel5A) was similar to that of EGI (Cel7B). It hydrolysed CMC (56 U/mg), Avicel (0.04 U/mg) and SEB (0.07 U/mg); however, it did not hydrolyse *p*NPG or PS. Since EGs are responsible for cleaving the amorphous regions of the cellulose chain, the high preference for CMC was expected (Karmakar and Ray, 2011). This was in agreement with Nakazawa *et al.* (2008) who showed that *T. reesei* EGII (Cel5A) displayed the highest activity on CMC (65 U/mg); however, it displayed no activity towards Avicel or *p*NPG. EGIIs (GH family 5) from different fungal sources, such as *P. equi*, *Thermotoga maritima, H. grisea, P. decumbens* and *P. pinophilum* also exhibited maximal activity towards CMC and had very low activity towards Avicel and *p*NPG (Eberhardt *et al.,* 2000; Mahadevan *et al*., 2008; Takashima *et al.,* 1997; Xiao-Min *et al.,* 2010; Yoon *et al.,* 2008).

BGL (Cel3A) rapidly hydrolysed *p*NPG (462 U/mg), but exhibited no activity towards CMC, Avicel, SEB or PS. BGLs are known to show high specificity towards cellobiose and cellodextrins, and are responsible for converting cellobiose to glucose molecules. *p*NPG is a chromogenic analog of cellobiose, thus BGL had high preference for this substrate (Van Rooyen *et al.,* 2005). This was in accordance with previous studies that had found BGL (Cel3A) from *S. fibuligera* to hydrolyse *p*NPG and cellobiose to a great extent, but had no activity towards Avicel or CMC (Gundllapalli *et al.,* 2007; Machida *et al.,* 1988). Furthermore, BGLs belonging to GH family 3, produced by *Aspergillus tubingensis* and *N. patricarium* similarly showed preference for *p*NPG and cellobiose as a substrate (Decker *et al.,* 2001; Hong *et al.,* 2007).

Temperature optimum and stability

CBHI (Cel7A) displayed maximal activity at 60ºC and displayed 50% activity at 40, 50 and 70ºC; however, it exhibited no activity at 20 and 30ºC (Figure 2.2A). This correlated well with Grassick *et al.* (2004) and Voutilainen *et al.* (2010) who determined *T. emersonii* CBHI displayed an optimum temperature of between 55 - 70ºC. CBHIs (Cel7A) produced by other fungi exhibited similar temperature optimum profiles to the CBHI used in this study (60ºC). *Trichoderma harzianum, T. reesei* and *Acremonium thermophilum* displayed optimum activity at 60ºC, whereas *T. aurantiacus* and *Chaetomium thermophilum* exhibited a temperature optimum of 65ºC (Colussi *et al*., 2012; Voutilainen *et al*., 2008). Thermostability studies (Figure 2.3A) showed that CBHI was stable at its optimum temperature.

Figure 2.2B showed that CBHII (Cel6A) exhibited a maximal activity at 60ºC and displayed ≥40% activity between 20 - 70ºC. This was in agreement with Bukhtojarov *et al.* (2004). Similarly, CBHIIs (GH 6) produced by *P. decumben*s and *M. grisea* displayed their maximum activities at 50ºC and 40ºC, respectively (Gao *et al*., 2011; Takahashi *et al*., 2010). Thermostability studies showed that *C. lucknowense* CBHII displayed high stability at its optimum temperature, and retained more than 80% residual activity over 96 hours (Figure 2.3B). These findings were in agreement, to some extent to that of Bukhtojarov *et al.* (2004) who determined that CBHII from *C. lucknowense* retains more than 90% of its activity for 5 hours.

EGI (Cel7B) had a temperature optimum of 60ºC and displayed ≥80% activity over a broad temperature range (20 - 70ºC) (Figure 2.2C). To the best of our knowledge, studies have not yet been conducted on the temperature optimum of *A. terreus* EGI from GH family 7. However, various studies have reported the temperature optima for EGIs produced by this fungus from GH family 12, and (similarly) these exhibited maximal activity between 50 - 60ºC (Gao *et al.,* 2008; Narra *et al.,* 2012; Nazir *et al*., 2009). Other GH family 7 EGIs produced by various fungi have been reported in literature. These were 60ºC for both *H. grisea* and *P. decumbens* (Takashima *et al.,* 1997; Xiao-Min *et al* 2010). EGI (Cel7B) was relatively stable for 96 hours at its optimum temperature, however, there was a 20% decrease in its residual activity between 24 - 48 hours (Figure 2.3C). Gao *et al.* (2008) found that *A. terreus* EGI (GH family 12) maintained 65% activity after incubation at 70ºC for 6 hours.

The results showed that EGII (Cel5A) was optimally active at 60ºC and DISPLAYED more than 45% activity between 20 - 70ºC (Figure 2.2D). This was in agreement with previous studies that had determined *T. reesei* EGII to be optimally active between 50 and 55ºC (Qin *et al.,* 2008; Samanta *et al.,* 2012). The optimum temperatures of EGIIs (GH family 5) produced by other fungi were 45ºC for *P. equi,* 60ºC for *Acidothermus cellulolyticus*, *P. decumbens and Fomitopsis pinicola*, 75ºC for *H. grisea,* and 80ºC for *T. maritima* (Eberhardt *et al.*, 2000; Mahadevan *et al*., 2008; Takashima *et al.,* 1997; Vlasenko *et al.*, 2010; Xiao-Min *et al*., 2010; Yoon *et al.,* 2008). The thermostability of EGII showed that it was stable for 96 hours at its optimum temperature; however, an unexpected 50% increase in activity was observed between 24 and 96 hours (Figure 2.3D). This may have been a result of extended incubation at a high temperature (96 hours at 60ºC), which may have led to a reduction in the volume of the enzyme solution, caused by evaporation. The thermostability profile of this cellulase was contradictory to that which was reported by Samanta *et al.* (2012) who had found the cellulase to lose activity after 40 min at 60ºC. Furthermore, Saloheimo *et al.* (1988) similarly showed the cellulase rapidly lost activity after 60 minutes at 50ºC.

BGL (Cel3A) exhibited maximum activity at 40ºC and rapidly lost activity (>65%) at higher temperatures of 60 and 70ºC (Figure 2.2E). This was in accordance with Gundllapalli *et al.* (2007) and Machida *et al.* (1988) who both determined BGL from *S. fibuligera* to display maximum activity at 40ºC and 50ºC, respectively. The optimum temperature was similar to the BGL (Cel3A) produced by *N. patriciarum* (Chen *et al.*, 2012); however, the temperature optimum was much lower than the BGL (Cel3A) produced by *T. reesei, T. aurantiacus, Aspergillus niger* and *T. emersonii,* which exhibited optimal activity at 70 - 72ºC (Chen *et al.,* 1992; Hong *et al.,* 2007; Murray *et al.,* 2004; Rashid and Siddqui, 1997; Yan *et al.,* 2012).

According to the thermostability assay, BGL was highly stable and maintained ~90% activity when incubated for 96 hours at its optimum temperature (Figure 2.3E).

pH optimum

The results showed that CBHI (Cel7A) displayed a pH optimum of 4.5 and displayed ≥50% activity between pH 4.0 - 6.5 (Figure 2.4A). There was a rapid loss in activity between pH 6.5 - 7.0 and the cellulase exhibited 0% activity at pH 7.0 - 8.0. This was in agreement to previous reports that determined that *T. emersonii* CBHI exhibits maximal activity between pH 3.6 and 5.0 (Grassick *et al.,* 2004; Tuohy *et al.,* 2002; Voutilainen *et al.,* 2010). The pH profiles of various fungal CBHs (GH family 7) have been characterised and displayed similar pH optima to *T. emersonii* CBHI. *T. reesei, A. thermophilum, Heterobasidion irregulare* and *C. thermophilum* displayed optimal activities ranging from pH 4.0 - 5.0, whereas *T. aurantiacus* exhibited a pH optimum of 5.5 (Boer and Kuivula, 2003; Hong *et al.,* 2003; Momeni *et al.,* 2013; Pingali *et al.,* 2011; Voutilainen *et al.*, 2008).

CBHII (Cel6A) displayed a pH optimum of 4.5 and displayed ≥60% activity between pH 4.5 and 7.0 (Figure 2.4B). This was in accordance with Bukhtojarov *et al.* (2004), who determined *C. lucknowense* CBHII to be optimally active between pH 4.5 and 5.5. Previous studies showed that CBHII (Cel6A) produced by *P. decumbens* and *M. grisea* exhibited similar pH optima (pH 4.5 - 5.0) to the CBHII (Cel6A) used in this study (Gao *et al.,* 2011; Takahashi *et al.,* 2010).

This study showed that EGI (Cel7B) displayed a pH optimum of 5.5 and displayed ≥ 80% activity between pH 5.0 and 6.5 (Figure 2.4C). At pH 7.0 - 7.5, more than 50% activity was displayed. To the best of our knowledge, no data has been published on the pH optima of *A. terreus* EGI belonging to GH family 5; however, there have been reports on the pH optimum of *A. terreus* EGI belonging to GH family 12. These pH optima ranged between pH 4.0 and 4.8 (Nazir *et al*., 2009; Narra *et al.,* 2012). EGIs (GH family 7) produced by *P. decumbens* and *T. reesei,* similarily displayed optimal activity at a pH of 4.0 and a pH of 5.0 - 5.5, respectively (Nakazawa *et al.,* 2008; Xiao-Min *et al.,* 2010).

EGII (Cel5A) was optimally active at pH 4.5 and displayed ≥60% activity between pH 4.0 and 6.5 (Figure 2.4D). However, a rapid decrease in activity was observed at a pH above 6.5 and no activity was observed at pH 7.5 - 8.0. This data was consistent with previous reports that determined *T. reesei* EGII (Cel5A) to be optimally active between pH 4.6 and 5.2 (Qin *et al*., 2008; Saloheimo *et al.,* 1988; Samanta *et al.,* 2012). EGIIs (Cel5a) produced by other fungi have been characterised with respect to their pH optima. The pH optimum was 5.0 for both *P. equi* and *T. maritima* and pH 4.0 for *P. decumbens* (Eberhardt *et al*., 2000; Mahadevan *et al*., 2008; Xiao-Min *et al*., 2010).

BGL (Cel3A) was active over a broad pH range and exhibited maximal activity at pH 5.5 (Figure 2.4E). BGL displayed ≥50% activity at pH 4.0 - 8.0. This was in accordance with Gundllapalli *et al.* (2007) and Machida *et al.* (1988) who showed BGL (Cel3A) from *S. fibuligera* to be optimally active at pH 5.0 and 5.5. This was also comparable to the pH optima exhibited by BGLs (Cel3A) produced by *T. aurantiacus, T. emersonii, A. niger* and *Paecilomyces thermophile,* which ranged between pH 4.0 and 6.0 (Hong *et al.,* 2007; Murray *et al.,* 2004; Rashid and Siddqui, 1997; Yan *et al.,* 2012).

Kinetic Parameters

The kinetic parameters for all five cellulases were analysed using double reciprocal Lineweaver-Burk plots and are listed in Table 2.3. CBHI (Cel7A) exhibited a K_M of 1.36 mg/mL, a V_{max} of 0.23 µmol/min, a k_{cat} of 23 min^{-1} and a k_{cat}/K_M of 16.9 $min^{-1}mg^{-1}$ mL, using Avicel as a substrate. The K_M was low, indicating that CBHI had a high affinity for Avicel. These kinetic parameters were lower than the reported values of Segato *et al.* (2012), who estimated the K_M, V_{max}, k_{cat} and k_{cat}/K_M to be 18.27 mg/mL, 24.81 µmol/min, 22.22 min^{-1} and 1.22 $min^{-1}mg^{-1}$ mL, respectively. The difference in results may be attributed to the fact that their enzymes were purified before kinetic analyses was performed, whereas the enzymes in this study were only partially purified.

Kinetic analysis on Avicel showed that CBHII (Cel6A) displayed a K_M (mM), V_{max} (µmol/min), k_{cat} (min^{-1}) and k_{cat}/K_M ($min^{-1}mM^{-1}$) of 3.3, 0.4, 40 and 12.12, respectively. The low K_M value indicated that CBHII has high affinity for Avicel. To the best of our knowledge, no data has been published on the kinetic parameters of CBHIIs, belonging to GH family 6, using Avicel as a substrate.

The K_M, V_{max}, k_{cat} and k_{cat}/K_M values of EGI (Cel7B) were 2.1 mg/mL, 149 µmol/min, 59600 min^{-1} and 28380 $min^{-1}mg^{-1}$ mL, respectively. The low K_M and high V_{max} values indicated that EGI had a high affinity towards CMC. The reported K_M value was lower than the K_M reported for *A. terreus* from GH family 12, whereas the estimated V_{max} value of *A. terreus* (GH family 12) was lower than what was reported in this study. The K_M and V_{max} values for *A. terreus* (GH family 12) were 12 mg/mL and 16.1 µmol/min, respectively (Narra *et al.*, 2012).

EGII (CEL5A) exhibited a K_M of 1.55 mg/mL, a V_{max} of 85 µmol/min, a k_{cat} of 34188 min^{-1} and a k_{cat}/K_M of 22792 $min^{-1}mg^{-1}$ mL for CMC. These results indicated that the EGII had a high affinity towards CMC, which was in accordance with Samanta *et al.* (2012). The K_M (2.1 mg/mL) reported in this study was similar to the findings of Samanta *et al*. (2012); however, the V_{max} value was determined to be lower to that reported in literature (220.57 µmol/min). The K_M (mg/mL) and V_{max} (µmol/min) of EGIs (Cel5a) produced by different fungal strains were 1.08 and 226 for *P. pinophilum*, 1.74 for 0.63 for *Daldinia eschscholzii* and 11.6 and 1250 for *F. pinicola*, respectively (Karnchanatat *et al.,* 2007; Yoon *et al.,* 2008).

The K_M (mM), V_{max} (µmol/min), k_{cat} (min^{-1}) and k_{cat}/K_M ($min^{-1}mM^{-1}$) obtained for *p*NPG by BGL (Cel3A) were estimated to be 1.46, 63.29, 63290 and 43349, respectively. To the best of our knowledge, no data has been reported on the kinetic parameters of BGL (Cel3A) from *S. fibuligera*. In comparison, the BGLs (Cel3A) from different fungal sources have been documented. *Stachybotrys* BGL exhibited a lower K_M value (0.27 mM) and a similar V_{max} (78 µmol/min) value to what was reported in this study, whereas *D. eschscholzii* displayed a similar K_M value (1.52 mM), but a lower V_{max} value (3.21 µmol/min) (Amouri and Gargouri, 2006; Karnchanatat *et al.,* 2007). Furthermore, *P. purpurogenum* exhibited a higher K_M (5.1 mM) and V_{max} (934 µmol/min) compared to the BGL used in this study (Jeya *et al.,* 2010).

2.6 Conclusions

In this study, five cellulases from different fungal sources were successfully characterised with respect to their molecular size, substrate specificities, optimum conditions required for maximal activity and their kinetic parameters. The molecular masses of the enzymes were confirmed and the results revealed that the expressed cellulases were larger than their expected theoretical sizes (Den Haan *et al.,* 2013; Qin *et al.,* 2008; Wei *et al.,* 2014). Substrate specificity studies showed that CBHs exhibited a substrate preference for the crystalline substrate, Avicel, whereas EGs exhibited substrate preference for the amorphous substrate, CMC. Furthermore, BGL had substrate preference for *p*NPG.

Similar results were observed from the temperature and pH optima data compared to that previously published. To the best of our knowledge, this was the first report on the temperature and pH optimum of *A. terreus* from GH family 7. The cellulases exhibited optimal activity at 60ºC, with the exception of BGL, which exhibited optimal activity at 40ºC. The pH optima were 4.5 for CBHI, CBHII, EGII and 5.5 for EGI and BGL. Furthermore, the enzymes were stable for 96 hours at their temperature optima, thus making them good candidates for industrial applications.

Kinetic characterisation showed that CBHs displayed high affinity for Avicel, whereas the EGs displayed high affinity for CMC and BGLs for *p*NPG. There was a difference difference in the results reported in this study, compared to that previously reported in literature, and may be attributed to the difference in experimental conditions. To the best of our knowledge, the kinetic parameters determined for *C. lucknowense* CBHII (Cel6A) on Avicel and the kinetic parameters of BGL (Cel3A) from *S. fibuligera* constitute novel data.

Chapter 3: Substrate characterisation, inhibition and adsorption studies

3.1 Introduction

The characteristics of a substrate, such as composition, DP and recalcitrance, is one of the major factors known to influence enzyme activity (Leu and Zhu, 2012; Yang *et al.,* 2011). To achieve efficient cellulose hydrolysis, it is important to understand the characteristics of a substrate, as this will provide useful insights into substrate-enzyme interactions (McMillan, 1994; Yang *et al.,* 2011). This study investigated the characteristics of three cellulosic substrates, namely steam exploded bagasse (SEB) (crop residue), paper sludge (PS) (municipal residue) and Avicel, a model micro-crystalline substrate (>90% glucan) which served as a reference substrate for this study (Esteghlalian *et al.,* 2002).

Sugarcane bagasse (SCB), the main residue obtained after sugarcane harvesting (Figure 3.1), has been the subject of countless bioconversion studies (Badsah *et al.,* 2012; Cardona *et al.,* 2010; De Albuquerque Wanderley *et al.*, 2013; Rocha *et al.*, 2011; Martín *et al*., 2008; Rabelo *et al*., 2011; Rivera *et al.*, 2010). Large quantities of sugarcane bagasse are produced annually throughout the world (8 billion dry tonnes in South Africa alone), however, only 50% of it is utilised as an energy source in sugar mills, and the remaining material is considered as waste (Botha and von Blottnitz, 2006; Cerqueira *et al.*, 2007; Leibbrandt *et al.*, 2011; Rabelo *et al*., 2011). It has been reported that its composition (dry weight) is composed of approximately 42% cellulose, 28% hemicellulose and 22% lignin (Quensanga and Picard, 1988). The large percentage of unutilised polysaccharide content in SCB makes it a well-suited candidate for bioconversion into value-added products.

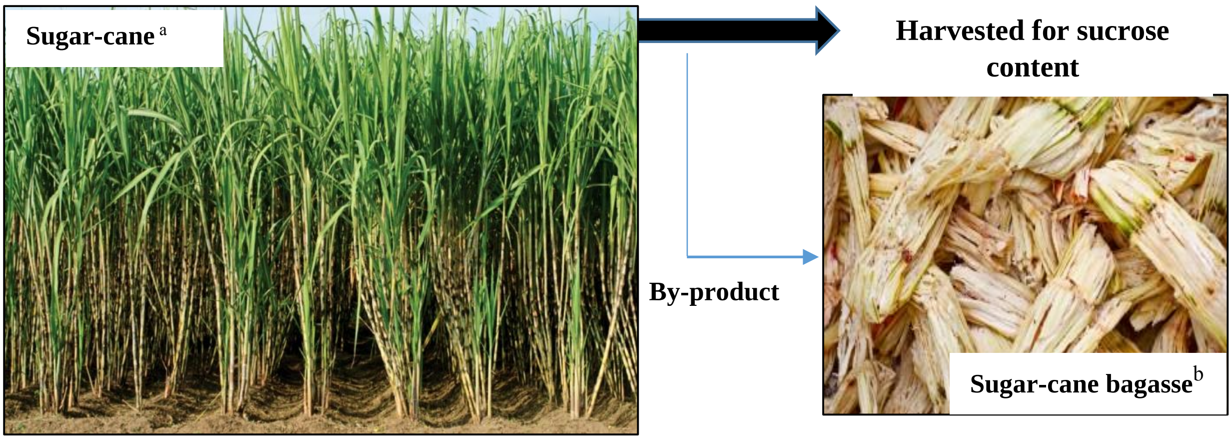

Figure 3.1. SCB, a potential feedstock for biofuel production, is the residue obtained from sugar cane harvesting (Adapted from Agrodaily, 2013[a]; Jadhav, 2014[b]).

In addition, paper sludge, the solid waste material from the paper industry (generated during wastewater treatment), has received significant attention in bioconversion studies (Pézsa and Ailer, 2011; Prasetyo, 2011). Globally, the paper industry produces approximately 40 - 50 kg of paper sludge for every tonne of paper produced, and it thus represents a major disposal problem to the paper industry (Fan *et al.,* 2003; Guerfali *et al.,* 2014; Yamashita *et al.,* 2010). Although some of the PS is recycled back into the mills, the majority of PS is incinerated or dumped into landfills, thereby contributing to current environmental concerns. Conversely, its high polysaccharide content, composed of approximately 34 - 50% cellulose and 12 - 15% hemicellulose, makes it an ideal candidate for bioethanol production (Kang *et al.,* 2010; Kim *et al.,* 2014; Marques *et al.,* 2008; Peng and Chen, 2011; Yamashita *et al.,* 2011). Figure 3.2 presents an overview of how paper sludge is generated.

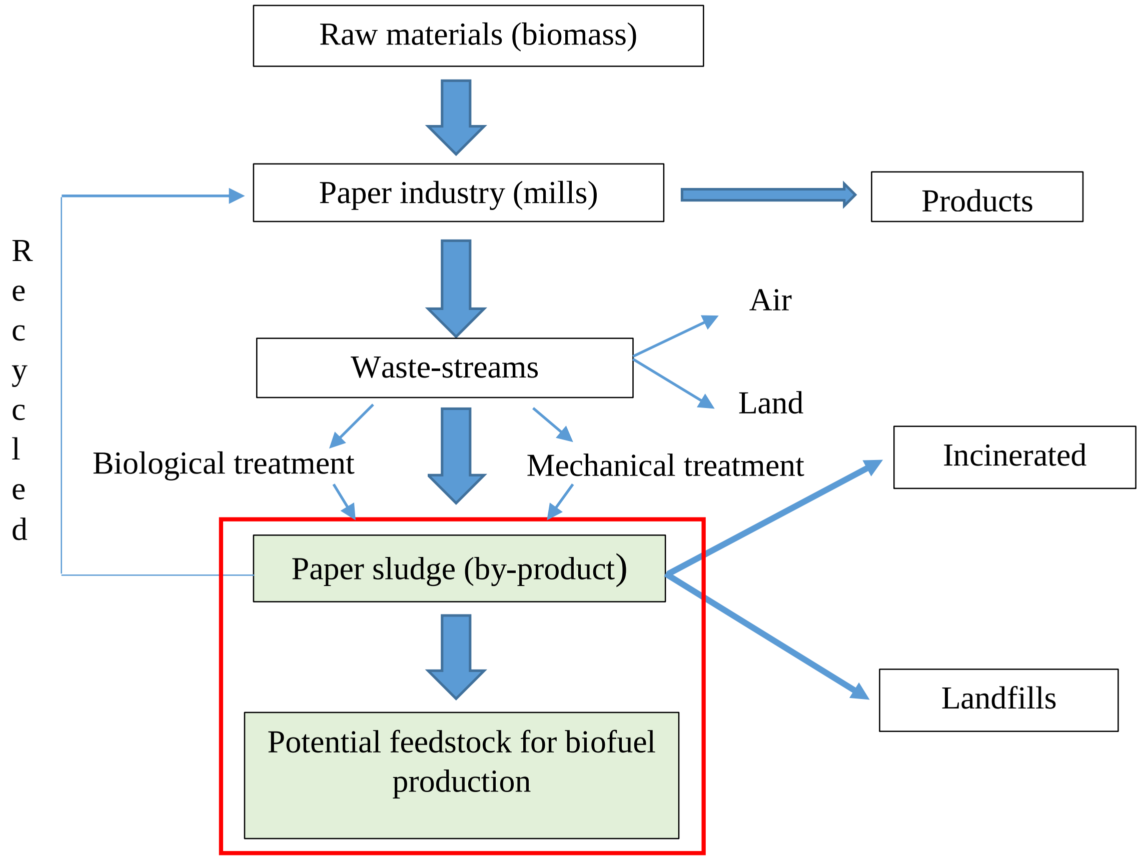

Figure 3.2. Schematic overview on the generation of paper sludge (Modified from Bayer *et al.*, 2007).

One of the major limiting factors to achieving efficient hydrolysis is overcoming substrate recalcitrance (Botha and von Blottnitz, 2006; Leibbrandt *et al.*, 2011; Pandey *et al.*, 2000). Thus, pre-treatment has been considered crucial for reducing biomass recalcitrance and improving cellulose accessibility (Chandra *et al.,* 2007; Himmel *et al.*, 2007; Van Dyk and Pletschke, 2012). One of the most widely used pre-treatment methods includes steam explosion, which is the process whereby a substrate is treated with hot steam (180 - 240ºC) under high pressure (1- 3.5 MPa). This is followed by a rapid drop in pressure, causing biomass separation (Karp *et al.,* 2013; McMillan, 1994; Ohgren *et al.,* 2007; Sun and Cheng, 2002). During the process, lignin is redistributed or partially removed from the biomass, however, numerous studies have found the lignin content to increase after steam explosion (De Albuquerque Wanderley *et al*., 2013; Pan *et al.,* 2005). Although the fundamental understanding behind this phenomenon is not understood, it has been proposed that this is caused by xylan degradation products, which produce insoluble pseudo-lignin (Sannigrahi *et al.,* 2011; Vivekanand *et al.,* 2014). It has been reported that SEB contains approximately 45% cellulose, 15% hemicellulose and 35 - 40% lignin (Martín *et al.*, 2008; Vivekanand *et al.,* 2014).

Although pre-treatment is an important cost driver for efficient cellulose degradation, the process may result in the formation of inhibitory compounds that could potentially hamper enzyme hydrolysis (García-Aparicio *et al.,* 2006; Kont *et al.,* 2013; Ximenes *et al.,* 2011). These inhibitory compounds include: i) sugars (oligomers); ii) phenolics (hydroxybenzoic acid, gallic acid and vanillin); iii) weak organic acids (acetic, succinic, levulinic and formic acids) and iv) furans (furfural and hydroxymethylfurfural) (Brodeur *et al.,* 2011; Hendriks and Zeeman, 2009; Xiemenes *et al.,* 2011; Zha *et al.,* 2014). An added concern relating to the inefficiency of substrate hydrolysis, is the non-productive binding of cellulases to lignin (Leu and Zhu, 2012; Liu and Zhu, 2013; Rahikainen *et al.*, 2013). While this interaction is yet to be fully elucidated, several researchers have proposed that this may be linked to the hydrophobic, electrostatic and hydrogen bonding interactions between the substrate and enzyme (Berlin *et al.,* 2006; Eriksson *et al.,* 2002; Moxley *et al.,* 2012; Nakagame *et al.*, 2011).

Since lignin is a rate-limiting factor in the efficient hydrolysis of cellulose, it is important to determine whether a substrate contains a high lignin content (Lee *et al.,* 2014; Zhao *et al.,* 2012). In addition to chemical compositional analysis, various techniques have been developed to determine the lignin distribution in various biomass substrates (Sant'Anna and de Souza, 2012). Histochemical assays, such as the Wiesner (phloroglucinol-HCL) and Mäule (potassium permanganate) methods are well established staining methods which allows for visualising the content and localisation of syringyl and guaiacyl lignin in a substrate (Trabucco *et al.,* 2013). In the presence of lignin, the dyes (phloroglucinol-HCL and potassium permanganate) react with aromatic aldehydes in lignin, causing an acid-catalysed condensation reaction (Figure 3.3), resulting in a colour change (Stange *et al.*, 2011). Phloroglucinol-HCl stains lignin a red-violet colour, whereas potassium permangenate stains angiosperm and gymnosperm lignin a brown and magenta colour, respectively (Dean, 1997; Trubucco *et al.*, 2013).

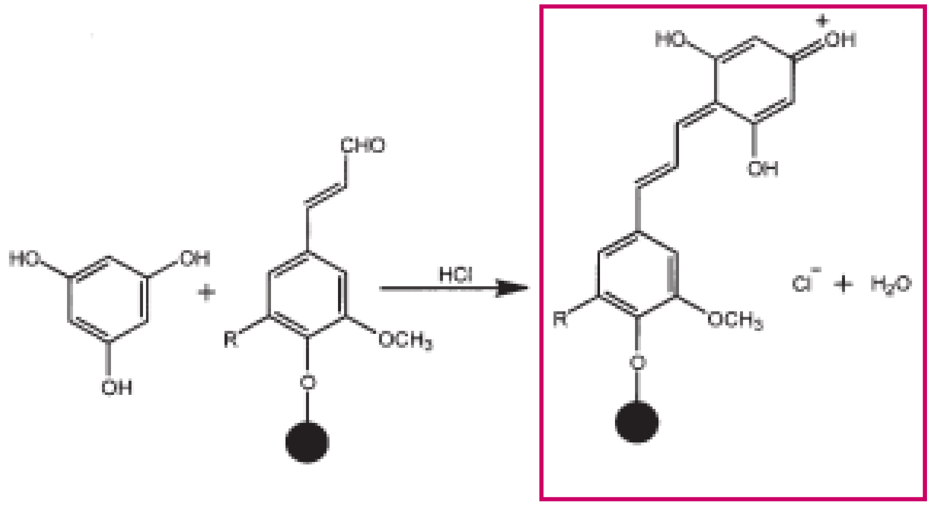

Figure 3.3. Proposed reaction of the Wiesner staining method. Phloroglucinol-HCL reacts with aromatic aldehydes that are present in the lignin, causing a colour change (Adapted from Pomar *et al.,* 2002).

The most crucial step in cellulose hydrolysis is the adsorption of cellulases to the substrate, and it has been reported that the presence of a CBM plays a crucial role in cellulase adsorption (Kim *et al.,* 2014). However, the adsorption characteristics of an enzyme is dependent on the structural characteristics of the substrate (accessibility to binding sites on the cellulose surface) (Zhang and Lynd, 2004). Du *et al.* (2012) reported that cellulases can remain bound to the cellulose surface or can be found free in solution, and that binding can be reversible or irreversible. The presence of lignin may cause unproductive binding of cellulases, which in turn affects the overall rate of cellulose hydrolysis. One of the simplest methods to assess how much protein has adsorbed to the substrate is to estimate the amount of dissolved protein by the Bradford method and enzyme activity assays (Kumar and Wyman, 2008).

It is important to understand the characteristics of a particular substrate as this could aid in unlocking fundamental information for elucidating substrate-enzyme interactions. By gaining an understanding of these interactions, optimal enzyme cocktails can be designed, which could ultimately make the current technologies more feasible (Leu and Zhu, 2012; Palonen *et al.,* 2004; Rahikainen *et al.,* 2013; Yang *et al.,* 2011).

3.2 Aims and Objectives

3.2.1 Aims

- To determine the characteristics of complex cellulosic substrates (Avicel, SEB and PS);
- To investigate the factors that affect substrate-enzyme interactions.

3.2.2 Objectives

- To determine the chemical composition of Avicel, SEB and PS, using HPLC and various sugar kits;
- To perform histochemical assays to identify the lignin content in each substrate;
- To investigate the inhibitory effects of compounds present in the substrates on enzyme activity;
- To investigate the adsorption/desorption patterns of cellulases to the different substrates by determining the protein content in the supernatant (Bradford assay) as well as assessing enzyme activity (DNS assay);
- To carry out SDS-PAGE.

3.3 Methods

3.3.1 Substrate preparation

Avicel was used as a reference substrate and SEB and PS were used as natural materials for representatives of agricultural and municipal residues, respectively (Refer to section 2.3.3). All substrates were prepared to a 2% (w/v) final concentration in sodium citrate buffer (pH 5.0; 0.05 M).

3.3.2 Substrate composition analysis

The natural substrates were characterized according to a modified sulphuric acid method by Sluiter *et al*. (2010), developed by the National Renewable Energy Laboratory (NREL, U.S.A). Substrate (300 mg) was hydrolysed with 72% (w/v) sulphuric acid (300 mg in 3 mL sulphuric acid) and incubated at 30ºC for 1 hour, with regular mixing. The samples were diluted with deionised water (74 mL) and then autoclaved for 1 hour. The resulting mixture was filtered to remove insoluble lignin. The solid fraction was dried at 50ºC for 48 hours and weighed to determine the amount of insoluble lignin, and the liquid fraction was analysed for monosaccharide sugars. D-sugar kits (Megazyme International, Bray, Ireland) were used to estimate the amount of monomeric sugars (glucose, galactose, xylose and mannose). The phenolic content was estimated using the Folin-Ciocalteu method and a Shimadzu HPLC, equipped with a Refractive Index Detector and Shodex column (8.0 mm ID x 300 mm L, SP-0810, Japan), was used to detect the presence of cellobiose and arabinose (Abboo *et al.*, 2014).

3.3.3 Light microscopy (Histochemical assays for lignin)

3.3.3.1 Mäule staining

Mäule staining was carried out by staining the substrates with 1% (w/v) potassium permanganate solution. After 5 minutes, the samples were rinsed with water until the potassium permanganate was no longer visible in the solution (Dean *et al*., 1997). The presence of lignin was visualized using an Olympus BX40 light microscope and the images were captured using an Olympus DP72 digital camera.

3.3.3.2 Wiesner staining

Wiesners staining was carried out by staining the substrates with phloroglucinol solution (2 volumes of 1% (w/v) phloroglucinol in 95% (v/v) ethanol) were mixed with 1 part 50% (v/v) HCl) (Dean, 1997; Tao *et al*., 2009). The samples were incubated at room temperature for 5 minutes prior to use. The presence of lignin was visualized using an Olympus BX40 light microscope and the images were captured using an Olympus DP72 digital camera.

3.3.4 Inhibition/activation studies

The inhibitory effects of by-products present in the substrates (SEB and PS) were tested by preparing the substrates in sodium citrate buffer (pH 5.0; 0.05 M). After 24 hours of mixing, the samples were centrifuged for 10 minutes (16 060 x *g*) and the supernatant (wash) was kept aside. Cellulase activity assays were performed as previously described in section 2.3.6, using their respective substrates that were diluted in the wash. Reactions set up included a positive control which contained the substrate without the enzyme; and enzyme controls, which contained only the enzyme without substrate.

3.3.5 Adsorption studies

The adsorption of CBHI, EGII and BGL (25 µg) to Avicel, SEB and PS was conducted at 50ºC and followed for 120 minutes in sodium citrate buffer (pH 5.0; 0.05 M). These three enzymes were chosen as representatives for each major cellulase class (E.C), based on their modes of action. Samples were prepared in separate assay tubes and were removed at various time intervals (10, 20, 30, 60, 90 and 120 minutes) and centrifuged for 5 minutes at 16 060 x *g*. The protein concentrations in the supernatant were measured as described previously (section 2.3.5). The amount of non-adsorbed protein was determined from the supernatant with activity assays described previously (section 2.3.6) and further assessed by running the samples on a

SDS-PAGE gel as described in section 2.3.7. Partially purified cellulase samples (positive control) were run in parallel with the supernatants from the binding assays.

3.4 Results

3.4.1 Chemical compositional analysis of natural substrates

The chemical composition of SEB and PS was determined using the sulphuric acid method as described in section 3.3.2. The composition of Avicel has been reported in literature and is said to be composed of >90% glucan. Table 3.1 showed that both the natural substrates had a high polysaccharide content. SEB was made up of 42% glucan, 7.2% xylan, 5.8% mannan and 2.3% arabinan, while PS was composed of 48% glucan, 2.7% xylan, 2.2% mannan and 3.9%. Both the substrates had a high lignin content – 41.2% and 40% in SEB and PS, repectively. Only small amounts of soluble lignin were detected in each substrate (1.2%).

Table 3.1. Compositional analysis of SEB and PS.

Content (%)	**Steam exploded bagasse**	**Paper sludge**
Glucan[a]	42	48
Xylan[a]	7.2	2.7
Mannan[a]	5.8	2.2
Galactan[a]	0	3.9
Arabinan[b]	2.3	0
Soluble phenolics[c]	1.2	1.2
Insoluble lignin and ash[d]	41.2	40

[a-]Megazyme sugar kits, [b-]HPLC, [c-]Folin-Ciocalteu method, [d-]Weighing balance. Data represent the mean values of triplicates (n=3; SD <10%)

3.4.2 Light microscopy (Histochemical assays for lignin)

The presence of syringyl and guaiacyl lignin in the three substrates were determined histochemically, as described in section 3.3.3. Figure 3.4 (A+D) showed that Avicel did not contain any lignin, since the observed staining was not a brown or magenta colour (which are indications of lignin by the Mäule and Wiesner methods, respectively). The Mäule method showed that SEB (Figure 3.4B) and PS (Figure 3.4C) had a high lignin content, as evident by the dark brown colouration observed for both substrates. The Wiesner method also indicated the high lignin content in SEB (Figure 3.4E) and PS (Figure 3.4F), apparent from the dark brown and red-violet colour observed in each substrate, respectively.

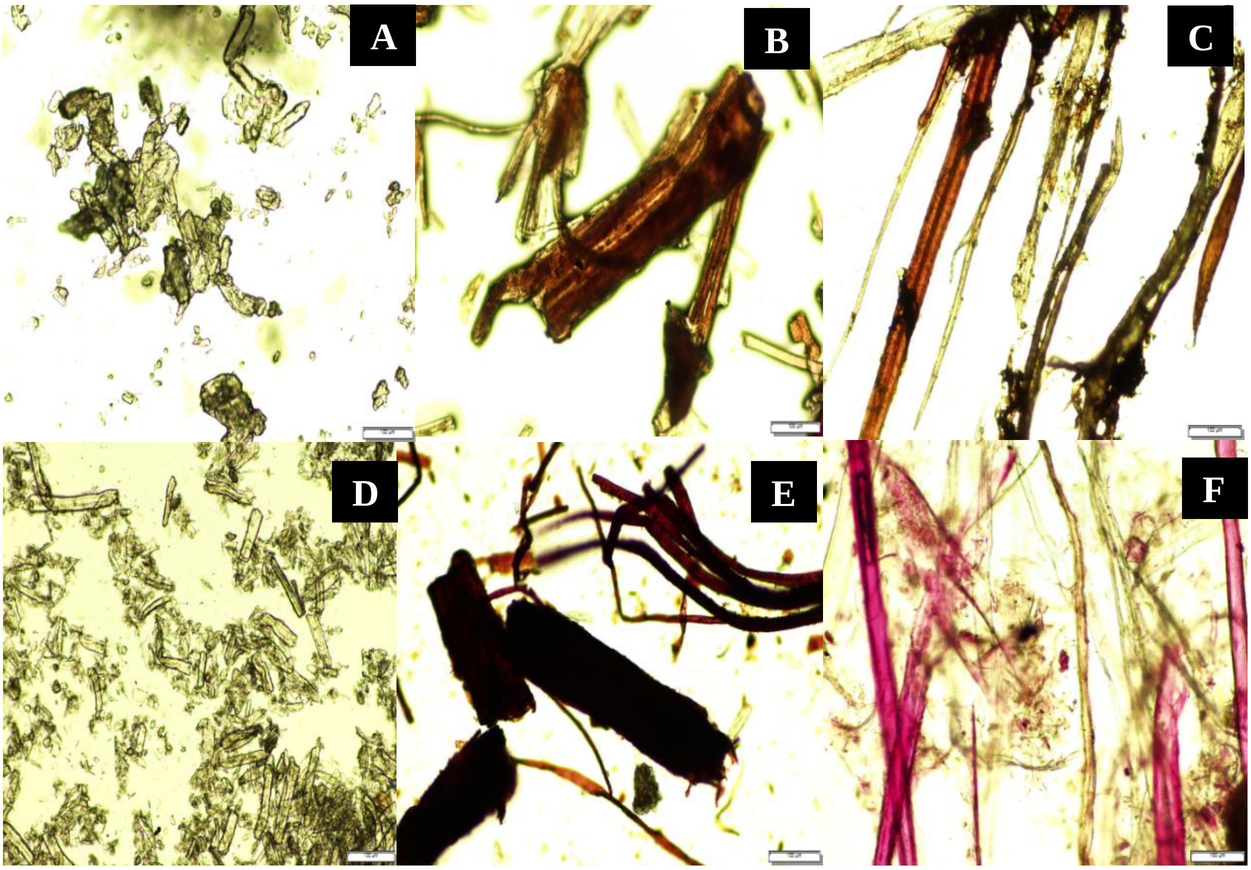

Figure 3.4. Histochemical analysis for syringyl and guaiacyl lignin in Avicel, SEB and PS. (A): Avicel; (B): SEB; (C): PS, after potassium permanganate staining (Mäule method) and (D): Avicel; (E): SEB; (F): PS, after phloroglucinol-HCl staining (Wiesner method). Scale bar: 100 µm; 10 x magnification.

3.4.3 The effect of by-products/chemicals from pre-treatment on cellulase activity

The effect of potential by-products in SEB and PS, on cellulase activities, were assessed (section 3.3.4). Inhibition from the SEB wash was observed for Avicel hydrolysis (Figure 3.5A). The activities of CBHI, CBHII and BGL were inhibited by 40, 20 and 80%, respectively. No inhibitory effects were observed for EGI and EGII; their activities were activated by 5 and 50%, respectively. Furthermore, the data in Figure 3.5B showed that no inhibition from the PS wash on Avicel hydrolysis took place. In fact, the activities of CBHI, CBHII, EGI, EGII and BGL were activated by 157, 158, 34, 72 and 17%, respectively. These results indicated that SEB and PS contained compounds and/or chemicals, which may have led to the inhibition and activation profiles of the cellulases.

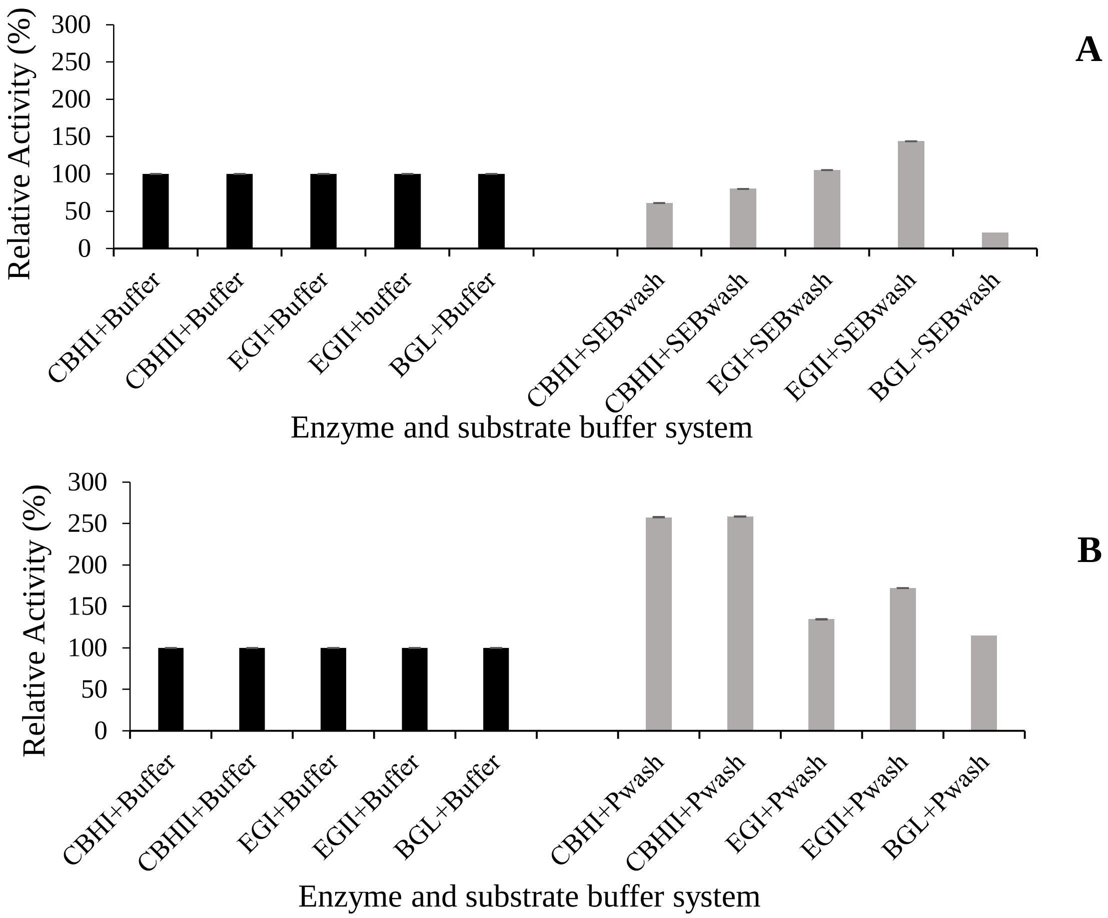

Figure 3.5. Effect of degradation products and chemicals present in SEB and PS on Avicel hydrolysis. Cellulase activities were measured in the presence of (A): SEB wash and (B): PS wash (Grey bars). Hydrolysis controls (100%) are represented by the black bars (enzyme activity assays on their respective substrates). Values are represented as mean values ± SD (n=3).

3.4.4 Binding assays

The adsorption profiles of CBHI, EGII and BGL were performed as described in section 3.3.5. Adsorption was rapid for all three substrates, with maximum adsorption taking place in the first 10 minutes (Figure 3.6). The cellulases completely bound to Avicel and remained adsorbed to the substrate during hydrolysis (Figure 3.6A), whereas the cellulases desorbed from SEB and PS throughout hydrolysis (Figure 3.6 B and C, respectively). Approximately 75% protein bound to SEB, whereas, for PS, only CBHI remained bound to the substrate. Approximately only 50% of EGII remained bound to PS, whereas BGL desorbed rapidly after 30 minutes, with 40% protein bound to the substrate after 120 minutes. Despite the low relative protein content of EGII observed from the Bradford assay, the activity assays on the supernatants showed the presence of EGII after adsorption. The results indicated that approximately 85% and 70% of EGII did not bind to Avicel and SEB, respectively. Another interesting observation made was the activated EGII activity (>40%) in the supernatant after adsorption to PS.

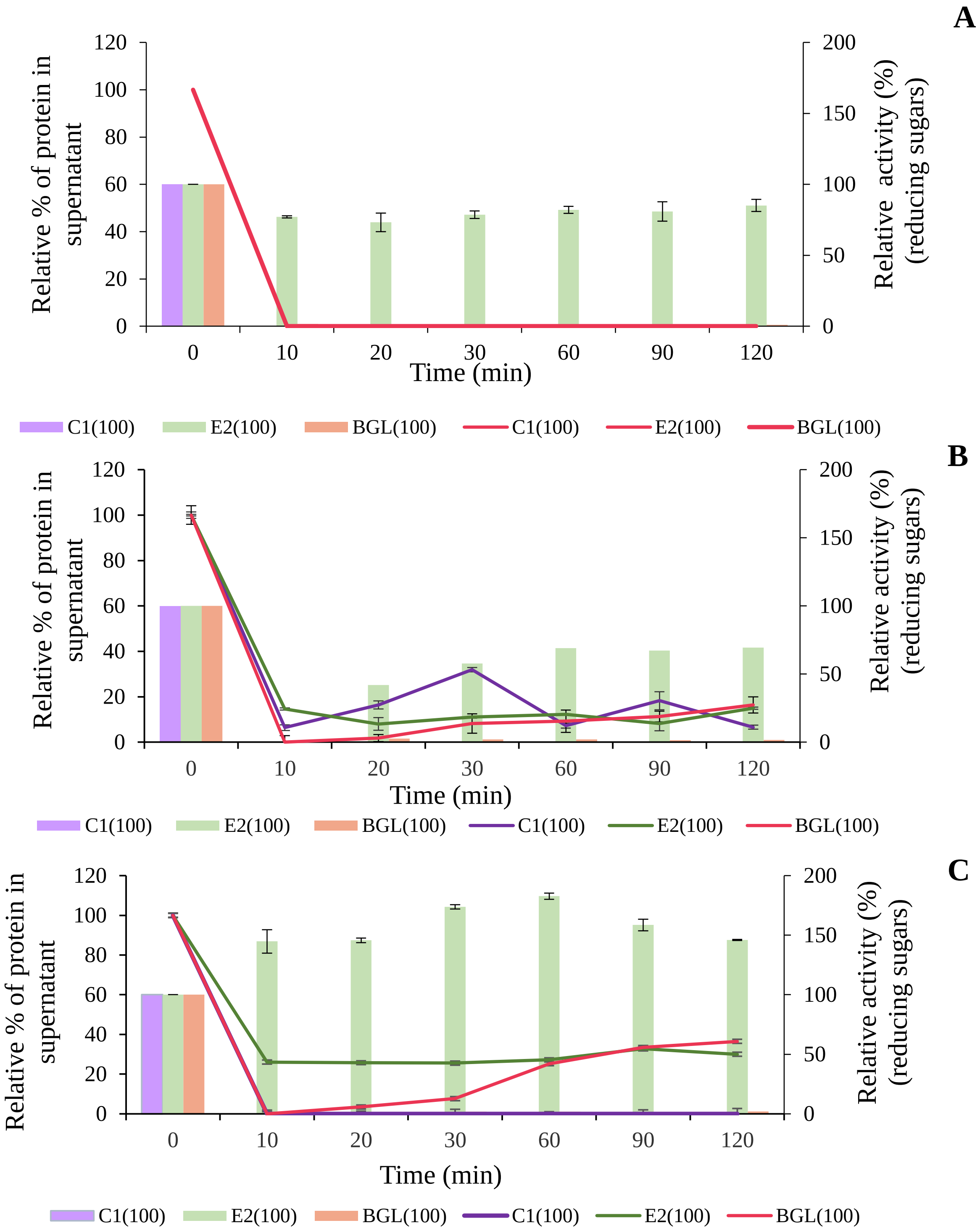

Figure 3.6. Cellulase adsorption profiles on complex substrates. Cellulase adsorption and activities were measured from the hydrolysis of (A): Avicel; (B): SEB and (C): PS. The lines represent cellulase adsorption and the bars represent cellulase activity in the supernatant (non-adsorbed protein). Values are represented as mean values ± SD (n=3).

3.4.5 SDS-PAGE analyses after 120 h

To further investigate the adsorption of the cellulases, SDS-PAGE was carried out on non-adsorbed cellulases present in the supernatants after adsorption studies for each substrate (Figure 3.7). As shown from the SDS-PAGE gel, the cellulases were not present in the supernatant fraction (lanes C; E and G). This was probably due to substrate binding which confirmed the adsorption profiles reported in section 3.4.4

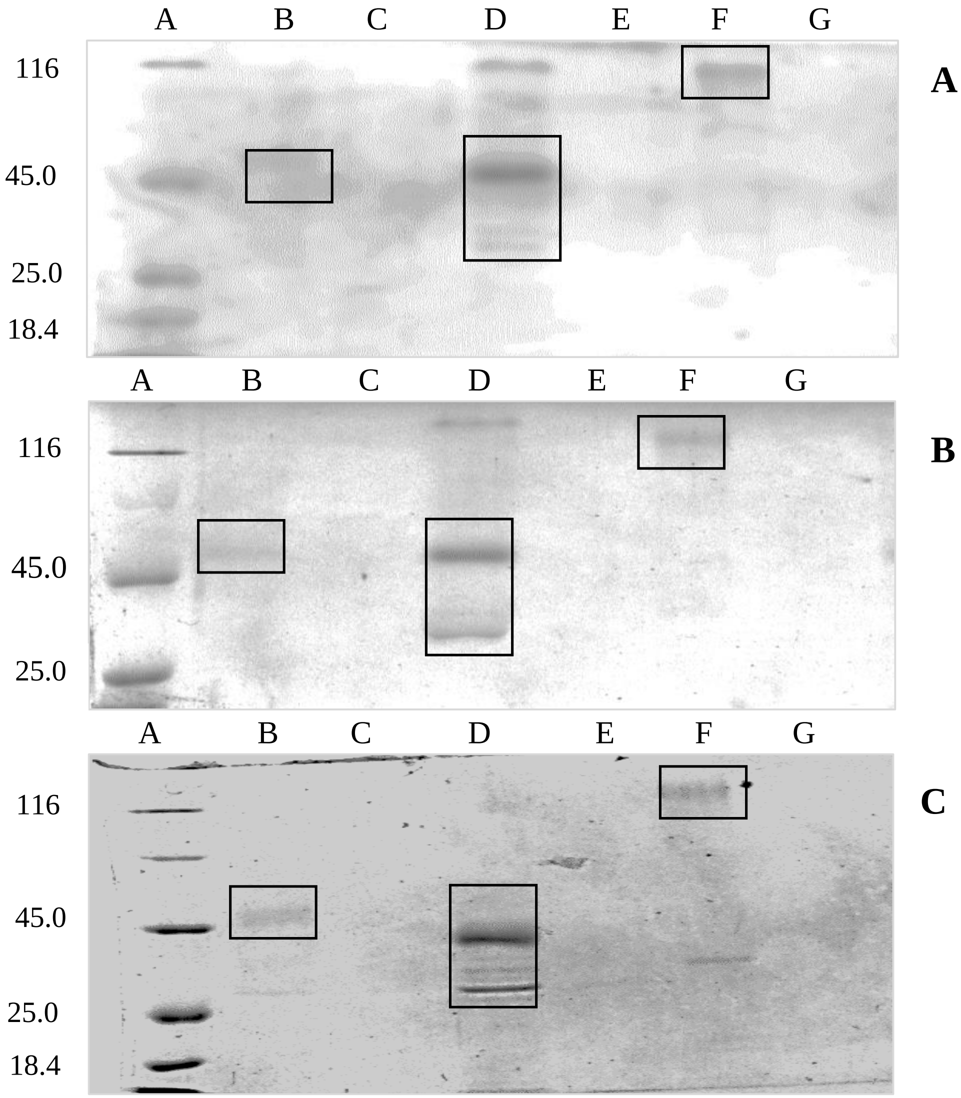

Figure 3.7. SDS-PAGE analyses of cellulases in the supernatant after hydrolysis of A: Avicel; B: SEB; C: PS after 120 h. 15 µl of each cellulase and 5 µl of prestained marker was loaded onto a 10% (w/v) SDS-PAGE gel and proteins were stained with Coomassie Blue. Lane (A): Prestained molecular marker; lane (B): CBHI; lane (C): CBHI in supernatant; lane (D): EG1; lane (E): EGI in supernatant; lane (F): BGL and lane (G): BGL in supernatant. Molecular masses (kDa) of marker proteins are shown on the left. Boxes represent positive controls, containing partially purified cellulase samples before hydrolysis.

3.5 Discussion

Lignocellulosic biomass has gained significant attention as a potential feedstock for biofuel production, due to its abundance and high sugar content (Cardona *et al.,* 2010; Wyman, 2007). However, the structural characteristics of a substrate plays a significant role in the efficiency of enzymatic hydrolysis (McMillan, 1994; Sun and Cheng, 2002). Thus, substrate characterisation proved crucial for providing insights for future experiments. In this study, a model substrate (Avicel) and two natural substrates (SEB and PS) were characterised.

Chemical composition of substrates

Results from literature have reported that Avicel contains a high polysaccharide content (>90% glucan) and no lignin (Esteghlalian *et al.,* 2002; Qing and Wyman, 2011).

SEB was composed of 42% glucan, 7.2% xylan, 5.8% mannan and 2.3% arabinan, 40% insoluble lignin and ash, and 1.2% soluble phenolics (Table 3.1). This was similar to the analysis carried out by Martín *et al.* (2008), who determined the composition of SEB to be 45% glucan, 12.9% xylan, 1.4% arabinan, 23.1% Klason lignin and 13.8% ash and other extractives. Vivekanand *et al.* (2014), similarly, found SEB to contain 38 - 41% glucan, 8.1 - 12.7% xylan, 0.2 - 0.7% arabinan, 0 - 0.1% galactan and 26.5 - 46% lignin. The polysaccharide content demonstrates the capacity of SEB to be converted into fermentable sugars, ultimately making it an attractive feedstock for biofuel production (Pandiyan *et al.,* 2014). However, it is important to note that SEB contained a high lignin content, which may cause unproductive enzyme binding onto the lignin surface.

PS displayed a similar composition to SEB, and was composed of 48% glucan, 2.7% xylan, 2.2% mannan and 3.9%, 41.2% lignin and ash, and 1.2% soluble phenolics (Table 3.1). These results were similar to the findings of Dobson (2013), who had determined PS to be composed of 34% cellulose, 14.26% hemicellulose and 32.72% lignin and ash. Furthermore, Kim *et al.* (2000) determined the cellulose, hemicellulose and lignin content of paper sludge to be 58, 12 and 20%, respectively. Cavka *et al.* (2013) alternatively found PS to contain a much higher glucan content (69.1 - 89.7%) and lower lignin and ash content (2.5 - 7.2%) than what was reported in this study. Although the PS in this study contained as much as 41.2% insoluble lignin and ash, its high polysaccharide content makes it a feasible substrate for bioconversion.

Light microscopy (Histochemical assays for lignin)

Lignin was not detected in Avicel after being stained with potassium permanganate (Mäule method) and phloroglucinol-HCL (Wiesner method) (Figure 3.4 A+D). Although a green-yellow stain was observed, it is important to note that it is not an indication of lignin, and may have been caused by the staining of polysaccharides.

The natural substrates showed the presence of lignin, which was evident from both staining methods (Figure 3.4 B+C+E+F). Both SEB (Figure 3.4B) and PS (Figure 3.4C) turned brown in colour after being stained with potassium permanganate, indicating the presence of guaiacyl (gymnosperm) lignin. After being stained with phloroglucinol-HCL, SEB turned dark brown in colour (Figure 3.4E), indicating the presence of highly lignified tissue (Trabucco *et al.*, 2013). PS turned a red-violet colour (Figure 3.4F) which indicated cell wall lignification at an early stage (Pomar *et al.*, 2002).

The effect of by-products/chemicals from SEB and PS treatment on cellulase activity

Figure 3.5A showed that the activities of CBHI, CBHII and BGL were inhibited by the SEB wash (supernatant) by 40, 20 and 80%, respectively, whereas the activities of EGI and EGII were activated by 5 and 50%, respectively (Grey bars). This was evident by comparison to their activities on their respective substrates, which served as the controls for this study (Black bars). According to Kont *et al.* (2013), inhibitory compounds are generated during pre-treatment which may hamper enzyme activity. A study conducted by Martín *et al.* (2002) found that steam explosion of sugarcane bagasse resulted in the formation of inhibitory by-products, including furfural, formic acid, acetic acid, levulinic acid and phenolic compounds. Similarly, steam exploded *Lespedeza* stalks and wheat straw also produced these inhibitory compounds (Feng *et al.*, 2006; Moreno *et al.*, 2013). Steam explosion of barley straw produced these inhibitory compounds, but the results indicated that sugars had a higher inhibitory effect than the degradation by-products (García-Aparicio *et al.,* 2006). The activation of the endoglucanases were unexpected. However, a study performed by Pecarovicova *et al.* (1989) showed that several phenolic compounds had activating effects on the cellulases from *T. reesei* QM 9414, whereas Panagiotou and Olsson (2007) similarly found that acetosyringone and guaiacol activated enzyme activity. Identification of the exact inhibitors present in the SEB wash was beyond the scope of this study and would require additional experimental procedures such as gas chromatography–mass spectrometry (GC-MS) and liquid chromatography-mass spectrometry (LC-MS) (Jönsson *et al.,* 2013; Martín *et al.,* 2002).

Figure 3.5B showed that no inhibition was exhibited by the PS wash on Avicel hydrolysis; however, the activities of CBHI, CBHII, EGI, EGII and BGL were activated by 157, 158, 34, 72 and 17%, respectively (Grey bars). Limited studies have been conducted on the effects of PS on enzyme activity; however, studies have reported that filler materials such as kaolin and calcium carbonate as well as ash may have inhibitory effects on cellulase activity (Kang *et al.,* 2010; Nikolov *et al.,* 2000). To the best of our knowledge, no studies have reported enzyme activation from PS on Avicel hydrolysis, however, Beukes *et al.* (2006) reported that sulphide and sulphite may have activating effects on enzyme activity. The waste-water streams in the paper and pulp industry contain large amounts of sulphur compounds, which may still be present in the sludge after biological and mechanical treatment (Paula and Foresti, 2009). Furthermore, Scott and Smith (1997) reported that phthalates, naphthalene, chloroform, wood derivatives (abietic acid and retene), phosphorous, nitrogen and calcium are present in sludge and thus we proposed that these compounds may also have caused enzyme activation. However, further analysis would be required, such as GC-MS or LC-MS to detect the exact compounds present in PS, followed by inhibition studies on those compounds (Jönsson *et al.,* 2013; Martín *et al.,* 2002). This would assist in identifying the compounds that activated enzyme activity.

Adsorption studies

Adsorpton of cellulases on a substrate is a prerequisite for hydrolysis (Zhang and Lynd, 2004). Figure 3.6A showed that CBHI, EGII and BGL rapidly adsorbed to Avicel and had completely bound to the substrate in the first 10 minutes and remained bound during the course of hydrolysis (line-graph). This was further confirmed by analysis of SDS-PAGE in Figure 3.7. Lanes C, E and G represented the supernatant fractions after protein adsorption studies (no protein detected on the gel). This was consistent with the finding of Kumar and Wyman (2009) who reported that cellulase adsorption to Avicel took place rapidly, and that maximum adsorption occurred in the first 10 minutes. Singh *et al.* (1991) and Steiner *et al.* (1988) also reported that cellulases rapidly bound to Avicel, with maximum adsorption occurring within the first 1 - 2 minutes.

Enzymes containing CBMs (such as the CBHI used in this study), are thought to enhance enzyme-substrate binding (Kim *et al.,* 2014), thus presenting a possible explanation for the rapid adsorption of CBHI to Avicel; however, EGII used in this study did not contain a CBM but still rapidly adsorbed to Avicel. This may further be linked to the availability of binding sites on its surface (accessibility of cellulose) (Hu *et al.,* 2015; Palonen *et al.,* 2004). From the histochemical analyses in Figure 3.4, it was observed that Avicel had no lignin or hemicellulose, thus the absence of these two components aided in rapid cellulase adsorption to Avicel. The ability of BGL to rapidly bind to Avicel was interesting, since BGLs are known to initiate their activities on cellobiose and binding to Avicel was not expected (Haven and Jørgensen, 2013). However, numerous studies have reported that BGL adsorbs to cellulose, but the reasons for this are unknown (Pareek *et al.,* 2013; Pribowo *et al.,* 2012; Várnai *et al.,* 2010). Although the results showed that EGII was bound to the substrate, activity assays performed on the supernatant after adsorption studies showed that it was found free in solution (bar-graphs). It was proposed that the Bradford assay and the Coomassie stain were not sensitive enough to detect proteins at low concentrations. More sensitive methods, such as the Lowry assay for protein estimation and silver staining to assess the amount of non-adsorbed proteins in the supernatant could be conducted in future assays.

Figure 3.6B showed that CBHI, EGII and BGL rapidly adsorbed to SEB and approximately 10% of protein remained unbound after 120 hours. This was further confirmed by SDS-PAGE analysis in Figure 3.7B, which showed that the supernatant fractions in lanes C, E and G contained no protein after adsorption studies. According to Haven and Jørgensen (2013), adsorption of cellulases to pre-treated substrates takes place at a rapid rate. However, the rapid adsorption may be linked to the presence of lignin. SEB in this study contained approximately 40% insoluble lignin and ash, which may have caused non-productive binding of the cellulases. It has been reported that non-productive binding of cellulases to lignin occurs through hydrophobic interactions, thus leading to lower hydrolysis rates (Haven and Jørgensen, 2013; Leu and Zhu, 2012; Liu and Zhu, 2013; Rahikainen *et al.,* 2013). It is therefore essential to differentiate between enzymes binding to cellulose or lignin-rich fractions, however, this was outside the scope of the study. Additional experiments could include lignin-rich fractions, to assess whether the enzymes bind to the lignin and to what extent. The addition of BSA would also be useful to block non-cellulosic surfaces, thus developing a better understanding of enzyme-substrate interactions (Arantes and Saddler, 2010). A more developed technique could include an ELISA-based method. This method is based on attaching an enzyme with antibodies that will allow for monitoring and quantifying each enzyme during the hydrolysis of a particular substrate (Pribowo *et al.*, 2012). EGII and BGL partially desorbed from the substrate and had reached equilibrium at 30 minutes, whereas CBHI partially desorbed from the substrate and then re-adsorbed onto the substrate throughout the course of hydrolysis. Den Haan *et al.* (2013) reported that desorption and re-adsorption takes place as result of enzymes attaching to available substrate binding sites, thus forming an enzyme-substrate complex. Once the sites have been hydrolysed, the enzyme detaches and desorption takes place. Desorption could also be attributable to enzymes competing for binding sites on the surface. Since SEB is more varied in composition than Avicel, the available surface for enzyme binding may have been limited (Palonen *et al.*, 2004). It would have been advantageous to do Simons' staining, which is a microscopic method used to visualise cellulosic surface accessibility, by staining cellulose yellow/orange (Hu *et al.*, 2015; Xiaochun *et al.*, 1995).

Figure 3.6C showed that CBHI, EGII and BGL rapidly adsorbed to PS within 10 minutes. After hydrolysis, CBHI remained bound to the substrate (possibly linked to the CBM), whereas approximately only 60% of BGL and EGII remained bound to the substrate. SDS-PAGE analysis in Figure 3.7C, showed that the supernatant fractions in lanes C, E and G contained no protein after adsorption studies. Although approximately 40% of BGL and EGII were found free in solution, these were not observable on the gel. This may be linked to the sensitivity of the Coomassie staining method, as it is unable to detect proteins at low concentrations. In addition to silver staining, the proteins could have been concentrated by methods such as acetone or ammonium sulphate precipitation to allow for better detection on the gel. Since PS contains a high percentage of lignin (41.2%), it was inconclusive whether adsorption was linked to the enzyme binding to the substrate or rather the non-productive binding to lignin (Haven and Jørgensen, 2013; Leu and Zhu, 2012; Liu and Zhu, 2013; Rahikainen *et al.*, 2013). The presence of a CBM may also enhance the non-productive binding of the enzyme onto lignin, due to its hydrophobic affinity (Guo *et al.* 2014). Furthermore, the enzyme assays on the supernatant after adsorption studies, further confirmed that CBHI had completely bound to the substrate. Activity by EGII in the supernatant after adsorption studies was exhibited, which was expected since 40% of protein remained free in solution. It is important to note though, that the activity of EGII was activated. This correlates well with the data in section 3.5B, which found that the presence of chemicals/by-products in PS may have had a positive effect on cellulase activity. Unexpectedly, no BGL activity was detected in the supernatant after adsorption studies (DNS assay), although 40% remained free in solution (Bradford assay). A possible explanation for this may be enzyme inactivation/denaturatiom. A study performed by Ye (2006) reported an overall loss in activity due to substrate - enzyme interactions, which caused the enzyme to become inactivated. According to Pribowo *et al* (2012), proteins become denatured due to irreversible adsorption to the interface.

25

3.6 Conclusions

In this study, three cellulosic substrates were successfully characterised with respect to their chemical composition, inhibition characteristics and adsorption/desorption profiles. The chemical composition analysis showed that both natural substrates contained a high polysaccharide content, making them good candidates for hydrolysis studies. The results also revealed that the natural substrates contained a large amount of lignin, which may be detrimental for efficient substrate hydrolysis (Leu and Zhu, 2012; Liu and Zhu, 2013; Rahikainen *et al.*, 2013).

It was observed that the SEB and PS washes had an effect on enzyme activity for Avicel hydrolysis. Inhibition of CBHI, CBHII and BGL took place in the presence of SEB, whereas the EGs were activated. Furthermore, all the enzymes activities were activated in the presence of the PS wash. The exact compounds present in the substrates could not be identified, as methods such as GC-MS and LC-MS would have been required (Jönsson *et al.*, 2013; Martín *et al.*, 2002). However, it is assumed that potential by-products such as phenolics, acids and furans from pre-treatment and compounds present in SEB and sulphur compounds in the PS may have caused these effects (Beukes and Pletschke, 2010; Kang *et al.*, 2010; Martín *et al.*, 2002). To the best of our knowledge, this is the first study that has found activating effects on cellulase activity from PS, thus presenting a novel finding.

This study provided an understanding of enzyme-substrate interactions. Adsorption studies showed that the cellulases rapidly bound to the substrates within 10 minutes, however, it was unclear whether it was due to the enzyme binding to the substrate or lignin. Further experiments such as including lignin-rich fractions or ELISA-based methods may aid towards a better understanding of enzyme adsorption.

It has been reported that the characteristics of a substrate may influence the activities of enzymes, which in turn, has an affect on the synergistic interactions established them. Thus, substrate characterisation in this study allowed for a better understanding of the factors that affect enzyme-substrate interactions, thus provided useful insights for synergy studies in Chapter 4.

Chapter 4: Enzyme synergy on complex substrates

4.1 Introduction

The conversion of cellulosic biomass into fermentable sugars is hindered by its recalcitrant structure (Bayer *et al.,* 1998; Limayem and Ricke, 2012; Zhao *et al.,* 2012). Consequently, multiple cellulases are required to act in synergy for complete cellulose degradation (Ganner *et al.,* 2012; Horn *et al.,* 2012). The concerted action of these enzymes significantly enhances bioconversion as opposed to when the enzymes are acting individually on a substrate (Boisset *et al.,* 2000; Converse and Optekar, 1993; Kostylev and Wilson, 2012; Väljamäe *et al.,* 1999; Van Dyk and Pletschke, 2012). Consequently, this phenomena has gained worldwide attention in research pertaining to the biofuel industry (Hall *et al.,* 2010; Horn *et al.,* 2012; Mohanram *et al.,* 2013; Yang *et al.,* 2011).

In efforts to obtain high degrees of synergy (DS) and enhanced cellulose hydrolysis, several researchers have strived to optimise cellulase cocktails (Boisset *et al.,* 2001; Den Haan *et al.,* 2013; Gusakov *et al.,* 2007; Kallioinen *et al.*, 2014; Meyer *et al.,* 2009; Mohanram *et al.*, 2013; Nidetzky *et al.,* 1994; Zhou *et al.,* 2009). Despite the extensive number of studies that have been reported in literature, large variations exist in the results obtained. Consequently, the exact mechanism by which these enzymes initiate their attack on a substrate and act synergistically is yet to be fully elucidated (Ganner *et al.,* 2012; Irwin *et al*., 1993; Jeoh *et al.,* 2006; Medve *et al*., 1994; Woodward *et al*., 1988). For that reason, further investigation into enzyme synergy is essential for gaining a deeper understanding of what takes place at a molecular level (Jalak *et al.,* 2012; Kostylev and Wilson, 2012; Lynd *et al.,* 2002; Yang *et al.,* 2011). In addition to cellulase synergy, studies have reported that cellulose degradation can be improved to an even greater extent by using a combination of cellulases and xylanases (Bura *et al.,* 2003; Choudhary *et al.,* 2014; García-Aparicio *et al.,* 2007; Hu *et al.,* 2011; Kumar and Wyman, 2009; Moraïs *et al.,* 2010; Selig *et al.,* 2008). This is based on the assumption that xylanases make the cellulose more accessible to the cellulases by removing xylan that may be covering the cellulose polymer (Kumar and Wyman, 2009; Hu *et al.,* 2011; Qing *et al.,* 2010; Zhang *et al.*, 2011). Although this chapter primarily focused on obtaining insights into the synergistic interactions between various cellulases, synergy between cellulases and a bacterial xylanase was included to determine whether this interaction could boost cellulose degradation.

Factors such as time and the characteristics of an enzyme and substrate are believed to be major contributors to enzyme synergy (Kostylev and Wilson, 2012; Van Dyk and Pletschke, 2012; Yang *et al.,* 2011). Therefore, this chapter explored the synergistic interactions of cellulases on various complex substrates, and investigated the effect of time on enzyme synergy. In an attempt to understand cellulase mechanisms, model substrates such as Avicel has been the substrate of choice of many researchers (Converse and Optekar, 1993; Woodward *et al*., 1988). Conversely, insufficient data has been published on the synergistic interactions between enzymes on natural cellulosic substrates. Therefore, by conducting synergy studies on Avicel, steam exploded bagasse and paper sludge, this study provided an interesting approach for comparing differences in the synergistic interactions of selected enzymes on a model substrate compared to more natural substrates. Furthermore, conflicting results have been reported on the effect of time on enzyme synergistic interactions, thus presenting a knowledge gap that requires further investigation

Since the recalcitrant structure of cellulose is the major technical and economical bottleneck in the conversion into fermentable sugars, enzyme synergy has become a key topic in current research pertaining to the biofuel industry. This chapter investigated the interactions between various enzymes on complex substrates to hopefully pave way for a better understanding into enzyme synergy.

4.2 Aims and Objectives

4.2.1 Aims

To develop a better understanding of enzyme interactions on complex cellulosic substrates, with a specific focus on how enzyme synergy is affected by different substrates. This was conducted by:

-Investigating the synergistic interactions between different combinations of endo and exo acting cellulases on the hydrolysis of a model substrate and two natural substrates;

-Investigating the synergistic interactions between an optimal cellulase cocktail and a bacterial xylanase for the hydrolysis of Avicel, SEB and PS.

4.2.2 Objectives

- To conduct simultaneous bi-synergy studies between various cellulase combinations on Avicel, SEB and PS and determine the optimal enzyme combinations required for the hydrolysis of each substrate;

- To investigate the effect of time on synergy for each substrate, using the optimal enzyme combination obtained from the bi-synergy studies;
- To observe structural changes in the substrates after enzyme hydrolysis by scanning electron microscopy (SEM);
- To conduct simultaneous tri-synergy studies between the optimal cellulase combination and a bacterial xylanase on each substrate.

4.3 Methodology

4.3.1 Enzyme preparation

The cellulases used in this study were described in section 2.3.1. A bacterial xylanase (a putative *Bacillus* species) was isolated and partially purified by Dr. A. Bhattacharya and kindly provided for this study. The enzymes were diluted in sodium citrate buffer (pH 5.0; 0.05 M) to a final concentration of 0.1 mg/mL.

4.3.2 Substrate preparation

Substrates were prepared as described in section 2.3.3.

4.3.3 Bi-synergy studies

Bi-synergy studies between the cellulases were conducted on Avicel, SEB and PS, by varying the protein ratios (0 - 100%) in the reaction mixture of the total protein concentration (25 µg) (Appendix 4A). The cellulases used in the experiments were based on the lowest protein concentration that released at least 0.2 mg/mL (quantifiable concentration using the DNS assay) of reducing sugars after 24 hours on Avicel hydrolysis. The assays were made up to a final volume of 400 µL with sodium citrate buffer (pH 5.0; 0.05 M). β-glucosidase was added at 10% total protein loading in all the reaction mixtures to avoid product inhibition. Assays were performed in triplicate at 50°C for 24 hours for Avicel hydrolysis and 72 hours for PS and SEB hydrolysis. After hydrolysis, the samples were centrifuged (16 060 x *g*) for 5 minutes and the supernatants were assayed for the release of reducing sugars, as described in section 2.3.7. The release of reducing sugars was expressed as mg/mL and the DS was calculated by dividing the activities of the combined enzymes by the theoretical sum of their individual activities.

4.3.4 Effect of time on enzyme synergy

The effect of time on enzyme synergy was investigated for the optimal binary enzyme combination established for the hydrolysis of each of the three substrates. The assays were made up to a final volume of 1200 µL with sodium citrate buffer (pH 5.0; 0.05 M) (Appendix 4B). β-glucosidase was added at 10% total protein loading in all the reaction mixtures to avoid product inhibition. Samples were taken at 24 hour intervals from the same reaction tube for a total of 120 hours and the amount of reducing sugars was measured as described in section 2.3.7.

4.3.5 SEM

Supramolecular structures of hydrolysed and un-hydrolysed substrates (control) were observed by SEM. Prior to analysis, the substrates were freeze-dried for 24 hours and added to a metal stub. Samples were coated with a thin layer of gold and observed using SEM (Vega© Tescan) at 2000 magnification (Cross, 2001).

4.3.6 Tri-synergy studies between cellulases and a xylanase

A xylanase was added at varying amounts (25, 50 and 75%) to a cellulase cocktail, while keeping the protein concentration in the reaction mixture constant (25 µg) (Appendix 4C). The ratio between cellulases required for optimal hydrolysis of each substrate was kept the same. The assays were made up to a final volume of 400 µL with sodium citrate buffer (pH 5.0; 0.05 M). β-glucosidase was added at 10% total protein loading in all the reaction mixtures to avoid product inhibition. Assays were performed in triplicate at 50°C for 24 hours for Avicel hydrolysis and 72 hours for PS and SEB hydrolysis. After hydrolysis, the samples were centrifuged (16 060 x *g*) for 5 minutes and the supernatants were assayed for the release of reducing sugars, as described in section 2.3.7.

4.4 Results

4.4.1. Bi-synergy studies

Synergy between CBHI, CBHII, EGI and EGII on the hydrolysis of Avicel, SEB and PS was determined as described in section 4.3.3.

4.4.1.1 Bi-synergy studies on Avicel hydrolysis

Figure 4.1 shows the synergistic interactions between (A) CBHI and CBHII (B) EGI and EGII (C) CBHI and EGI; (D) CBHI and EGII; (E) CBHII and EGI; (F) CBHII and EGII on the hydrolysis of Avicel after 24 hours. All combinations, except for the EGI: EGII combination enhanced Avicel hydrolysis as opposed to when the enzymes were used individually. Furthermore, synergy was observed between all combinations, except for the EGI: EGII and CBHII: EGII combinations. The general trend observed by all combinations was that hydrolysis was enhanced when the ratio of CBH to EG was higher in a reaction mixture. The highest quantity of reducing sugars of 0.88 mg/mL was produced by the enzyme combination 75% CBHI: 25% EGII, which exhibited a DS of 1.38 (Figure 4.1D). However, it was interesting to note that the combinations 50% CBHI: 50% CBHII (Figure 4.1A) and 75% CBHII: 25% EGI (Figure 4.1E) produced similar results of 0.83 mg/mL and 0.86 mg/mL in reducing sugars, respectively and exhibited a DS of 1.31 and 1.37, respectively. Thus, the optimal ratio required for Avicel hydrolysis was not conclusive.

4.4.1.2 Bi-synergy studies on SEB hydrolysis

Figure 4.2 shows the synergistic interactions between (A) CBHI and CBHII (B) EGI and EGII (C) CBHI and EGI; (D) CBHI and EGII; (E) CBHII and EGI; (F) CBHII and EGII on the hydrolysis of SEB after 72 hours. It was found that the only enzyme combination to considerably enhance SEB hydrolysis was the 75% CBHI: 25% EGI enzyme combination (Figure 4.2C). All the other combinations were found to only slightly enhance SEB hydrolysis or in some cases found to decrease hydrolysis. This optimal combination [CBHI (75): EGI (25)] liberated 0.75 mg/mL of reducing sugars and exhibited a DS of 1.07. This was an indication that the enzymes did not act synergistically on SEB. Similar to Avicel hydrolysis, a higher ratio of CBH to EG was required for SEB hydrolysis.

4.4.1.3 Bi-synergy studies on PS hydrolysis

Figure 4.3 shows the synergistic interactions between (A) CBHI and CBHII (B) EGI and EGII (C) CBHI and EGI; (D) CBHI and EGII; (E) CBHII and EGI; (F) CBHII and EGII during the hydrolysis of PS after 72 hours. It was found that only a few enzyme combinations resulted in the release of reducing sugars, whereby the 75% CBHI: 25% EGII combination produced the highest quantity of reducing sugars (0.49 mg/mL) (Figure 4.3D). This was the same enzyme combination that was optimal for Avicel hydrolysis. When the enzymes were used individually, even at 100% protein loading, they could not release sugars. Thus, the DS could not be determined, but the concerted action of enzymes enhanced PS hydrolysis to a large extent.

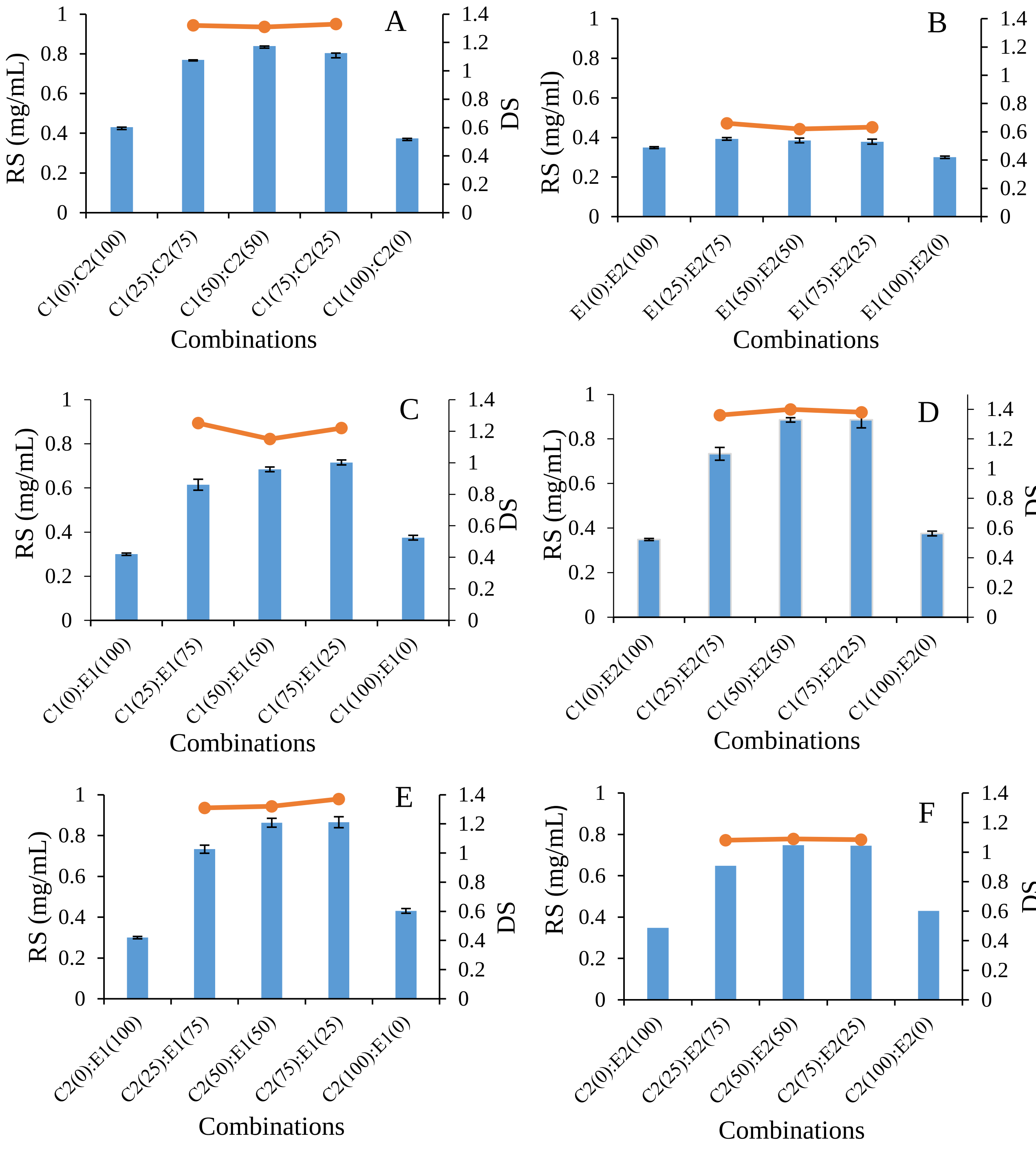

Figure 4.1. Synergy between various enzyme combinations in the hydrolysis of Avicel. (A): CBHI and CBHII; (B): EGI and EGII; (C): CBHI and EGI; (D): CBHI and EGII; (E): CBHII and EGI; (F): CBHII and EGII. Hydrolysis was carried out for 24 h at 50ºC. Bar graphs represent the release of reducing sugars (RS) and line graphs represent the DS. Data represent the mean values of triplicates (n=3).

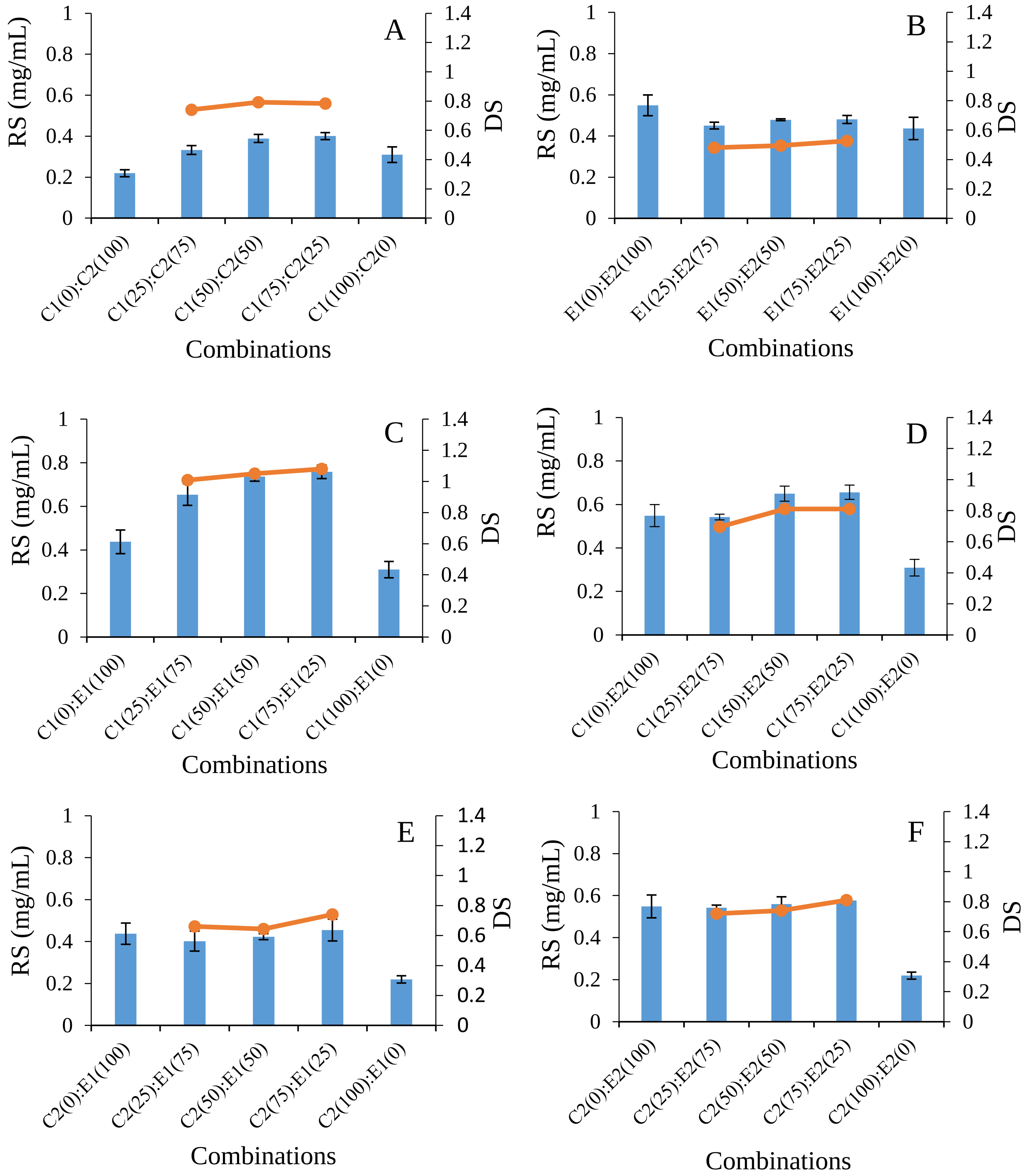

Figure 4.2. Synergy between various enzyme combinations in the hydrolysis of SEB. (A): CBHI and CBHII; (B): EGI and EGII; (C): CBHI and EGI; (D): CBHI and EGII; (E): CBHII and EGI; (F): CBHII and EGII. Hydrolysis was carried out for 72 h at 50°C. Bar graphs represent the release of reducing sugars (RS) and line graphs represent the DS. Data represent the mean values of triplicates (n=3).

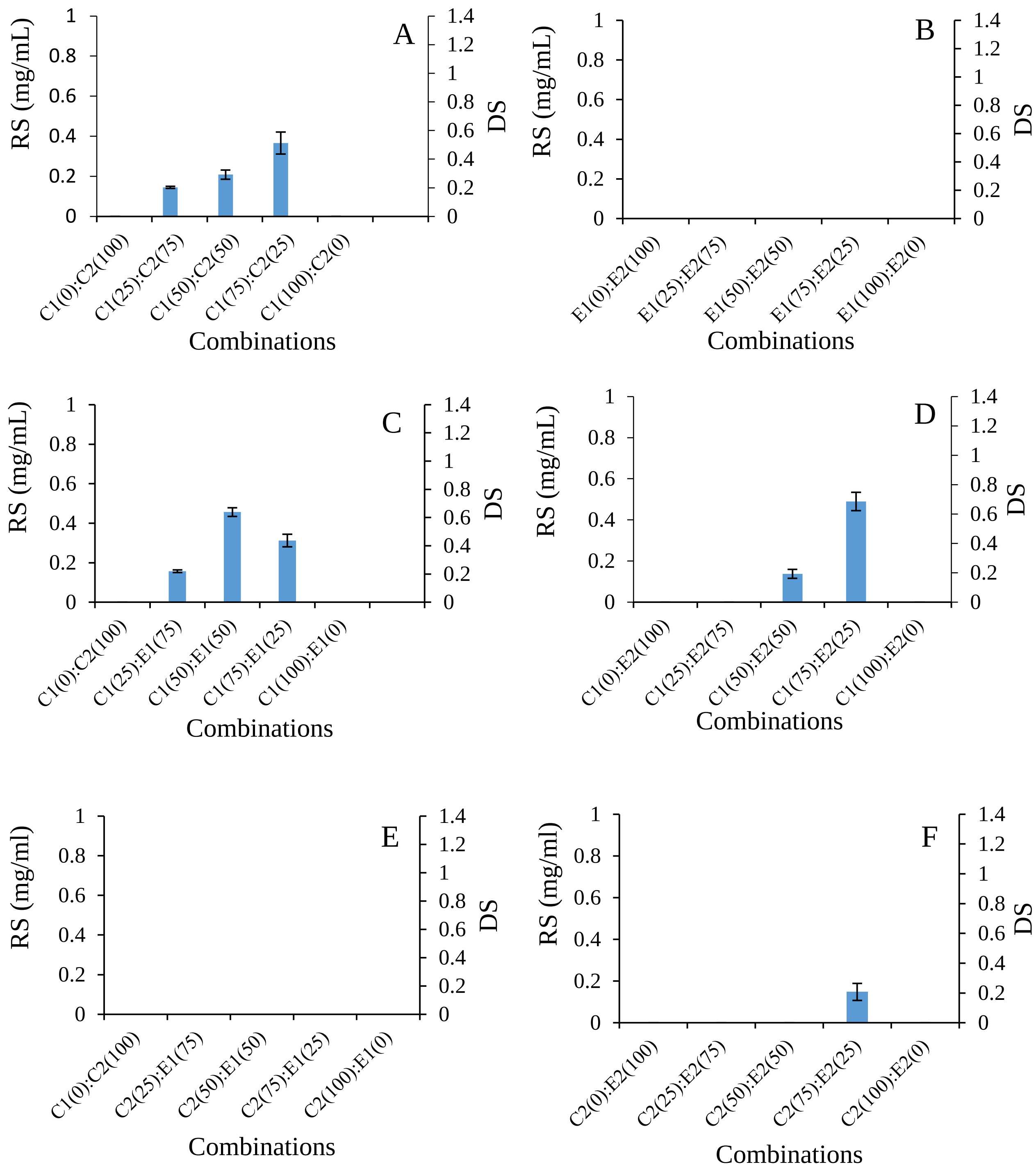

Figure 4.3. Synergy between various enzyme combinations in the hydrolysis of PS. (A): CBHI and CBHII; (B): EGI and EGII; (C): CBHI and EGI; (D): CBHI and EGII; (E): CBHII and EGI; (F): CBHII and EGII. Hydrolysis was carried out for 72 h at 50ºC. Bar graphs represent the release of reducing sugars (RS) and line graphs represent the DS. Data represent the mean values of triplicates (n=3).

4.4.2 Effect of time on enzyme synergy

Time course hydrolyses were conducted to further assess the synergistic interactions between the optimal binary enzyme combinations for each substrate (Figure 4.4). Synergy was determined as described in section 4.3.3 and 4.3.4.

4.4.2.1 Avicel Hydrolysis

Figure 4.4A shows that the amount of reducing sugars liberated by Avicel hydrolysis increased over time. After 120 hours, the liberation of reducing sugars for 100% EGII, 100% CBHI and 75% CBHI: 25% EGII were 0.95 mg/mL, 1.95 mg/mL and 2.2 mg/mL, respectively. Optimal synergy occurred at 24 hours (DS: 1.53) and decreased over time with a DS of 1.41 and 1.17 observed at 48 and 72 hours, respectively (data not shown). At 96 hours, a DS of 1 was observed whereas no synergy was observed at 120 hours. It was thus apparent that synergy was vital in the initial stages of Avicel hydrolysis.

4.4.2.2 SEB Hydrolysis

Figure 4.4B shows that the amount of reducing sugars released by SEB hydrolysis increased over time. After 120 hours, the release of reducing sugars for 100% EGI, 100% CBHI and 75% CBHI: 24% EGI were 0.81 mg/mL, 0.89 mg/mL and 1.83 mg/mL, respectively. At 24 hours, the DS was 1, but increased to 1.25 at 48 hours (data not shown). At 72 hours, the DS decreased to 1.15 and decreased again to 1.05 at 96 hours. However, at 120 hours, an increase in DS was observed and a DS of 1.28 was attained. It was thus apparent that the synergistic behaviour between the enzymes varied throughout the course of hydrolysis and their synergistic interactions were unpredictable. In this regard, no distinct synergistic trend was observed.

4.4.2.3 PS Hydrolysis

Figure 4.4C shows that the amount of reducing sugars released by PS increased over time. After 120 hours, 100% EGII, 100% CBHI and 75% CBHI: 25% EGII liberated 0.13 mg/mL, 0.43 mg/mL and 1.13 mg/mL of reducing sugars, respectively. High degrees of synergy (>2) were observed throughout hydrolysis (data not shown). The DS was lower at the initial stage of hydrolysis, with an observed DS of 2.15. The DS increased substantially to 4.52 at 48 hours and increased to 5.26 and 5.66 at 72 and 96 hours, respectively. A decrease in DS was observed at 120 hours, exhibiting a DS of 2.43. It was therefore apparent that synergy was lower at the beginning and end of hydrolysis, with optimal synergy occurring during the middle to later stages of hydrolysis.

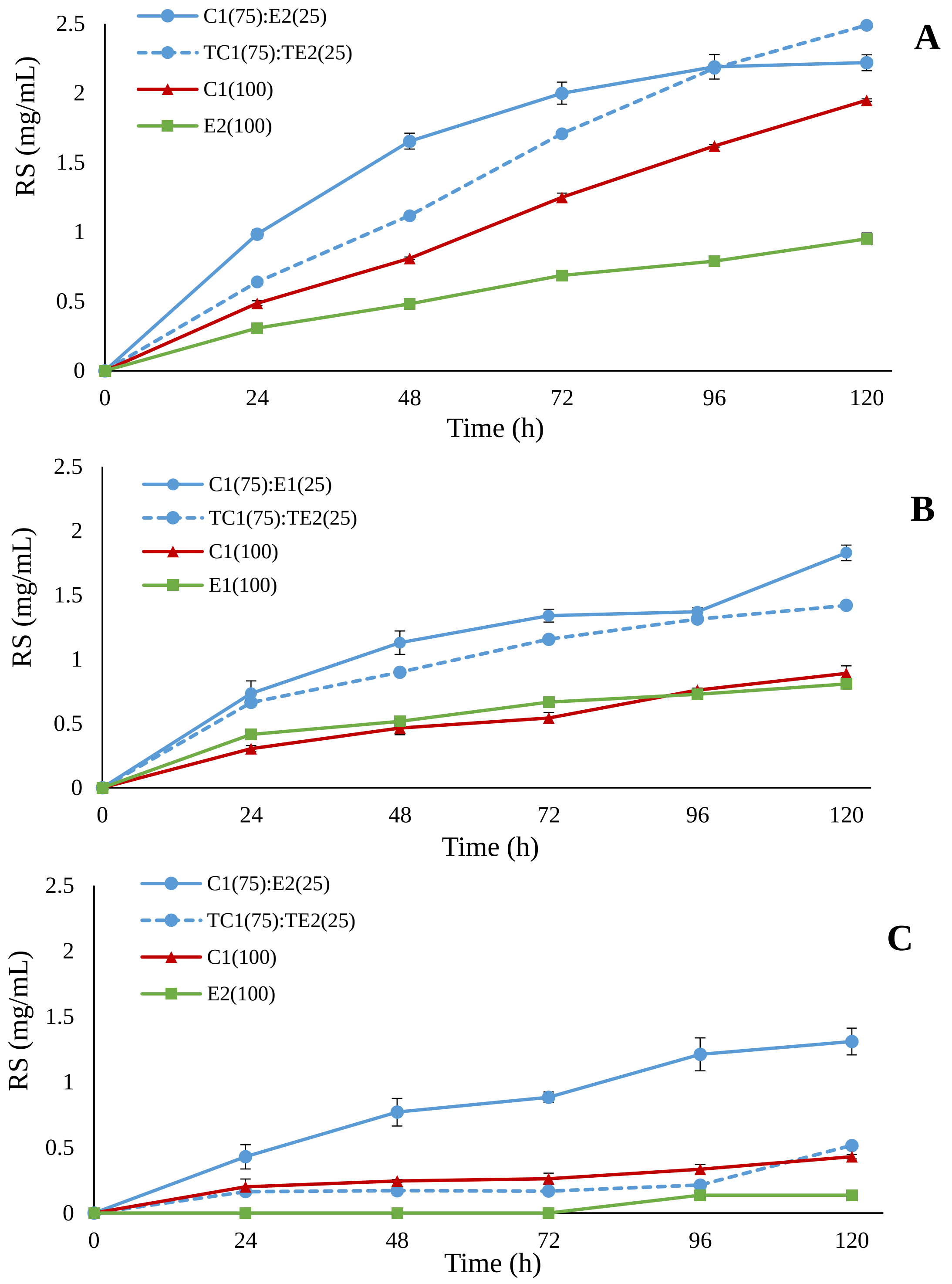

Figure 4.4. Synergy between cellulases in the time course hydrolysis of (A): Avicel; (B): SEB and (C): PS. Solid lines represent the release of reducing sugars (RS) by the binary cocktail and the dotted lines represent the theoretical sum of the reducing sugars (RS) liberated by each enzyme. Data represent the mean values of triplicates (n=3).

4.4.3 SEM analysis of hydrolysates

The hydrolysis samples from the temporal studies were visualised by SEM and compared to un-hydrolysed substrates (Figure 4.5). The SEM micrographs showed that the hydrolysed substrates had undergone structural changes. This was made evident by the less ordered (amorphous) fibres (right) opposed to the more ordered (crystalline) fibres (left) displayed by the un-hydrolysed substrates.

Un-hydrolysed substrates **Hydrolysed substrates**

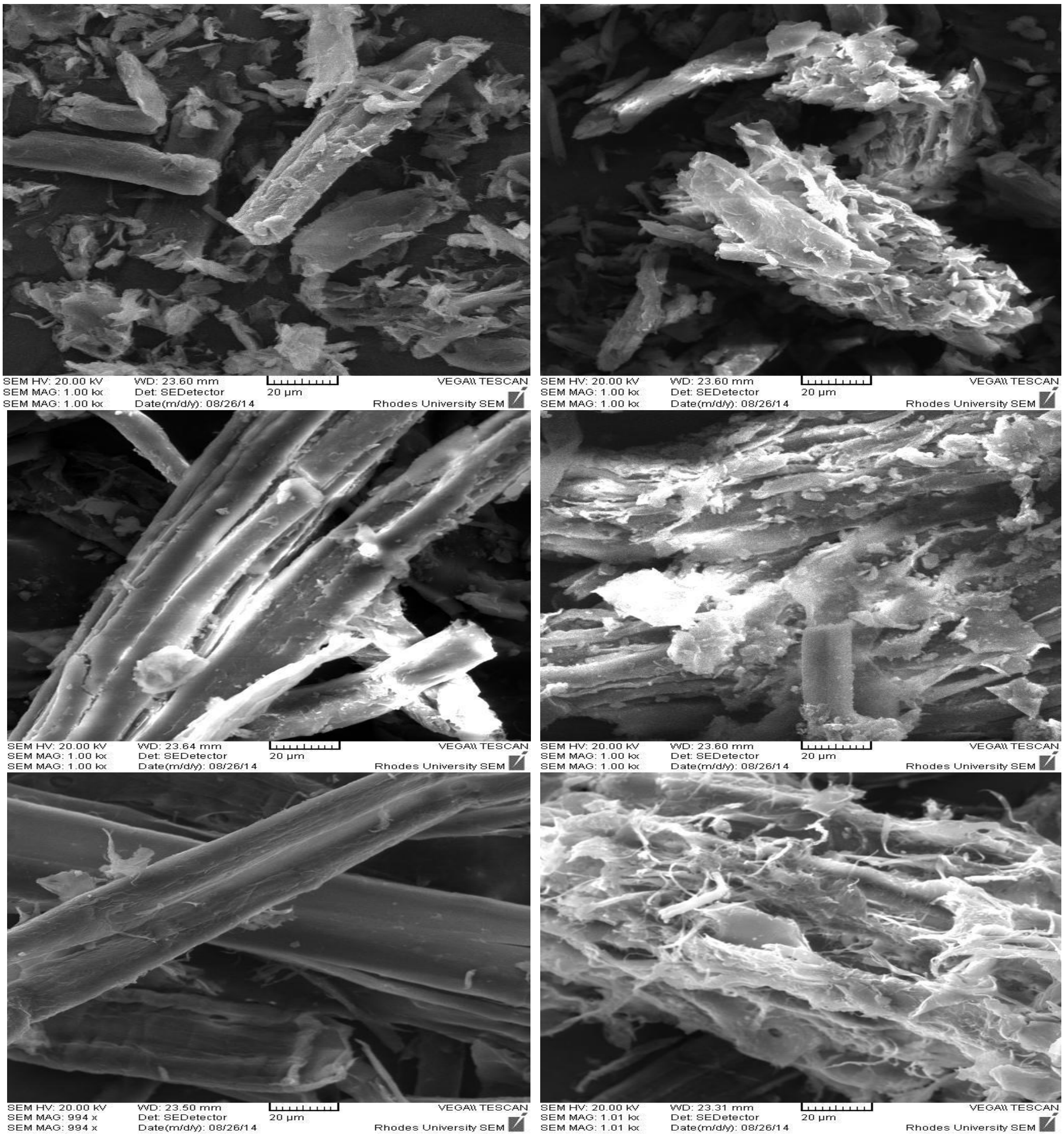

A

B

C

Figure 4.5. SEM images of (A): Avicel; (B): SEB; (C): PS before and after 120 h enzymatic hydrolysis. The images on the left represent the unhydrolysed samples and the images on the right represent the hydrolysed samples. Bars: 20 µm, 2000 magnification.

4.4.4 Tri-synergy studies between cellulases and a xylanase

Tri-synergy studies were performed between the optimal cellulase combination and a bacterial xylanase on the hydrolysis of all three substrates, to assess whether the addition of xylanase could further enhance cellulose degradation (Figure 4.6). Figure 4.6 indicates that the xylanase, even at low concentrations, did not enhance cellulose degradation and that the cocktail consisting of only cellulases [100% C: 0% X] liberated the highest quantity of reducing sugars for all three substrates. No synergy was exhibited for the hydrolysis of Avicel and SEB, however, a DS of 1.23 was observed on PS hydrolysis, when the ratio of xylanase to cellulase was low (25% to 75%, respectively).

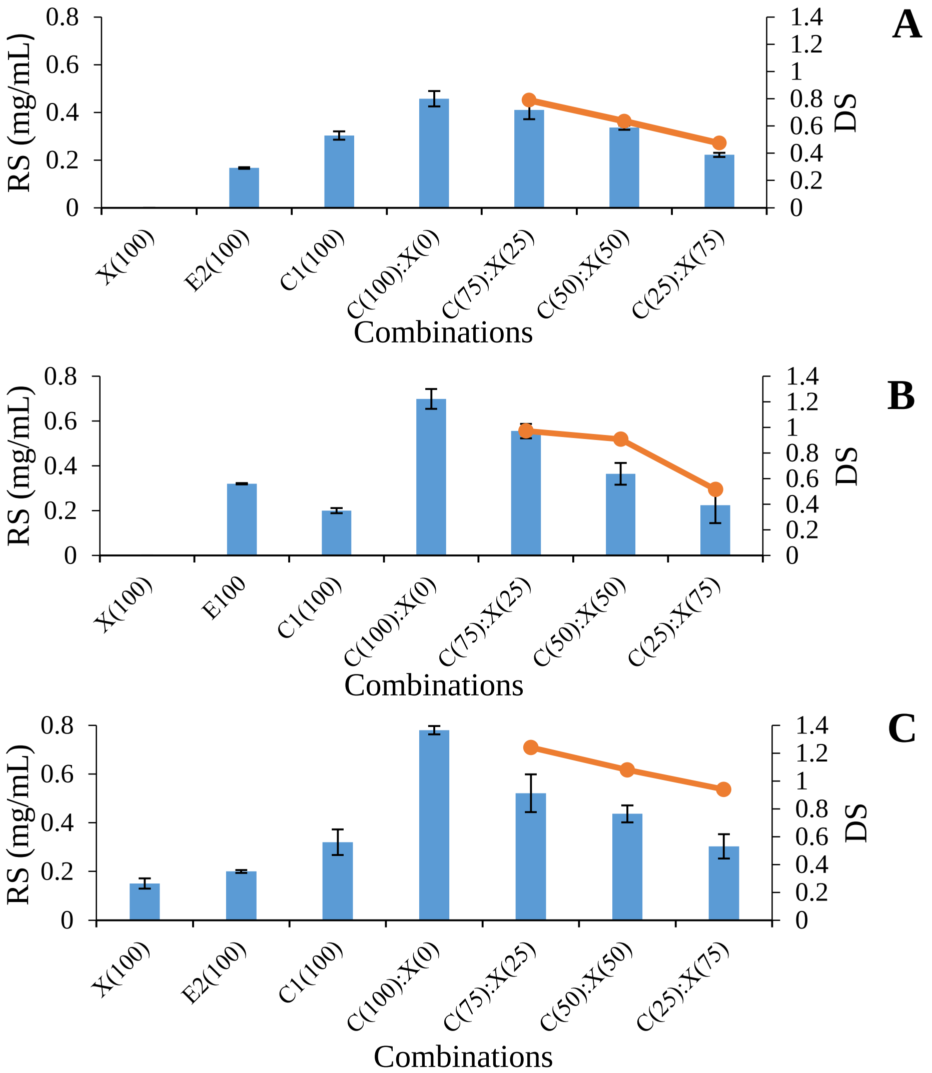

Figure 4.6. Synergy between an optimal cellulase cocktail and bacterial xylanase for the hydrolysis of (A): Avicel; (B): SEB and (C): PS Hydrolysis was carried out for 24 h for Avicel and 72 h for SEB and PS at 50ºC. Bar graphs represent the reducing sugars (RS) released and line graphs represent the DS. Data represent the mean values of triplicates (n=3).

4.5 Discussion

Bi-synergy studies

The efficient degradation of cellulose is a major bottleneck in biomass conversion (Bayer *et al.,* 1998; Kumar and Murthy, 2013; Zhao *et al.,* 2012). However, it has been well documented that the synergistic interactions of cellulases improves cellulose degradation (Den Haan *et al*., 2013; Ganner *et al.,* 2012; Henrissat *et al*., 1985; Ilmén *et al*., 2011; Nidetzky *et al*., 1994; Teeri, 1997; Tomme *et al*., 1990). This has led researchers to optimise cellulase cocktails with hopes of reducing costs for industrial applications (Balan, 2014; Mohanram *et al*., 2013; Pirota *et al.,* 2014). In this study the synergistic effects between various enzyme combinations were investigated for the degradation of complex cellulosic substrates.

Understanding enzyme interactions on cellulosic biomass has been difficult to elucidate due to the differences in biomass chemical compositions (Kostylev and Wilson, 2012; Zhang *et al.,* 2012). For the purpose of this study, Avicel was chosen as a reference substrate, as it is commercially available and represents a well-defined microcrystalline substrate (Vazana *et al*., 2013; Peciulyte *et al*., 2014). This provided a good comparison between enzyme synergy on model compared to natural substrates. Furthermore, it allowed for determining whether model substrates are still applicable when conducting enzyme synergy studies. The observed synergy between the cellulases during Avicel hydrolysis are shown in Figure 4.1. It was found that the enzyme combination 75% CBHI: 25% EGII released the highest quantity of reducing sugars of 0.88 mg/mL and exhibited a DS of 1.38 (Figure 4.1D). However, the combination of 75% CBHII: 25% EGI, similarly produced 0.86 mg/mL of reducing sugars and exhibited a DS of 1.37 (Figure 4.1E). Thus, the optimal enzyme cocktail required for Avicel hydrolysis was in-conclusive. The endo-exo synergism observed in this study was in agreement with Den Haan *et al.* (2013), who studied the synergistic interactions between the same recombinant cellulases used in this study. It was reported that EGII synergistically interacted with CBHI and CBHII, and that optimal synergy and enhanced hydrolysis was exhibited by the CBHI and EGII combination. Furthermore, endo-exo synergism has been reported by Henrissat *et al.* (1985); Phillips (2011) and Woodward *et al*. (1988), who determined the best enzyme combinations for Avicel hydrolysis to be 50% CBHI to 50% EGII; 97.4% CBHs to 2.6% EG and 67% CBHs to 33% EGII, respectively. We assumed that the concerted action of these enzymes enhanced hydrolysis because EGII induced the synergistic effect by providing accessible sites for the action of CBHI on Avicel (Beldman *et al.,* 1988; Ganner *et al.,* 2012; Henrissat *et al.,* 1985; Jalak *et al.,* 2012; Nidetzky *et al.,* 1994). This further agreed with the endo-exo synergism model proposed by Wood and Mcrae (1979). However, this model is an over-simplification of a complex process that still needs to be elucidated (Kostylev and Wilson, 2014). Different endo-exo synergy models have been proposed in literature, including the surface erosion model by Väljamäe *et al.* (1998), who hypothesised that the action of CBHI generates obstacles on a substrate that prevents it from exhibiting further activity; however, it makes the substrate more hydrolysable for EG. Furthermore, Igarashi *et al.* (2011) hypothesised that synergy takes place as a result of a "traffic jam effect". This model suggests that an enzyme can become "stuck" on the substrate, due to obstacles in the crystalline cellulose chain. However, the accumulation of blocked enzymes that are congested behind the obstructed enzyme enables it to overcome these obstacles. This facilitated action results in increased substrate hydrolysis. Ganner *et al.* (2012), on the contrary, suggested that synergism takes place via a "polishing" effect, whereby the amorphous material is degraded first by the EGs so to expose the hidden crystalline regions, which requires the activity of CBHI for its degradation.

An interesting observation was the synergistic interaction that occurred between the CBHs. A combination of 50% CBHI: 50% CBHII produced as much as 0.83 mg/mL of reducing sugars and exhibited a DS of 1.31 (Figure 4.1A). This phenomenon (exo-exo synergism) has been reported by Den Haan *et al*. (2013), Fägerstam and Pettersson. (1980), Henrissat *et al*. (1985), Ilmén *et al*. (2011), Nidetzky *et al*. (1994) and Tomme *et al*. (1990). According to this model, synergism takes place because the CBHs attack from either side of the cellulose chain (reducing and non-reducing ends) (Barr *et al.*, 1996; Nutt *et al.*, 1998; Wood and Mcrae, 1979). Furthermore, Den Haan *et al*. (2013) suggested that CBHII aids in opening up the substrate, therefore allowing CBHI to bind and degrade it. However, Ganner *et al.* (2012) proposed that CBHII does more than just attack from the non-reducing end. AFM revealed that CBHII exhibited EG activity, as it displayed activity on the amorphous regions. Thus, it polished the substrate, exposing crystalline sites for CBHI. However, the CBHII in this study showed no activity on CMC (Table 2.2), therefore our study did not agree with this model. The only combinations that did not exhibit synergy were the EGI: EGII combinations (DS<1) (Figure 4.1B). This is in agreement with Woodward *et al.* (1988), who suggested that the EGs compete with each other for the same binding sites on Avicel. Competition takes place as a result of enzymes having the same or overlapping functions, thus unable to enhance cellulose degradation (Van Dyk and Pletschke, 2012). Although similar results were demonstrated by the combinations 75% CBHI: 25% EGII; 75% CBHII: 25% EGI and 50% CBHI: 50% CBHII, a key observation made from these findings was that CBHs were the key enzymes required for efficient cellulose hydrolysis. In the endo-exo binary combination, a higher ratio of CBH to EG was required. This was consistent with Andersen *et al*. (2008); Den Haan *et al.* (2013); Hu *et al.* (2015) and Woodward *et al.* (1988). Den Haan *et al.* (2013) and Hu *et al.* (2015) reported that CBH could hydrolyse cellulose; however, when EG was added (in small quantities), it boosted the overall hydrolysis. Due to the discrepancies reported in literature and the observations made in this study, it was concluded that as long as one enzyme renders the substrate more accessible for the action of another enzyme, cellulose degradation may be enhanced by their concerted action. For the purpose of this study, the combination 75% CBHI and 25% EGII was selected for further investigation into enzyme synergy for Avicel hydrolysis.

The synergistic interactions on SEB hydrolysis are shown in Figure 4.2. It was found that the highest release of reducing sugars (0.75 mg/mL) was produced by the enzyme combination 75% CBHI: 25% EGI (Figure 4.2C). The quantity of reducing sugars was less than that produced by Avicel hydrolysis, which was an indication that SEB had a more complex structure than Avicel (as expected). Avicel is a defined micro-crystalline substrate, and it is assumed that it would have more accessible sites than SEB. The results from binding assays (Figure 3.3) also showed that the % of cellulase adsorption was lower for SEB than what it was for Avicel, which (in turn) would have an effect on the efficiency of cellulose hydrolysis. The high lignin content (40%) in SEB (in this study) may also have contributed to the lower hydrolysis rates, as it may have restricted the accessibility of the cellulases to the substrate. Hu *et al.* (2015) reported that the non-cellulosic components that remain in the substrate after pre-treatment have shown to hamper the efficiency of enzyme hydrolysis. With respect to the DS, this enzyme combination exhibited a DS of 1.07, which indicated that the enzymes did not act in a synergistic manner and could independently hydrolyse the substrate (Figure 4.3C) (Kostylev and Wilson *et al.,* 2012; Van Dyk and Pletschke, 2012). This may be related to substrate pre-treatment which reduces the degree of polymerisation (DP) (Karp *et al.,* 2013; Ramos, 2003). The degree of polymerisation describes the length of a cellulose polymer, based on the number of linked glucose molecules that make up a cellulose chain and when the DP decreases, cellulose becomes more recalcitrant (crystalline) (Bayer *et al.,* 1998; Festucci-Buselli *et al.,* 2007; Lynd *et al.,* 2002). Zhang and Lynd (2006) proposed a functional model whereby a lower DP results in a lower DS. A study by Väljamäe *et al.* (1999) confirmed this model and found that when bacterial cellulose was treated with acid, the DP decreased, resulting in lower endo-exo synergism. Based on these findings, we suggest that steam explosion reduced the DP of sugar cane bagasse, thus leading to the formation of accessible sites for the action of CBHI (crystalline cellulose). Consequently, the activity of EGI was no longer pivotal for CBHI activity, however, it still contributed to the overall degradation (Zhang and Lynd, 2006). With respect to the other combinations investigated, a DS of less than 1 was exhibited by all the combinations investigated (Figure 4.2A, B, D and E), indicating that the enzymes did not interact synergistically or that they competed for the same binding sites (Kostylev and Wilson, 2012; Van Dyk and Pletschke, 2012). The results also revealed that SEB hydrolysis was marginally enhanced by the combined cellulase activities, whereas in some occurrences, the core enzyme (100%) released the same or even more reducing sugars than the binary combinations. This phenomenon was reported by Väljamäe *et al.* (2001), who similarly found that a combination of CBH and EG yielded less activity, as opposed to when CBH was used independently. It was therefore proposed that the synergistic co-operation between the enzymes were inhibited by the substrate and could not hydrolyse the substrate efficiently, and by lowering the substrate to enzyme ratio, inhibition could be reduced (Väljamäe *et al.*, 2001). The presence of lignin may also have contributed to low hydrolysis rates. In Chapter 3, it was reported that SEB contained as much as 40% insoluble lignin and ash (Table 3.1). This may have led to non-productive binding of the cellulases to its surface, thus lowering substrate hydrolysis (Guo *et al.*, 2014; Mansfield *et al*., 1999). A further contributing factor may be a result of enzyme deactivation (Bansal *et al*., 2009). This phenomenon takes place when an enzyme becomes trapped on the substrate, ultimately preventing it from carrying out its function (Bansal *et al.*, 2009; Väljamäe *et al.*, 1998). Similar to Avicel hydrolysis, a higher ratio of CBH to EG (75%: 25%) was required for efficient SEB hydrolysis, confirming the importance of CBH as a key enzyme in cellulose degradation.

The synergistic interactions of cellulases on PS hydrolysis are shown in Figure 4.3. It was evident that PS was more recalcitrant than Avicel and SEB, since only a few enzyme combinations led to its hydrolysis. The combination 75% CBHI: 25% EGII produced the highest quantity of reducing sugars of 0.49 mg/mL, which further indicated that PS was more recalcitrant than Avicel and SEB, as it produced the lowest amount of reducing sugars compared to Avicel (0.88 mg/mL) and SEB (0.75 mg/mL). The results from the binding assays (Figure 3.3C) showed that the % adsorption was the lowest for PS, which suggested that the structure of PS contained less available sites for binding, which in turn may have had an affect on hydrolysis efficiency. The low enzyme activity may also be attributed to the high content of lignin (41%) in PS (Table 3.1). The DS could not be determined, since the enzymes were unable to hydrolyse PS independently (Figure 4.3D). It was therefore proposed that a strong synergistic association existed between the cellulases and that the hydrolysis of PS was only attainable by the concerted action of these enzymes. Furthermore, we suggest that the high composition of lignin (41%) (Table 3.1) may have restricted the activity of the cellulases, due to the unproductive binding of enzymes to its surface (Guo *et al.,* 2014; Mansfield *et al*., 1999).

Temporal studies

The effect of time was shown to play a significant role on the observed DS. This was carried out using the optimal enzyme combinations obtained from the binary studies for each substrate. Figure 4.4A showed that over time, the DS decreased with respect to Avicel hydrolysis. At the initial stages of hydrolysis (24 hours), the DS was 1.52, whereas at 120 hours, a DS of less than 1 was observed. This was in agreement with the model proposed by Warden *et al.* (2011), who determined the DS to be optimal during the initial stages of crystalline hydrolysis. The DS between Cel6B and Cel9A on bacterial microcrystalline cellulose (BMCC) hydrolysis also exhibited a high DS at the initial stages of hydrolysis (Jeoh *et al*., 2006). It was thus put forward that enzymes are required to co-operate more efficiently during the initial stages of hydrolysis to unravel the substrate. Both enzymes are required because the substrate is composed of both amorphous and crystalline cellulose. At the initial stages of hydrolysis, the EGs hydrolyse the amorphous cellulose at a rapid rate, providing sites for the CBHs; thus a high DS is observed. However, over time, the amorphous cellulose becomes fragmented into shorter fibers, resulting in more crystalline regions (Arantes *et al*., 2014). These regions are are no longer specific for the EGs, and require the activities of CBHs for its efficient hydrolysis. Ultimately, less co-operation between the enzymes takes place over time, resulting to a lower DS (Andersen *et al.,* 2008; Arantes *et al.,* 2014; Hu *et al.,* 2014).

The rate of hydrolysis for SEB (Figure 4.4B) was determined to be slower than Avicel hydrolysis (Figure 4.4A). This was likely due to their substrate compositions, which has a profound effect on the co-operativity between enzymes (as mentioned earlier) (Andersen, 2008). In turn, this would have a direct impact on the DS established between enzymes (Hu *et al.,* 2015). It was found that the DS varied throughout the course of SEB hydrolysis; however, it is important to consider that the DS established between enzymes on a model substrate and a natural substrate will not be the same at the same time, due to their substrate complexeties. At the beginning of hydrolysis, a DS of 1 was observed which increased to 1.25 at 48 hours. At 72 and 96 hours however, a decrease in synergy was observed, with DS reaching 1.15 and

1, respectively. A further increase in synergy was shown at 120 hours (DS: 1.28). This may have been a result of the substrate opening up in layers. According to Arantes *et al.* (2014), hydrolysis takes place in an “onion peeling” fashion, whereby the outer layer is “peeled” to expose a new surface layer (similarly containing the same morphology of crystalline and amorphous regions to that of the previous layer). We believe that pre-treatment decreased the DP of the substrate, making it more crystalline to begin with, and therefore a low degree of co-operativity was observed in the initial stages (requiring CBH). We further proposed that pre-treatment does not reach all the cellulose fibres and that cellulose fibres consisiting of amorphous and crystalline cellulose exist, even after pre-treatment. These layers (consisting of amorphous and crystalline regions) are exposed from enzymes “peeling” the substrate. The degree of co-operativity will be high in the initial stages of hydrolysis, due to the amorphous regions; however once the amorphous cellulose have been hydrolysed, the fibril is left with intact crystalline regions, which are more difficult to degrade (i.e. the DS will be lower). The enzymes will start degrading the next fibril in the same manner, resulting in a DS that will increase and decrease throughout hydrolysis.

The synergistic trend observed during the time course hydrolysis of PS (Figure 4.4C) showed that the DS was higher during the middle stages of hydrolysis (4.52; 5.25 and 5.66 for 48, 72 and 96 hours, respectively), whereas a DS of 2.15 and 2.53 was observed at 24 and 120 hours, respectively. Based on our findings, we propose that, at the initial stages of hydrolysis, the structure is more ordered (crystalline), which is more specific for the action of one enzyme (CBH in this study). Due to the limited accessibility to chain ends, a lower DS is observed. However, while the substrate unravels, sites that are specific for the other enzyme (EGI in this study) become more accessible during hydrolysis and thus the enzymes can facilitate the activities of each other for efficient cellulose degradation. This ultimately results in a high DS as hydrolysis progresses. Towards the end of hydrolysis, a lower degree of cooperation between the enzymes is required since the substrate is less ordered and more exposed, thus a low DS is observed. This proposed theory contradicts the hypothesis put forward for the synergistic pattern observed during Avicel hydrolysis. However, this was attributable to the characteristics of the substrates.

SEM analysis of hydrolysates

It has been reported that substrate structural modifications occur during the course of enzymatic hydrolysis (Jeoh *et al.,* 2013). SEM micrographs were observed to confirm the surface structural modifications that took place during the hydrolysis of Avicel, SEB and PS, after 120 hours. As seen in Figure 4.5, all the substrates had changed in their surface structural topology. The un-hydrolysed samples appeared to have highly ordered structures (smooth fibres), whereas the hydrolysed substrates had undergone modifications, as made evident by the less-ordered/amorphous structures (rough fibres). This demonstrated that the substrate became more fragmented by the concerted hydrolytic action of cellulases.

Tri-synergy studies with a xylanase

Numerous studies have reported that the addition of a xylanase to a cellulase cocktail leads to enhanced cellulose degradation (Bura *et al.,* 2003; Choudhary *et al.,* 2014; García-Aparicio *et al.,* 2007; Hu *et al.,* 2011; Kumar and Wyman, 2009; Moraïs *et al.,* 2010; Selig *et al.,* 2008). It is believed that xylanases make the cellulose more accessible to the cellulases by removing xylan that may be covering the cellulose polymer (Kumar and Wyman, 2009; Hu *et al.,* 2011; Qing *et al.,* 2010; Zhang *et al*., 2011). For this reason, we investigated the synergistic interactions between a cellulase cocktail and a xylanase to determine whether cellulose degradation could be enhanced.

Figure 4.6A showed that the cellulases and xylanase could not interact synergistically on Avicel and that a cellulose: xylanase cocktail did not enhance degradation. Furthermore, the higher ratio of xylanase to cellulases in a reaction mixture resulted in a decrease in the reducing sugars released. This was expected, since Avicel is a model microcrystalline substrate, containing no xylan, and therefore only requires the activities of cellulases for its complete degradation (Vazana *et al*., 2013; Peciulyte *et al*., 2014).

Figure 4.6B shows that a synergistic interaction between the cellulases and a xylanase could not be established and that the addition of a xylanase did not enhance cellulose degradation. The binary combination [C(100): X(0)] which consisted of CBHI 75% and EG1 25% was still the best combination for efficient SEB hydrolysis. However, the findings of Zhang and Viikari (2014) reported that the addition of a xylanase led to enhanced hydrolysis of steam pretreated corn stover. However, it was found that the severity of the pre-treatment had a direct effect on the results obtained. At a higher severity (42% cellulose and 2% xylan), a lower DS (with respect to glucose formation) was observed between the cellulase and xylanase, whereas at a lower severity (44.8% cellulose and 4.8% xylanase), the DS (with respect to glucose formation) between the cellulases and xylanase increased. It was reported that at a higher cellulose: xylanase ratio, less xylan coated the cellulose microfibrils, which led to lower synergism. In this study, SEB contained 7.2% xylan (Table 3.1), which was higher than what was reported by Zhang and Viikari (2014). Although they reported that a substrate with a higher xylan content results in a higher DS, we propose that this would be dependent on the 3D structure (whether or not xylan forms a coat over cellulose), rather than the xylan composition of a substrate. If the xylan and cellulose are not intertwined, the cellulases would not require the activity of xylanases.

Figure 4.6C demonstrates that a cocktail consisting of only cellulases released the highest quantity of reducing sugars and that PS hydrolysis was not enhanced by the addition of a xylanase. Suprisingly, a DS of 1.24 was observed when the cellulase to xylanase ratio was 25% to 75%, although the hydrolysis was not improved. The observations made in this study were also contradictory to what has been reported previously where it was found that a xylanase boosted cellulose hydrolysis. It is therefore suggested that the small percentage of xylan (2.7%) present in PS did not interfere with cellulose hydrolysis.

4.6 Conclusions

In this study, the synergistic interactions between enzymes on complex substrates were extensively studied. The optimal binary combinations for the hydrolysis of Avicel, SEB and PS were established and it was found that CBHI was the key enzyme required for cellulose degradation. The ratio of CBH to EG (75:25) was optimal for all three substrates, indicating that, irrespective of the substrate, a higher ratio of CBH to EG was required for cellulose degradation. The patterns of synergism varied between substrates. This was proposed to be due to their different substrate compositions. SEM micrographs showed that the hydrolytic activities of the enzymes caused morphological changes on the substrate surface. This study also demonstrated that the addition of a xylanase could not enhance cellulose degradation and this may be related to the 3D structure of the substrate.

Although enzyme synergy is a topic that requires further research to elucidate the exact mechanisms behind enzyme interactions, this chapter provides a few insights into the proposed mechanisms behind enzyme synergy. However, more advanced methods such as real time studies (AFM), staining methods (tagging of enzymes and substrates) and various sugar kits would provide a more in-depth understanding of these synergistic interactions.

Chapter 5: General discussion and future recommendations

5.1 General discussion and conclusions

Enzymatic conversion of cellulosic biomass is considered a promising technology for addressing the current environmental issues associated with crude oil usage (Mohanram *et al.*, 2013; Sweeney and Xu, 2012). However, the recalcitrant structure of biomass, low enzyme activities on the substrate, and high enzyme production costs impose major economic challenges for the production of cellulosic fuels (Limayem and Ricke, 2012; Zhao *et al.*, 2012). Unravelling the complex mechanisms behind enzyme synergy would aid in improving the current facilities by optimising enzyme cocktails to achieve higher hydrolysis rates. Therefore, this study investigated:

i) The conditions required for optimal cellulase activity of five fungal cellulases;
ii) The characteristics of complex cellulosic substrates and the factors that influence substrate-enzyme interactions;
iii) The synergistic associations between cellulases;
iv) The synergistic associations between cellulases and a xylanase.

Fungal cellulases have been studied extensively due to their ability to degrade cellulose, a linear polymer made up of β 1, 4-linked glucose monomers (Bayer *et al.*, 1998; Gusakov *et al.*, 2006). Many fungal cellulases have been characterised, of which cellulases produced by *T. reesei* have attracted the most attention in bioconversion studies (Peterson *et al.*, 2008; Voutilainen *et al.*, 2010). For this study, five recombinant cellulases from different fungal species (expressed in *S. cerevisiae)* were investigated for their potential to act synergistically to enhance cellulose hydrolysis. The cellulases used were cellobiohydrolases Cel7A (CBH1, EC 3.2.1.176 from *T. emersonii* with C-terminally-fused CBM from *T. reesei*) and Cel6A (CBHII, EC 3.2.1.91 from *C. lucknowense*), endoglucanases Cel7B (EGI, EC 3.2.1.4 from *A. terreus*) and Cel5A (EGII, EC 3.2.1.4 from *T. reesei*) and β-glucosidase (Cel3A, EC 3.2.1.21 from *S. fibuligera*).

First and foremost, it was important to characterise the cellulases, to understand the factors that influence their activities. Understanding the conditions required for optimal enzyme activity, provided a platform for future experiments. The findings in this study were in agreement with literature reports, regarding the enzymes' biochemical properties (molecular weight), substrate specificities, physico-chemical characteristics and kinetic characteristics. However, to the best of our knowledge, this was the first study to characterise *A. terreus* EGI from GH family 7 and the first kinetic characterisation of CBHII from *C. lucknowense* from GH family 6 and *S. fibuligera* BGL. With respect to their specific activities, the studied enzymes had preferences for different substrates which are attributable to the 3D structures of their active sites (Vlasenko *et al.*, 2010). Cellobiohydrolases, endoglucanases and β-glucosidases showed a preference for crystalline cellulose (Avicel), amorphous cellulose (CMC) and *p*NPG, respectively (Table 2.2). They had high affinities for their substrates, as evident by their low K_M values, and the rate at which the EGs and BGL hydrolysed their preferred substrates were high (i.e. high V_{max} values), while the V_{max} for the CBHs were low. The enzymes displayed optimum activity at pH 4.5 - 5.5 and at 60^{o}C (with the exception of BGL, which exhibited optimum activity at 40^{o}C). The cellulases also showed great stability over time (Figure 2.1). Stability is a great advantage to enzymes, especially in industrial applications (Thomas and Scopes, 1998).

Understanding enzyme synergy has been an ongoing challenge for many years. Most studies have used model substrates such as Avicel or filter paper to optimise enzyme cocktails. However, substrate characteristics have a major influence on the way enzymes carry out their functions (Leu and Zhu, 2012; Yang *et al.,* 2011). It is acknowledged that using model substrates may provide unreliable insights into how enzymes would perform when hydrolysing natural lignocellulosic substrates. SEB and PS are two major by-products generated from agricultural and municipal processes, respectively. These substrates were selected as suitable candidates to investigate how different substrate characteristics may influence enzyme synergy. Prior to enzyme synergy studies, the substrates were characterised to identify factors that may affect substrate-enzyme interactions.

Chemical composition analyses showed that SEB and PS contained high polysaccharide as well as high lignin content, which was in agreement with the studies performed by Martín *et al.* (2008) for SEB and the studies performed by Kim *et al.* (2000) for PS. It is well known that a high polysaccharide content provides the platform for subsequent conversion into fermentable sugars; however, the presence of lignin is a major obstacle for achieving efficient biomass conversion. During pre-treatment, biomass recalcitrance is reduced by removing or relocating lignin that forms a sheath over cellulose (Chandra *et al.,* 2007; Himmel *et al.*, 2007). During the process, many by-products may however be formed, which could potentially have an inhibitory effect on enzyme activity (García-Aparicio *et al.,* 2006; Kont *et al.,* 2013; Ximenes *et al.,* 2011). This was assessed by conducting activity assays using the supernatant (wash) from SEB and PS. The activities of CBHI, CBHII and BGL were inhibited by the SEB wash, but activated by the PS wash. The activities of EGI and EGII were activated by both washes. This indicated that compounds were present in the natural substrates which, in turn, had an effect on enzyme activities. The exact compounds were not identified which could, in future, be carried out using LC-MS. Martín *et al.,* (2002) found that steam explosion of sugarcane bagasse resulted in the formation of inhibitory by-products, including furfural, formic acid, acetic acid, levulinic acid and phenolic compounds, whereas it is proposed that sulphur compounds present in the PS may have had an activating effect on enzyme activity (Beukes and Pletschke, 2011). To assess this, future work could be carried out by adding different concentrations of sulphur-containing compounds to the reaction to assess whether they activate enzyme activity.

A prerequisite for hydrolysis includes the adsorption of cellulases to the substrate surface (Zhang and Lynd, 2004). It was found that the enzymes adsorbed to the substrates within 10 minutes, which was in agreement with Kumar and Wyman (2009), who reported that enzyme binding takes place rapidly. The % adsorption of cellulases was higher for Avicel, followed by SEB and then PS, which could be attributable to differences in the availability of binding sites and the composition of each substrate. The presence of lignin is said to cause non-productive binding of cellulases; however, whether adsorption could be attributed to unproductive binding to lignin (for the natural substrates) is not clear.

The information obtained in Chapter 3 (substrate characterisation) was useful for unravelling some of the phenomena observed for enzyme synergy in Chapter 4. Synergy studies showed that, irrespective of the type of substrate, a higher CBH to EG ratio was required to achieve higher hydrolysis yields, indicating that CBHs are the key enzymes required for cellulose hydrolysis. This was in agreement with previous studies which had reported that the addition of EG boosted CBH activity, resulting in an overall increase in cellulose hydrolysis (Den Haan *et al.,* 2013; Hu *et al.,* 2015; Shahbazi *et al.,* 2014). The binary cocktails which liberated the highest quantity of reducing sugars were 75% CBHI: 25% EGII for Avicel and PS, and 75% CBHI: 25% EGI for SEB. Synergistic interactions were established for Avicel and PS hydrolysis, but not for SEB hydrolysis (DS = 1). However, the combined activities (75% CBHI: 25% EGI) were still more efficient at hydrolysis then when the enzymes were used at 100% loading. The proposed model for cellulose hydrolysis was based on the endo-exo model by Wood and Mcrae (1979), whereby new sites are constantly being created to facilitate the activity of the other enzyme. However, this is an over-simplification of endo-exo synergism and updated models, such as the surface erosion model, substrate polishing effect and traffic jam effect which have been proposed (See Chapters 1 and 4).

For a more in-depth understanding of enzyme synergy, temporal studies were conducted using the optimal binary cocktails for each substrate. The results (with respect to the DS) varied between the substrates. For Avicel hydrolysis, the DS was higher at the beginning of hydrolysis, suggesting that enzymes were required to co-operate during the initial stages of hydrolysis to open up the substrate, which agreed with the findings of Andersen *et al.* (2008). The DS varied throughout hydrolysis of SEB and it was hypothesised that the substrate was opened up in layers, which is in agreement with the study performed by Arantes *et al.* (2014). In contrast, PS had a higher DS towards the mid-to-later stages of hydrolysis which was suggested to be as a result of a limited number of binding sites available at the beginning of hydrolysis; however, the number of binding sites increased over time. The patterns of synergism observed varied between the substrates, and it was hypothesised that the characteristics of a substrate had a direct impact on the interactions established between the enzymes.

Numerous studies have reported that the addition of a xylanase can boost cellulose hydrolysis due to cellulose and xylanase being intertwined with each other (Hu *et al.*, 2014; Li *et al.*, 2014; Zhang and Viikari, 2014). Therefore, cellulose accessibility can be increased by the removal of xylan by a xylanase. Our study showed that the addition of a bacterial xylanase did not increase cellulose hydrolysis. Zhang and Viikari *et al.* (2013) reported that lower synergy is observed when the ratio of cellulose to xylan is high, since there is less xylan to coat the cellulose microfibrils. Both the natural substrates in this study contained xylan, however we suggest that xylan did not coat the cellulose fibrils, and a xylanase was therefore not required to increase cellulose hydrolysis.

In conclusion, this study confirmed that cellulose hydrolysis can be enhanced by the activities of endo and exo acting enzymes. However, the characteristics of a particular substrate has a direct impact on their hydrolysis rates and the synergistic interactions that are established between them. Although this study provided useful insights into enzyme synergy and the proposed mechanisms behind their interactions, elucidating their exact mechanisms still requires extensive in-depth investigation.

5.2 Future perspectives

This study showed that the characteristics of a substrate plays a major role in hydrolysis, which, in turn, has an effect on the degree of synergy. Future work would entail using un-treated and pre-treated substrates, as this would allow for a better understanding of how the structural changes from pre-treatment innfluences hydrolysis and enzyme synergy. Substrates would need to be assessed better to elucidate their 3D structures. Methods such as determining the crystallinity index, DP, and staining of the different polymers by Simons' staining would be beneficial for obtaining a better understanding of the substrate characteristics that influence enzyme-substrate interactions.

Binding assays require more insight as to where the enzyme is binding. This could be conducted by ELISA-based methods, by tagging enzyme and staining polymers. A better understanding of enzyme binding is crucial for obtaining an understanding of their binding capacity. This could potentially lead to enzyme engineering, whereby CBMs can be truncated if the enzyme binds to non-cellulosic components (lignin), or by engineering a CBM to the enzyme (if it doesn't contain one) for better substrate binding.

The compounds present in the substrate washes could be analysed by LC-MS. Once the compounds have been identified, model binding of the enzyme-to-compound could be carried out to assess the effects of each individual compound on enzyme activity. The structural changes of the enzyme could be visualised by CD spectroscopy. Knowing which compounds cause inhibition or activation would be beneficial when selecting enzymes that are tolerant to these compounds.

Real time studies such as AFM and SPR would also assist to better elucidate the synergistic interactions that exist between these enzymes.

References

Abboo, S. (2014). TILE-Bioreactor system for fruit waste water treatment: reactor kinetics and analysis of digestion products. PhD Thesis (In preparation). Rhodes University, South Africa.

Allen, S.G., Kam, L.C., Zemann, A.J., Antal, M.J. (1996). Fractionation of sugarcane with hot, compressed liquid water. *Industrial and Engineering Chemistry Research.* 35 (8), 2709-2715.

Alvira, P., Negro, M.J., Ballesteros, M. (2011). Effect of endoxylanase and α-L-arabinofuranosidase supplementation on the enzymatic hydrolysis of steam exploded wheat straw. *Bioresource Technology*. 102: 4552-4558. *Industrial and Engineering Chemistry Research.* 35 (8), 2709-2715.

Amouri, B. and Gargouri, A. (2006). Characterization if a novel β-glucosidase from a *Stachybotrys* strain. *Biochemical Engineering*. 32 (3), 191-197.

Andersen, N., Johansen, K.S., Michelsen, M., Stenby, E.H., Krogh, K.B.R.M., Olsson, L. (2008). Hydrolysis of cellulose using mono-component enzymes shows synergy during hydrolysis of phosphoric acid swollen cellulose (PASC), but competition on Avicel. *Enzyme and Microbial Technology*. 42 (4), 362-370.

Arantes, V. and Saddler, J.N. (2010). Access to cellulose limits the efficiency of enzymatic hydrolysis: the role of amorphogenesis. *Biotechnology for Biofuels.* 3 (4).

Arantes, V., Gourlay, K., Saddler, J.N. (2014). The enzymatic hydrolysis of pretreated pulp fibers predominantly involves peeling/erosion modes of action. *Biotechnology for Biofuels.* 7 (87).

Arfi, Y., Shamshoum, A., Rogachev, I., Peleg, Y., Bayer, E.A. (2014). Integration of bacterial lytic polysaccharide monooxygenases into designer cellulosomes promotes enhanced cellulose degradation. *Proceedings of the National Academy of Sciences*. 111 (25), 9109-9114.

Aspenborg, H., Coutinho, P., Wang, Y., Brumer, H., Henrissat, B. (2012). Evolution, substrate specificity and subfamily classification of glycoside hydrolase family 5 (GH5). *BMC Evolutionary Biology*, 12 (186).

Babajide, O. (2013). Sustaining biodiesel production via value-added applications of glycerol. *Energy*. 2013. 1-7.

Badsah, M., Lam, D.M., Mattiasson, J.J.B. (2012). Use of an automatic methane potential test system for evaluating the biomethane potential of sugarcane bagasse after different treatments. *Bioresource Technology*. 114, 262–269.

Balan, V. (2014). Current challenges in commercially producing biofuels from lignocellulosic biomass. *Biotechnology*. 2014, 1-31.

Banerjee, G., Scott-Craig. J.S., Walton, J.D. (2010). Improving enzymes for biomass conversion: A basic research perspective. *Bioenergy Resources.* 3, 82-92.

Bansal, P., Hall, M., Realff, M.J., Lee, J.H., Bommariu, A.S. (2009). Modelling cellulase kinetics on lignocellulosic substrates. *Biotechnology Advances.* 27, 833-848.

Barr, B. K., Hsieh, Y. L., Ganem, B., Wilson, D. B. (1996). Identification of two functionally different classes of exocellulases. *Biochemistry*. 35, 586- 592.

Bastawde, K.B. (1992). Xylan structure, microbial xylanases, and their mode of action. *World Journal of Microbiology and Biotechnology.* 8 (4), 353-368.

Bayer, E.A., Chanzy, H., Lamed, R. and Shoham, Y. (1998). Cellulose, cellulases and celllosomes. *Current Opinion in Structural Biology*. 8 (5), 548-557.

Bayer, E.A., Lamed, R., Himmel, M.E. (2007). The potential of cellulases and cellulosomes for cellulosic waste management. *Current Opinion in Biotechnology.* 18 (3), 237-25.

Beckham, G.T., Dai, Z., Matthews, J.F., Momany, M., Payne, C.M., Adney, W.S., Baker, S.E., Himmel, M.E. (2012). Harnessing glycosylation to improve cellulase activity. *Current Opinion in Biotechnology.* 23 (3) 338-345.

Beldman, G., Voragen, A.G.J., Rombouts, F.M., Pilnik, W. (1988). Synergism in cellulose hydrolysis by endoglucanases and exoglucanases purified from *Trichoderma viride*. *Biotechnology and Bioengineering*. 31, 173-178.

Benko, Z., Siika-aho, M., Viikari, L., Reczey, K. (2008). Evaluation of the role of xyloglucanase in the enzymatic hydrolysis of lignocellulosic substrates. *Enzyme and Microbial Technology*. 43 (2), 109-114.

Berg, J.M., Tymoczko, J. L., Stryer, L. (2002). *The Michaelis-Menten Model Accounts for the Kinetic Properties of Many Enzymes* In: Biochemistry. 5th edition. W H Freeman: New York.

Berlin, A., Gilkes, M., Kadla, J., Maximenko, V., Kubo, S., Saddler, J. (2006). Inhibition of cellulase, xylanase and beta-glucosidase activities by softwood lignin preparations. *Biotechnology*. 84-86, 693-705.

Beukes, N. and Pletschke, B.I. (2006). Effect of sulfur-containing compounds on *Bacillus* cellulosome-associated 'CMCase' and 'Avicelase' activities. *Microbiology Letters.* 264 (2), 226-231.

Beukes, N. and Pletschke, B.I. (2010). Effect of lime-pretreatment on the synergistic hydrolysis of sugarcane bagasse by hemicellulases. *Bioresource Technology.* 101, 4472-4478.

Beukes, N. and Pletschke, B.I. (2011). Effect of lime pre-treatment on enzyme synergy for efficient hemicellulose hydrolysis in sugarcane bagasse. *Bioresource Technology.* 102, 5207-5213.

Bhat, M.K. and Bhat S. (1997). Cellulose degrading enzymes and their potential industrial applications. *Biotechnology Advances*. 15, 583–620.

Boer, H. and Koivula, A. (2003). The relationship between the thermal stability and pH optimum studied with wild-type and mutant *Trichoderma reesei* cellobiohydrolase Cel7A. *Biochemistry.* 270 (5), 841-848.

Boisset. C., Fraschini. C., Schulein, M., Henrissat. B., Chanzy, H. (2000). Imaging the enzymatic digestion of bacterial cellulose ribbons reveals the endo character of the cellobiohydrolase Cel6A from *Humicola insolens* and its mode of synergy with cellobiohydrolase Cel7A. *Applied Environmental Microbiology*. 66, 1444–1452.

Boisset, C., Pétrequin, C., Chanzy, H., Henrissat, B., Schülein, M. (2001). Optimised mixtures of recombinant *Humicola insolens* cellulases for the biodegradation of crystalline cellulose. 72(3), 339-345. *Biotechnology and Bioengineering.* 72 (3), 339-345.

Book, A.J., Yennamalli, R.M., Takasuka, T.E., Currie, C.R., Phillips, G.N., Fox, B.G. (2014). Evolution of substrate specificity in bacterial AA10 lytic polysaccharide monooxygenases. *Biotechnology for Biofuels.* 7 (109).

Botha, T. and Von Blottnitz, H. (2006). A comparison of the environmental benefits of bagasse-derived electricity and fuel ethanol on a life cycle basis. *Energy Policy.* 34, 2654-2661.

Bothwell, M.K., Walker, L.P., Wilson, D.B., Irwin, D.C., Price, M. (1993). Synergism between pure *Thermomonospora fusca* and *Trichoderma reesei* cellulases. *Biomass and Bioenergy.* 4 (4), 293-299.

Bradford, M.M. (1976). A rapid and sensitive method for the quantification of microgram quantities of protein utilizing the principle of protein-dye binding. *Analytical Biochemistry*. 72, 248-254.

Brodeur, G., Yau, E., Badal, K., Collier, J., Ramachandran, K.B., Ramakrishnan, S. (2011). Chemical and physiochemical pretreatment of lignocellulosic biomass: A Review. *Enzyme Research.* 2011, 1-17.

Bukhtojarov, F.E., Ustinov, B.B., Salanovich, T.N., Antonov, A.I., Gusakov, A.V., Okunev, O.N., Sinitsyn, A.P. (2004). Cellulase complex of the Fungus *Chrysosporium lucknowense*: Isolation and characterisation of endoglucanases and cellobiohydrolases. *Biochemistry*. 69 (5), 542-551.

Bura, R., Bothast, R.J., Mansfield, S.D., Saddler, J.N. (2003). Optimization of $S0_2$-catalaysed steam pretreatment of corn fiber for ethanol production. *Applied Biochemistry and Biotechnology*. 105, 319-335.

Bura, R., Chandra, R., Saddler, J. (2009). Influence of xylan on the enzymatic hydrolysis of steam-pretreated corn stover and hybrid Poplar. *Biotechnology Progress*. 25 (2), 315-322.

Camassola, M. and Dillon, A.J.P. (2009). Biological pretreatment of sugarcane bagasse for the production of cellulases and xylanases by *Peniciilium echinulatum. Industrial crops and Products*. 29 (203), 642-647.

Cardona, C. A., Quintero, J. A., & Paz, I. C. (2010). Production of bioethanol from sugarcane bagasse: Status and perspectives. *Bioresource Technology*. 10, 4754–4766.

Cavka, A., Guo, X., Tang, S-J., Winestrand, S., Jönsson, L., Hong, F. (2013). Production of bacterial cellulose and enzyme from waste fiber sludge. *Biotechnology for Biofuels.* 6 (25).

Cerqueira, D.A., Rodrigues, G., Meireles, C.D. (2007). Optimization of sugarcane bagasse cellulose acetylation. *Carbohydrate Polymers*. 69, 579–582.

Chandel, A.K., Kapoor, R.K., Singh, A., Kuhad, R.C. (2007). Detoxification of sugarcane bagasse hydrolysate improves ethanol production by *Candida shehatae* NCIM 3501. *Bioresource Technology*. 98, 1947-1950.

Chandra, R. P., Bura, R., Mabee, W. E., Berlin, A., Pan, X. Saddler, J. N. (2007). Substrate Pretreatment: The Key to Effective Enzymatic Hydrolysis of Lignocellulosics? *Advanced Biochemical Engineering and Biotechnolo*gy. 108, 67–93.

Chen, C., Hay, H., Esterbauer, H. (1992). Purification and characterisation of two extracellular beta-glucosidases from *Triochoderma reesei. Protein Structure and Molecular Enzymology* 1121 (1), 54-60.

Chen, Y.R., Sarkanen, S., Wang, Y.Y. (2012). Lignin degrading enzyme activities. *Methods in Molecular Biology*. 908, 251-268.

Chen, H.L., Chen, Y.C., Lu, M.J., Chang, J.J., Wang, H.C., Wang, T.Y., Ruan, S.K. and Li, W.H. (2012). A highly efficient beta-glucosidase from a buffalo rumen fungus *Neocallimastix patriciarum* W5. *Biotechnology for Biofuels*. 5 (24).

Chen, H., Vendetti, R., Gonzalez, R., Phillips, R., Jameel, H., Park, S. (2014). Economic utilization of the conversion of industrial paper sludge to ethanol. *Energy Economics*. 44, 281-290.

Choi, Y.J., Lee, J., Jang, Y-S., Lee, S.Y. (2014). Metabolic engineering of microorgansims for the production of higher alcohols. *Microbiology.* 5 (5).

Choudhary, J., Saritha, M., Nain, L., Arora, A. (2014). Enhanced Saccharification of steam pretreated rice straw by commercial cellulases supplemented with xylanase. *Bioprocessing and Biotechniques.* 4 (7).

Cockeril, S. and Martin, C. (2008). Are biofuels sustainable? The EU perspective. *Biotechnology for Biofuels.* 1 (9).

Colussi, F., Garcia, W., Rosseto, F.R., de Mello, B.L.S., de Oliviera, M. and Polikarpov, I. (2012). Effect of pH and temperature on the global compactness, structure and activity of cellobiohydrolase Cel7A from *Trichoderma harzianum. European Biophysics.* 41(1), 89.

Converse, A.O. and Optekar, J.D. (1993). A synergistic kinetics model for enzymatic hydrolysis compared to degree-of-synergism experimental results. *Biotechnology and Bioengineering*. 42, 145- 148.

Cross, R. (2001). The preparation of biological material for electron microscopy part 3: The preparation of material for scanning electron microscopy (SEM). Rhodes University Press. Grahamstown.

Cui, T., Li, J., Yan, Z., Menghui, Y., Li, S. (2014). The correlations between the enzymatic saccharfication and the multidimensional structure of cellulose changed by different pretreatments. *Biotechnology for Biofuels.* 7:134.

Daniel, R.M., Danson, M.J., Eisenthal, R., Lee, C.K., Peterson M.E. (2008). The effect of temperature on enzyme activity: new insights and their implications. *Extremophiles*. 12, 51–59.

Dashtban, M., Schraft, H. and Qin, W. (2009). Fungal bioconversion oflLignocellulosic residues; opportunities and perspectives. *Biological Sciences.* 5 (6), 578-595.

De Albuquerque Wanderley, M.C., Martín, C., Rocha, G.J.M. (2013). Increase in ethanol production from sugarcane bagasse based on combined pretreatments and fed-batch enzymatic hydrolysis. *Bioresource Technology.* 128, 448-453.

Dean, J.F.D. (1997). *Lignin analysis* In: Methods in Plant Biochemistry and Molecular Biology. CRC Press: Florida, 199–215.

Decker, C.H., Visser, J., Schreier, P. (2001). β-Glucosidase multiplicity from *Aspergillus tubingensis* CBS 643.92: purification and characterization of four β-glucosidases and their differentiation with respect to substrate specificity, glucose inhibition and acid tolerance. *Applied Microbiology and Biotechnology.* 55, 157-163.

Decker, S. R., Siika-Aho, M., Viikari, L. (2009). *Enzymatic depolymerization of plant cell wall hemicelluloses* In: Biomass Recalcitrance: Deconstructing the plant cell wall for bioenergy. E. Himmel, M. (Ed.). Blackwell Publishing Ltd: United Kingdom, 352-373.

Den Haan, R., Kroukamp, H., van Zyl, J-H.D., van Zyl, W.H. (2013). Cellobiohydrolase secretion by yeast: Current state and prospects for improvement. *Process Biochemistry.* 48 (1), 1-12.

Den Haan, R., van Zyl, J.M., Harms, T.M., van Zyl, W.H. (2013). Modeling the minimum enzymatic requirements for optimal cellulose conversion. *Environmental Research Letters.* 8 (2), 1-11.

Din, N., Damude, H.G., Gilkes, N.R, Miller, R.C., Warren, R.A.J., Kilburn, D.G. (1994). C1–Cx revisited: intramolecular synergism in a cellulase. *Proceedings of the National Academy of Sciences*. 91, 11383-11387.

Ding, S., Ge, W., Buswell, J.A. (2007). Molecular cloning and transcriptional expression analysis of an intracellular β-glucosidase, a family 3 glycosyl hydrolase, from the edible straw mushroom, *Volvariella volvacea*. *Microbiology Letters.* 267, 221-229.

Dobson, Rosemary. "The development of recombinant fungal enzyme cocktails for the hydrolysis of cellulosic waste products." iThemba Labs, Cape Town, August 2013. Conference Proceedings.

Du, R., Su, R., Li, X., Tantai, X., Liu, Z., Yang, J., Qi, W., He, Z. (2012). Controlled adsorption of cellulase onto pretreated corncob by pH adjustment. *Cellulose.* 19, 371-380.

Eberhardt, R.Y., Gilbert, H.J., Hazlewood, G.P. (2000). Primary sequence and enzymic properties of two modular endoglucanases, Cel5A and Cel45A, from the anaerobic fungus *Piromyces equi*. *Microbiology*. 146, 1999-2008.

El-Hefnawy, M.E., Sakran, M., Ismail, A., Aboelfetoh, E.F. (2014). Extraction, purification and thermodynamic properties of urease from germinating *Pisuym sativum L.* seeds. *Physical influences on stem cells.* 14 (15).

Eriksson, T., Karlsson, J. and Tjerneld, F. (2002). A model explaining declining rate in hydrolysis of lignocellulose substrates with Cellobiohydrolase I (Cel7A) and Endoglucanase I (Cel7B) of *Trichoderma reesei. Applied Biochemistry and Biotechnology*. 41 (101), 41-60.

Esteghlalian, A.R., Mansfield, S.D., Saddler, J.N. (2002). Cellulases: Agents for fiber modification or bioconversion? The effect of substrate accessibility on cellulose enzymatic hydrolyzability. *Biotechnology in the Pulp and Paper Industry*. 21, 21-36.

Fan, Z., South, C., Lyford, K., Munsie, J., van Walsum, P., Lynd, L.R. (2003). Conversion of paper sludge to ethanol in a semicontinuous solids-fed reactor. *Bioprocessing and Biosystems Engineering.* 26, 93-101.

Fägerstam, L.G. and Pettersson, G. (1980). The 1, 4 β-glucan cellobiohydrolases of *Trichoderma reesei.* QM 9414: A new type of cellulolytic synergism. *FEBS Letters.* 119 (1).

Feng, Y., Qi, X., Jian, H-L., Sun, R-C., Jiang, J-X. (2006). Effect of inhibitors on enzymatic hydrolysis and simultaneous saccharification fermentation for lactic acid production from steam explosion pretreated lespedeza stalks. *BioResources.* 7 (3), 3755.

Festucci-Bucelli, R.A., Otoni, W.C., Joshi, C.P. (2007). Structure, organisation, and functions of cellulose synthase complexes in higher plants. *Plant Physiology.* 19 (1), 1-13.

Forseberg, Z., Mackemzie, A.K., Sorlie, M., Rohr, A.K., Helland, R., Arvai, A.S., Vaaje-Kolstad, G., Eijsink, V.G.H. (2014). Structural and functional characterisation of a conserved pair of bacterial cellulose-oxidizing lytic polysaccharide monooxygenases. *Proceedings of the National Academy of Sciences*. 111 (23).

Fujita, Y., Ito, J., Ueda, M., Fukuda, H., Kondo, A. (2004) Synergistic saccharification, and direct fermentation to ethanol, of amorphous cellulose by use of an engineered yeast strain codisplaying three types of cellulolytic enzyme. *Applied and Environmental Microbiology*. 70, 1207–12.

Gandolfi, S., Ottolina, G., Riva, S., Fantoni, G.P., Patel, I. (2013). Complete chemical analysis of carmagnola hemp hurd and structural feature of its components. *BioResources.* 8 (2), 2641-2656.

Ganner, T., Bubner, P., Eibinger, M., Mayrhofer, C., Plank, H. Nidetzky, B. (2012). Dissecting and Reconstructing Synergism: In situ visualisation and cooperativity among cellulases. *Biological Chemistry*. 287 (52), 43215-43222.

Gao, J., Weng, H., Xi, Y., Zhu, D., Han, S. (2008). Purification and characterization of a novel endo-b-1, 4-glucanase from the thermoacidophilic *Aspergillus terreus*. *Biotechnology Letters.* 30, 323-327.

Gao, L., Wang, F., Gao, F., Wang, L., Zhao, J., Qu, Y. (2011) Purification and characterization of a novel cellobiohydrolase (PdCel6A) from *Penicillium decumbens* JU-A10 for bioethanol production. *Bioresource Technology*. 102 (17), 8339-8342.

García-Aparicio, M.P., Ballesteros, I., Gonzáles, A., Oliva, J.M., Ballesteros, M., Negro, M.J. (2006). Effect of Inhibitors Released During Steam-Explosion Pretreatment of Barley Straw on Enzymatic Hydrolysis. *Applied Biochemistry and Biotechnology*. 129 (1-3), 278-288.

García-Aparicio, M.P., Ballesteros, M., Manzanres, P., Ballesteros, I., Gonzalez, A., Negro, M.J. (2007). Xylanase contribution to the efficiency of cellulose enzymatic hydrolysis of barley straw. *Applied Biochemistry and Biotechnology.* 137, 353-336.

Granum, D.M., Schutt, T.C., Maupin, M. (2014). Computational Evaluation of the Dynamic Fluctuations of Peripheral Loops Enclosing the Catalytic Tunnel of a Family 7 Cellobiohydrolase. *Physical Chemistry*. 118 (20), 5340-5349.

Grassick, A., Murray, P.G., Thompson, R., Collins, C.M., Byrnes, L., Birrane, G., Higgins, T.M. Tuohy, M.G. (2004). Three dimensional structure of a thermostable native cellobiohydrolase and molecular characterisation of cel7 gene from the filamentous fungus *Talaromyces emersonii*. *Biochemistry.* 271, 4495–4506.

Guerfali, M., Saida, A., Gargouri, A., Belghith, H. (2014). Enhanced enzymatic hydrolysis of waste paper for ethanol production using separate saccharification and fermentation. *Applied Biochemistry and Biotechnology.* 171 (1), 25-42.

Gunawardena, J. (2012). Some lessons about models from Michaelis and Menten. *Molecular Biology of the Cell.* 23 (14), 2819.

Gundllapalli, S.N., Pretorius, I.S. and Cordero Otero, R.R. (2007). Effect of the cellulose-binding domain of β-glucosidase from *Saccharomycopsis fibuligera*. *Industrial Microbiology and Biotechnology*. 34, 413-421.

Guo, F., Shi, W., Sun, W., Xuezhi, L, Wang, F., Zhao, J., Qu, Y. (2014). Differences in the adsorption of enzymes onto lignins from diverse types of lignocellulosic biomass and the underlying mechanism. *Biotechnology for Biofuels.* 7 (38).

Gusakov, A.V., Salanovic, T.N., Antonov, A.I., Ustinov, B.B., Okunev, O.N., Burlingame, R., Emalfarb, M., Baez, M., Sinitsyn, A.P. (2007). Design of highly efficient cellulase mixture for enzymatic hydrolysis of cellulose. *Biotechnology and Bioengineering*. 97 (5), 1028-1038.

Hall, M., Bansal, P., Lee, J.H., Realff, M.J., Bommarius, A.S. (2010). Cellulose crystallinity- a key predictor of the enzymatic hydrolysis rate. *FEBS.* 277 (6), 1571-1582.

Haven, M. Ø. and Jørgensen, H. (2013). Adsorption of β-glucosidases in two commercial preparations onto pretreated biomass and lignin. *Biotechnology for Biofuels.* 6 (165).

Hendriks, A. T. W. M. and Zeeman, G. (2009). Pretreatments to enhance the digestibility of lignocellulosic biomass. *Bioresource Technology*. 100 (1), 10-18.

Henrissat. B., Driguez. H., Viet. C., Schülein. M. (1985). Synergism of cellulases from *Trichoderma reesei* in the degradation of cellulose. *Nature Biotechnology*. 3 (8), 722-726.

Henrissat, B. (1991). A classification of glycosyl hydrolases based on their amino acid sequences similarities. *Biochemistry*. 280, 309-316.

Herpoël-Gimbert, I., Margeot, A., Dolla, A., Jam, G., Molle, D., Lignon, S., Mathis, H., Sogoilloti, J.C., Monot, F. and Asther, M. (2008). Comparative secretome analyses of two *Trichoderma reesei* RUT-C30 and CL847 hypersecretory strains. *Biotechnology for Biofuels.* 1 (18), 1-12.

Himmel, M.E., Ding, S.Y., Johnsons, D.K., Adney, W.S., Nimlos, M.R., Brady, J.W. Foust, T.D. (2007). Biomass Recalcitrance: Engineering plants and enzymes for biofuel production. *Science*. 315 (5813), 804-807.

Hong, H., Tamaki, K., Y., Kumagai, H. (2003). Cloning of a gene encoding thermostable cellobiohydrolase from *Thermoascus aurantiacus* and its expression in yeast. *Applied Microbiology and Biotechnology*. 63 (1), 42-50.

Hong, J., Tamaki, H., Kumagai, H. (2007). Cloning and functional expression of thermostable β-glucosidase gene from *Thermoascus aurantiacus*. *Applied Microbiology and Biotechnology*. 73 (6), 1331–1339.

Horn, S.J., Vaaje-Kolstad, G., Westereng, B., Eijsink, V.G.H. (2012). Novel enzymes for the degradation of cellulose. *Biotechnology for Biofuels.* 5 (45).

Howard, R.L., Abotsi, E., Jansen van Rensburg, E.L., Howard, S. (2003). Lignocellulose biotechnology: issues of bioconversion and enzyme production. *Biotechnology*. 2 (12), 602-619.

Hu, J., Arantes, V., Saddler, J.N. (2011). The enhancement of enzymatic hydrolysis of lignocellulosic substrates by the addition of accessory enzymes such as a xylanase: is it an additive or synergistic effect? *Biotechnology for Biofuels.* 4 (36).

Hu, J., Gourlay, K., Arantes, V., Van Dyk, J.S., Pribowo, A., Saddler, J.N. (2015). The accessible surface influences synergism during the hydrolysis of lignocellulosic substrates. *ChemSusChem.* doi: 10.1002/cssc.201403335.

Igarashi, K., Koivula, A., Wada, M., Kimura, S., Penttilä, M. Samejima, M. (2009). High speed atomic force microscopy visualises processive movement of *Trichoderma reesei. Biological Chemistry*. 284, 36186-36190.

Ilmén, M., den Haan, R., Brevnova, E., McBride, J., Wiswall, E., Froelich, A., Koivula, A., Voutilainen, S.P., Siika-aho, M., la Grange, D.C., Thorngren, N., Ahlgren, S., Mellon, M., Deleault, K., Rajgarhia, V., van Zyl, W.H., Penttila, M. (2011). High level secretion of cellobiohydrolases by *Saccharomyces cerevisiae*. *Biotechnology for Biofuels.* 4 (30), 30.

Imai, T., Boisset, C., Samejima, M., Igarashi. K., Sugiyam, J. (1998). Unidirectional processive action of cellobiohydrolase Cel7A on Valonia cellulose microcrystals. *FEBS Letters*. 432 (3), 113-116.

Ioelovich, M., Leykin, A., Figovsky, O. (2010). Study of cellulose paracrystallinity. *BioResources.* 5 (3), 1393-1407.

Irwin, D.C., Spezio, M., Walker, L.P., Wilson, D.B. (1993). Activity studies of eight purified cellulases: specificity, synergism, and binding domain effects. *Biotechnology and Bioengineering*. 42, 1002-1013.

Jadhav, S.D. (2014). Ethanol Production from Sugarcane Bagasse without Enzymatic Saccarification – A Microbial Study. *Indian Streams Research Journal.* 5 (2).

Jahangeer, S., Khan, N., Jahangeer, S., Sohail, M., Shahzad, S., Ahmad, A., Khan, S.A. (2005). Screening and characterisation of fungal cellulases isolated from the native environmental source. *Pakistan Journal of Botany.* 37 (3), 739-745.

Jalak, J., Kurasin, M., Teugjas, H., Väljamäe, P. (2012). Endo-exo synergism in cellulose hydrolysis revisted. *The Journal of Biological Chemistry.* 287 (34), 28802-28815.

Jeoh, T., Wilson, D.B., Walker, L.P. (2006). Effect of cellulase mole fraction and cellulose recalcitrance on synergism in cellulose hydrolysis and binding. *Biotechnology Progress.* 22 (1), 270-277.

Jeoh, T., Santa-Maria, M.C., O'Dell, P.J. (2013). Assessing cellulose microfibrillar structure changes due to cellulase action. *Carbohydrate Polymers.* 97 (2), 581-586.

Jeya, M., Joo, A.R., Lee, K.M., Tiwara, M.K., Lee, K.M., Kim, S.H., Lee. J.K. (2010). Characterization of β-glucosidase from a strain of *Penicillium purpurogenum* KJS506. *Applied Microbiology and Biotechnology.* 86 (1), 1473- 1484.

Jönsson, L.J., Alriksson, B., Nilvebrant, N-O. (2013). Bioconversion of lignocellulose: inhibitors and detoxification. *Biotechnology for Biofuels.* 6 (16).

Jorgensen, H., Kristensen, J.B., Felby, C. (2007). Enzymatic conversion of lignocellulose into fermentable sugars: challenges and opportunities. *Biofuels, Bioproducts and Biorefineries.* 1, 119-134.

Kallioinen, A., Puranen, T., Siika-aho, M. (2014). Mixtures of thermostable enzymes show high performance in biomass saccharification. *Applied Biochemistry and Biotechnology.* 73 (5), 1038-1056.

Kang, L., Wang, W., Lee, Y.Y. (2010). Bioconversion of Kraft Paper mill sludges to ethanol by SSF and SSCF. *Applied Biochemistry and Biotechnology*. 161, 53-66.

Karmakar, M. and Ray, R.R. (2011). Current trends in research and application of microbial cellulases. *Microbiology*. 6 (1), 41-53.

Karnchanatat, A., Petsom, A., Sangvanich, P., Piaphukiew, J., Whalley, A.J.S., Reynolds, C.D., Sihanonth, P. (2007). Purification and biochemical characterization of an extracellular β-glucosidase from the wood-decaying fungus *Daldinia eschscholzii*. *Microbiology Letters.* 270 (1), 162-170.

Karp, S.G., Woiciechowski, A.L., Soccol, V.T., Soccol, C.R. (2013). Pretreatment strategies for delignification of sugarcane bagasse: A Review. *Brazilian Archives of Biology and Technology*. 56 (4), 679-689.

Khan, M.M. Khan, R.U., Khan, F.Z., Athar, M. (2013). Impacts of biodiesel on the environment. *Environmental Engineering and Management.* 4 (4), 345-350.

Kim, J.S., Lee, Y.Y., Park, S.C. (2000). Pretreatment of wastepaper and pulp mill sludge by aqueous ammonia and hydrogen peroxide. *Applied Biochemistry and Biotechnology*. 84-86, 129-139.

Kim, J., Lee, H.J., Choi, I.G., Kim, K.H. (2014). Synergistic proteins for the enhanced enzymatic hydrolysis of cellulose by cellulase. *Applied Microbiology and Biotechnology*. 98 (20), 8469-8480.

Kont, R., Kurašin, M., Teugjas, H., Väljamäe, P. (2013). Strong cellulase inhibitors from the hydrothermal pretreatment of wheat straw. *Biotechnology for Biofuels.* 6 (135).

Kostylev, M. and Wilson, D.B. (2012). Synergistic interactions in cellulose hydrolysis. *Biofuels*. 3, 61-70.

Kostylev, M., Wilson, D. (2014). A distinct model of synergism between a processive endocellulase (TfCel9A) and an exocellulases (TfCel48A) from *Thermobifida fusca*. *Applied Environmental Microbiology*. 80 (1), 339.

Krishnan, C., Sousa, L.C., Jin, M., Chang, L., Dale, B.E., Balan, V. (2010). Alkali based pretreatment for the conversion of sugarcane bagasse and cane leaf residues to ethanol. *Biotechnology and Bioengineering.* 107 (3), 441-450.

Kleman-Leyer, K.M., Siika-Aho, M., Teeri, T., Kirk, T.K. (1996). The cellulases endoglucanase I and cellobiohydrolase II of *Trichoderma reesei* act synergistically to solubilize native cotton cellulose but not decrease its molecular size. *Applied and Environmental Microbiology*. 62, 2883-2886.

Kumar, R. and Wyman, C. E. (2009). Effects of cellulase and xylanase enzymes on the deconstruction of solids from pretreatment of poplar by leading technologies. *Biotechnology Progress*. 25, 302-314.

Kumar, S., Salam, P.U., Shrestha, P., Ackom, E.K. (2013). An assessment of Thailand's biofuel development. *Sustainability*. 2013 (5), 1577-1597.

Kumar, R., Hu, F., Sannigrahi, P., Jung, S., Ragauskas, A.J., Wyman, C.E. (2013). Carbohydrate derived-pseudo-lignin can retard cellulose biological conversion. *Biotechnology and Bioengineering*. 110 (3), 737-753.

Kumar, D. and Murthy, G.S. (2013). Stochastic molecular model of enzymatic hydrolysis of cellulose for ethanol production. *Biotechnology for Biofuels*. 6 (63).

La Grange, D.C., den Haan, R., van Zyl, W.H. (2010). Engineering cellulolytic ability into bioprocessing organisms. *Applied Microbiology and Biotechnology*. 87, 1195–1208.

Lamed, R., Setter, E., Bayer, E.A. (1983). Characterization of a cellulose binding, cellulase-containing complex in *Clostridium thermocellum*. *Bacteriology*. 156, 828 – 836.

Langston, J.A., Shaghasi, T., Abbate, E., Xu, F., Vlasenko, E., Sweeney, M.D. (2011). Oxidoreductive cellulose depolymerization by the enzymes cellobiose dehydrogenase and glycoside hydrolase 61. *Applied and Environmental Microbiology*. 77, 7007-7015.

Lavoine, N., Desloges, I., Dufresne, A., Bras, J. (2012). Microfibrillated cellulose – Its barrier properties and applications in cellulosic materials: A review. *Carbohydrate Polymers*. 90 (2), 735-764.

Laemmli, U.K. (1970). Cleavage of structural proteins during the assembly of the head of bacteriophage T4. *Nature*. 227, 680.

Lee, J. (1997). Biological conversion of lignoellulosic biomass to ethanol. *Journal of Biotechnology*. 56, 1-24.

Lee, K.M., Joo, A.R., Jeya, M., Lee, K.M., Moon, H.J., Lee, J.K. (2011). Production and characterization of cellobiohydrolase from a novel strain of *Penicillium purpurogenum* KJS506. *Applied Biochemistry and Biotechnology*. 163, 25-39.

Lee, H.V., Hamid, S.B.A., Zain, S.K. (2014). Conversion of lignocellulosic biomass to nanocellulose: structure and chemical process. *The Scientific World Journal*. 2014, 1-20.

Leibbrandt, N. H., Knoetze, J. H., & J.F. Gorgens, J. F. (2011). Comparing biological and thermochemical processing of sugarcane bagasse: An energy balance perspective. *Biomass and Bioenergy*. 35, 2117-2126.

Leu, S.Y. and Zhu, J.Y. (2012). Substrate related factors affecting enzymatic saccharification of lignocellulose: Our recent Understanding. *Bioenergy Resources*. 6, 405–415.

Li, J., Zhou, P., Liu, H., Gong, Y., Xiao, W., Liu, Z. (2014). Monosaccharide and ethanol production from superfine sugarcane bagasse using enzyme cocktail. *BioResources*. 9 (2), 2529-2540.

Lima, D.U., Santos, H.P., Tiné, M.A., Molle, F.R.D., Buckeridge, M.S. (2001). Patterns of expression of expression of cell wall related genes in sugarcane. *Geneticsand Molecular Biology*. 24 (1-4), 191-198.

Lima, M.A., Oliveira-Neto, M., Kadowaki, M.A., Rosseto, F.R., Prates, E.T., Squina, F.M., Leme, A.F., Skaf, M.S., Polikarpov, I. (2013). *Aspergillus niger* β-glucosidase has a cellulase-like tadpole molecular shape: insights into glycoside hydrolase family 3 (GH3) β-glucosidase structure and function. *Biological Chemistry*. 288 (46), 32991-33005.

Limayem, A. and Ricke, S.C. (2012). Lignocellulosic biomass for bioethanol production: Current perspectives, potential issues and future prospectives. *Progress in Energy and Combustion Science*. 38, 449-467.

Liu, H. and Zhu, J.Y. (2013). Eliminating inhibition of enzymatic hydrolysis by lignosulfate in unwashed sulphite-pretreated aspen using metal salts. *Bioresource Technology*. 101, 9120-9127.

Lynd, L.R., Weimer, P.J., van Zyl, W.H., Pretorius, I.S. (2002). Microbial cellulose utilization: Fundamentals and Biotechnology. *Microbiology and Molecular Biology Reviews*. 66 (3), 506-577.

Machida, M., Ohtsuki, I., Fukui, S., Yamashita, I. (1988). Nucleotide sequences of *Sacharomycopsis fibuligera* gene for extracellular β-glucosidases as expressed in *Saccharomyces cerevisiae*. *Applied and Environmental Microbiology*. 54 (3), 3147-3155.

Macrelli, S., Mogensen, J., Zacchi, G. (2012). Techno-economic evaluation of 2nd generation bioethanol production from sugarcane bagasse and leaves intergrates with sugar-based ethanol process. *Biotechnology for Biofuels*. 5 (22).

Mahadevan, S.M., Wi, S.G., Lee, D.S., Bae, H.J. (2008). Site directed mutagenesis and CBM engineering of CEL5A (*Thermotoga maritima*). *Microbiology Letters*. 287 (2), 205-211.

Malgas, S., Van Dyk, J.S., Pletschke, B.I (2015). β-Mannanase (Man26A) and α-galactosidase (Aga27A) synergism – A key factor for the hydrolysis of galactomannan substrates. *Enzyme and Microbial Technology*. 70, 1-8.

Mansfield, S.D., Mooney, C., Saddler, J. N. (1999). Substrates and enzyme characteristics that limit cellulose hydrolysis. *Biotechnology Progress*. 15, 804-816.

Marques, S., Alves, L., Roseiro, J.C., Girio, F.M. (2008). Conversion of recycled paper sludge to ethanol by SHF and SSF using *Pichia stipites*. *Biomass and Bioenergy*. 32, 400-406.

Martín, C., Galbe, M., Nilvebrant, N-O., Jönsson, L.J. (2002). Comparison of the fermentability of enzymatic hydrolysates of sugarcane bagasse pretreated by steam explosion using different impregnating agents. *Applied Biochemistry and Biotechnol*ogy. 98–100.

Martín, C., Klinke, H.B., Thomsen, A.B. (2008). Wet oxidation as a pretreatment method for enhancing the enzymatic convertibility of sugarcane bagasse. *Enzyme and Microbial Technology*. 40 (3), 426–432.

Mason, G.F. and Lai, J.C.K. (2000). Nonlinear determination of Michaelis-Menten kinetics with model evaluation through estimation of uncertainties. *Metabolic Brain Disease.* 15 (2).

McCarter JD and Withers SG. (1994) Mechanisms of enzymatic glycoside hydrolysis. *Current Opinion in Structural Biolology*. 4 (6), 885-92.

McMillan, J.D. (1994). Pretreatment of lignocellulosic biomass. *Enzymatic Conversion of Biomass for Fuels Production.* 15, 292-324.

Medve, J., Stahlberg, J., Tjerneld, F. (1994). Adsorption and synergism of cellobiohydrolase I and II of *Trichoderma reesei* during hydrolysis of microcrystalline cellulose. *Biotechnology for Bioengineering*. 44, 1064–1073.

Medve, J., Karlsson, J., Lee, D. and Tjerneld, F. (1998). Hydrolysis of microcrystalline cellulose by cellobiohydrolase I and endoglucanase II from *Trichoderma reesei*: adsorption, sugar production pattern, and synergism of the enzymes. *Biotechnology and Bioengineering*. 59, 621-634.

Meyer, A.S., Rosgaard, L., Sorensen, H.R. (2009). The minimal enzyme cocktail concept for biomass processing. *Cereal Science.* 50, 337-344.

Miller, G. L. (1959). Use of dinitrosalicylic acid reagent for determination of reducing sugar. *Analytical Chemistry*. 31(3), 426-428.

Mohanram, S., Amat, S., Choudhary, J., Arora, A., Nain, L. (2013). Novel perspectives for evolving enzyme cocktails for lignocellulose hydrolysis in biorefineries. *Sustainable Chemical Processes.* 1 (15).

Momeni, M.H., Payne, C.M., Hansson, H., Mikkelsen, N.E., Svedberg, J., Engström, A., Sandgren, M., Beckham, G.T., Ståhlberg, J. (2013). Structural, biochemical, and computational characterization of the glycoside hydrolase family 7 of the tree-killing fungus *Heterobasidion irregulare. Enzymology.* 288 (8), 5861-5872.

Moon, R.J., Martin, A., Nairn, J., Simonsen, J., Youngblood, J. Cellulose nanomaterials review: structure, properties and nanocomposites. *Chemical Society Reviews.* 40, 3941- 3994.

Moraïs, S., Barak, Y., Caspi, J., Hadar, Y., Lamed, R., Shoham, Y., Wilson, D.B., Bayer, E.A. (2010). Cellulase-xylanase synergy in designer cellulosomes for enhanced degradation of a complex cellulosic substrate. *Microbiology.* 1 (5).

Moreira, L.R.S and Filho, E.X.F. (2008). An overview of mannan structure and mannan degrading enzyme systems. *Applied Microbiology and Biotechnology*. 79, 165-178.

Moreno, A.D., Tomás-Pejó, E., Ibarra, D., Ballesteros, M., Olsson, L. (2013). Fed-batch SSCF using steam-exploded wheat straw at high dry matter consistencies and a xylose-fermenting *Saccharomyces cerevisiae* strain: effect of laccase supplementation. *Biotechnology for Biofuels.* 6 (160).

Morgenstern, I., Powlowski, J., Tsang, A. (2014). Fungal cellulose degradation by oxidative enzymes: from dysfunctional GH61 family to powerful lytic polysaccharide monooxygenase family. *Briefings in Functional Genomics.* 1-11.

Morozova, V.V., Gusakov, A.V., Andrianov, R., Pravilnikov, A.G., Osipov, D.O., Sinitysyn, A.P. (2010). Cellulases of *Penicillium verruculosum. Biotechnology*. 5 (8), 871-880.

Moxley, G., Gaspar, A.R., Higgins, D., Xu, H. (2012). Structural changes of corn stover lignin during acid pretreatment. *Industrial Microbiology and Biotechnology*. 39, 1289-1299.

Müller-Langer, F., Majer, S., O'Keeffe, S. (2014). Benchmarking biofuels- a comparison of technical, economic and environmental indicators. *Energy, Sustainability and Society.* 4 (20).

Murray, P., Arob, N., Collins. C., Grassick, A., Penttilä, M., Saloheimo, M., Tuohy, M. (2004). Expression in *Trichoderma reesei* and characterisation of a thermostable family 3 β-glucosidase from the moderately thermophilic fungus *Talaromyces emersonii*. *Protein Expression and Purification*. 38, 248-257.

Naik, S.N., Goud, V.V., Rout, P.K., Dalai, A.K. (2010). Production of first and second generation biofuels: A comprehensive review. *Renewable and Sustainable Energy Reviews.* 14 (2), 578-497.

Nakagame, S., Chandra, R.P., Saddler, J.N. (2011). The influence of lignin on the enzymatic hydrolysis of pretreated biomass substrates. Sustainable production of fuels, chemicals, and fibers from forest biomass. *American Chemical Society.* Washington, DC. 146-167.

Nakazawa, H., Okada, K., Kobayashi, R., Kunota, T., Onodera, T., Ochiai, N., Omata, N., Wataru Ogasawara, W., Okada, H., Morikawa, Y. (2008). Characterization of the catalytic domains of *Trichoderma reesei*. *Microbiology and Biotechnology*. 81, 681-689.

Narra, M., Dixit, G., Divecha, J., Datta, M., Shah, A.R. (2012). Production of cellulases by solid state fermentation with *Aspergillus terreus* and enzymatic hydrolysis of mild-alkali treated rice straw. *Bioresource Technology*. 121, 355-361.

Naumoff, D.G. (2011). Hierarchical classification of glycoside hydrolases. *Biochemistry-Moscow*. 76 (6), 622-635.

Nazir, A., Somi, R., Saini, H.S., Manhas, R.K., Chadha, B.S. (2009). Purification and characterization of an endoglucanase from *Aspergillus terreus* highly active against barley a-glucan and xyloglucan. *Microbiology and Biotechnology.* 25, 1189-1197.

Nguyen, H.Q. and Quyen, D.I. (2010). Purification and properties of an endoglucanase from *Aspergillus oryzae* VTCC-F045. *Australian Journal of Basic and Applied Sciences.* 4 (12), 6217-6222.

Nidetzky, B., Steiner, W., Hayn, M., and Claeyssens, M. (1994). Cellulose hydrolysis by the cellulases from *Trichoderma reesei*: a new model for synergistic interaction. *Biochemistry*. 298, 705-710.

Nijikken, Y., Tsukada, T., Igarashi, K., Samjima, M., Wakagi, T., Shoun, T., Fushinobu. (2007). Crystal structure of intracellular family 1 β-glucosidase BGL1A from the basidiomycete *Phanerochaete chrysosporium. FEBS Letters.* 581 (7), 1514-1520.

Nikolov, T., Bakalova, N., Petrova, S., Benadova, R., Spasov, S., Kolev, D. (2000). An effective method for bioconversion of delignified waste cellulolse fibers from the paper industry with a cellulase complex. *Bioresource Technology.* 71, 1-4.

Nutt. A., Sild, V., Pettersson, G., Johansson, G. (1998). Progress curves - a mean for functional classification of cellulases. *Biochemistry.* 258 (1), 200–206.

Ohgren, K., Vehmaanpera, J., Silka-Aho, M., Galbe, M., Viikari, L., Zacchi, G. (2007). High termperature enzymatic prehydrolysis prior to simultaneous saccharification and fermentation of steam pretreated corn stover for ethanol production. *Enzyme and Microbial Technology.* 40 (4), 607-613.

Okada, H., Tada, K., Sekiya, T., Yokoyama, K., Takahashi, A., Tohda, H., Kumagai, H., Morikawa, T. (1998). Molecular characterization and heterologous expression of the gene encoding a low-molecular-mass endoglucanase from Trichoderma reesei QM9414. *Applied Environmental Microbiology*. 64, 555-563.

Olver, B., Van Dyk, J.S., Beukes, N., Pletschke, B.I. (2011). Synergy between EngE, XynaA and ManA from *Clostridium cellulovorans* on corn stalk, grass and pineapple pulp substrates. *3Biotech.* 1, 187-192.

O'Sullivan, A. C. (1997). Cellulose: the structure slowly unravels. *Cellulose.* 4, 173–207.

Palonen, H., Tjerneld, F., Zacchi, G., Tenkanen, M. (2004). Adsorption of *Trichoderma reesei.* CBHI and EGII and their catalytic domains on steam pretreated softwood and isolated lignin. *Biotechnology.* 107 (1), 65-72.

Pan, X., Xie, D., Gilkes, N., Gregg, J.D., Saddler, N.J. (2005). Strategies to enhance the enzymatic hydrolysis of pretreated softwood with high residual lignin content. *Applied Biochemistry and Biotechnology*. 121–124, 1069–1079.

Panagiotou, G. and Olsson, L. (2007). Effect of compounds released during pretreatment of wheat straw on microbial growth and enzymatic hydrolysis rates. *Biotechnology and Bioengineering.* 96 (2), 250-258.

Pandey. A., Soccol, C.R., Poonam Nigam, P., Soccol, V.T. (2000). Biotechnological potential of agro-industrial residues. I: sugarcane bagasse. *Bioresource Technology*. 7 (1), 69-80.

Pandiyan, K., Tiwari, R., Singh, S., Nain, P.K.S., Rana, S., Arora, A., Singh, S.B., Nain, L. (2014). Optimisation of enzymatic saccharification of alkali pretreated *Parthenium* sp using response surface methodology. *Enzyme Research.* doi: 10.1155/2014/764898.

Pareek, N., Gillgren, T., Jönsson, L.J. (2013). Adsorption of proteins involved in hydrolysis of lignocellulose on lignins and hemicelluloses. *Bioresource Technology.* 148, 70-77.

Park, S., O Baker, H., Himmel, M.E., Parilla, P.A., Johnson, D.K (2010). Cellulose crystallinity index: measurement techniques and their impact on interpreting cellulose performance. *Biotechnology for Biofuels.* 3 (10).

Pasquini, D., Pimenta, M.T.B., Ferreira, L.H., Curvelo, A.A.S. (2005). Extraction of lignin from sugarcane bagasse and *Pinus taeda* wood chips using ethanol-water mixtures and carbon dioxide at high pressures. *Supercritical fluids*. 36, 31-39.

Paula, D.R. and Foresti, E. (2009). Sulfide toxicity kinetics of a uasb reactor. *Brazilian of Chemical Engineering.* 26 (4).

Pecarovicova, A., Luzakova, V., Bystricky, S., Pecarovic, J., Kosik, M. (1989). An activation of effect of some phenolics on enzymatic hydrolysis of polysaccharides. *Cellulose Chemistry and Technology*. 23 (225).

Peciulyte, A., Anasontzis, G.E., Karlström, K., Larsson, P.T., Olsson, L. (2014). Morphology and enzyme production of *Trichoderma reesei* RUT C-30 are affected by the physical and structural characteristics of cellulosic substrates. *Fungal Genetics and Biology.* 72, 64-72.

Peng, L. and Chen, Y. (2011). Conversion of paper sludge to ethanol by separate hydrolysis and fermentation (SHF) using *Saccharomyces cerevisiae. Biomass and Bioenergy.* 25, 1600-1606.

Perez, J., Munoz-Dorado, J., Rubia, T. D. L. and Martinez, J. (2002). Biodegradation and biological treatments of cellulose, hemicellulose and lignin: An overview. *International Microbiology*. 5 (2), 53-63.

Perez-Rodriguez, F., Posada-Izquierd, G.D., Valero, A., García-Gimeno, R.M., Zurera G. (2013). Modelling survival kinetics of *Staphylococcus aureus* and *Escherichia coli* O157:H7 on stainless steel surfaces soiled with different substrates under static conditions of temperature and relative humidity. *Food Microbiology*. 33, 197–204.

Petkowicz, C.L.O., Reicher. F., Chanzy. H., Taravel, F.R, Vuong, R. (2001). Linear mannan in the endosperm of *Schizolobium amazonicum. Carbohydrate Polymers*. 44, 107–112.

Pézsa, N. and Ailer, P. (2011). Bioethanol production from paper sludge pretreated by subcritical water. *Hungarian Journal of Industrial Chemistry.* 39 (2), 321-324.

Phillips, C.M (2011). Enzymatic degradation of cellulose by the filamentous fungus *Neurospora crassa.* PhD Thesis. University of California, Berkeley.

Pierson, Y., Boobink, F., Yan, N. (2013). Alcohol mediated liquefaction of lignocellulosic materials: A mini review. *Chemical Engineering and Process Techniques.* 1 (2), 1014.

Pingali, S.V., O'Neill, H.M., McGaughey, J., Urban, V.S., Rempe, C.S., Petridis, L., Smith, J.C., Evans, B.R., Teller, W.T. (2011). Small angle neutron scattering reveals a pH-dependant conformation change in *Trichoderma reesei* cellobiohydrolase I: Implications for enzymatic activity. *Biological Chemistry.* 286, 32801-32809.

Pirota, R.D.P.B., Delabona, P.S., Farinas, C.S. (2014). Enzymatic hydrolysis of sugarcane bagasse using enzyme extract and whole solid-state fermentation medium of two newly isolated strains of *Aspergillus Oryzae. Chemical Engineering Transactions*. 38, 259-264.

Pomar, F., Merino, F., Barceló, A.R. (2002). O-4-Linked coniferyl and sinapyl aldehydes in lignifying cell walls are the main targets of the Wiesner (phloroglucinol-HCl) reaction. *Protoplasma.* 220 (1-2), 17-28.

Prasetyo, J., Naruse, K, M, Kato, C., Harashima, S., Park, E. (2011). Bioconversion of pape sludge to biofuel by simultaneous saccharification and fermentation using a cellulase of paper sludge origin and thermotolerant *Saccharomyces cerevisiae* TJ14. *Biotechnology for Biofuels.* 4 (35).

Pribowo, A., Arantes, V., Saddler, J.N. (2012). The adsorption and enzyme activity profiles of specific Trichoderma reesei cellulase/xylanase components when hydrolyzing steam pretreated corn stover. *Enzyme and Microbial Technology.* 50, 195-203.

Qin, Y., Wei, X., Liu, X., Wang, T., Qu, Y. (2008). Purification and characterization of recombinant endoglucanase of *Trichoderma reesei* expressed in *Saccharomyces cerevisiae* with higher glycosylation and stability. *Protein Expression and Purification.* 58, 162-168.

Qing, Q., Yang, B., Wyman, C.E. (2010). Xylooligomers are strong inhibitors of cellulose hydrolysis by enzymes. *Bioresource Technology.* 101, 9624-9630.

Qing, Q. and Wyman, C.E. (2011). Supplementation with xylanase and β-xylosidase to reduce xylo-oligomer and xylan inhibition of enzymatic hydrolysis of cellulose and pretreated corn stover. *Biotechnology for Biofuels.* 4 (18).

Quensanga, A. and Picard, C. (1988). Thermal Degradation of Sugar Cane Bagasse. *Thermochimica Acta*. 125, 89-97.

Quiroz-Castañeda, R. E., and Folch-Mallol, J. L. (2013). *Hydrolysis of biomass mediated by cellulases for the production of sugars* In: Sustainable degradation of lignocellulosic biomass - Techniques, applications and commercialization; Chandel, .A.K and da Silva, S.S. (Eds), 275.

Rabelo, S.C., Carrere, H., Filho, M., Costa, A.C. (2011). Production of bioethanol, methane and heat from sugarcane bagasse in a biorefinery concept. *Bioresource Technology*. 102, 7887-7895.

Rabelo, S.C., Amezquita Fonseca, N.A., Andrade, R.R., Maciel Filho, R., Costa, A.C. (2011). Ethanol production from enzymatic hydrolysis of sugarcane bagasse pretreated with lime and alkaline hydrogen peroxide. *Biomass and Bioenergy*. 35 (7), 2600-2607.

Raman, S. and Mohr, A. (2014). Biofuels and the role of space in sustainable innovation journeys. *Cleaner Production.* 65, 224-233.

Ramos, L.P. (2003). The chemistry involved in the steam treatment of lignocellulosic materials. *Quim Nova.* 26 (6), 863-871.

Rahikainen, J.L., Marin-Sampedro, R., Heikkinen, H., Rovio, S., Marjamaa, K., Tamminen, T., Rojas, O.J., Kruus, K. (2013). Inhibitory effect of lignin during cellulose bioconversion: the effect of lignin chemistry on non-productive enzyme adsorption. *Bioresource Technology*. 133, 270-278.

Rahikainen, J.K., Evans, J.D., Mikander, S., Kalliola, A., Puranen, T., Tamminem, T., Marjamaa, K., Kruus, K. (2013). Cellulase-lignin-interactions- The role of carbohydrate-binding module and pH in non-productive binding. *Enzyme and Microbial Technology*. 53 (5), 315-321.

Rashid, M.H., Siddqui. (1997). Purification and Characterisation of a beta-glucosidase from *Aspergillus niger*. *Microbiology*. 42 (6), 544-550.

Rivera, E.C., Rabelo, S.C., Garcia, D.R., Maciel Filho, R., Costa, A.C. (2010). Enzymatic hydrolysis of sugarcane bagasse for bioethanol production: determining optimal enzyme loading using neural networks. *Chemical Technology and Biotechnology*. 85, 983–992.

Rocha, G.J.M, Martin, C., Soares, I.B., Maior, A.M.S., Baudel, H.M., de Abreu, C.A.M. (2011). Dilute mixed-acid pretreatment of sugarcane bagasse for ethanol production. *Biomass and Bioenergy*. 35 (1), 663-670.

Rocha, G.J.M, Goncalves, A.R., Oliveira, B.R., Olivares, E.G., Rossell, C.E.V. (2012) Steam explosion pretretament reproduction and alkaline delignification reactions performed on a pilot scale with sugarcane bagasse for bioethanol production. *Industrial Crops and Products.* 35, 274-279.

Rodrigue, J-P. (2013). *Transport, Energy and Environment.* In: The Geography of Transport Systems, 3rd edition. Routledge: New York.

Ryu, J.S., Shary, S., Houtman, C.J., Panisko, E.A., Korripally, P., St John, F.J., Crooks, C., Siika-aho, M., Magnuson, J.K., Hammel, K.E. (2011). Proteomic and functional analysis of the cellulase system expressed by *Postia placenta* during brown rot of solid Wood. *Applied and Environmental Microbiology*. 77 (22), 7933-7941.

Saloheimo, M., Lehtovaara, P., Penttila, M., Teeri, T.T., Stahlberg, J., Johansson, G., Pettersson, G., Claeyssens, M., Tomme, Knowles, J.J.C. (1988). EGII, a new endoglucanase from *Trichoderma reesei:* the characterisation of both gene and enzyme. *Gene*. 63 (1), 11-21.

Samanta, S., Basu, A., Halder. U.C., Sen, S.K. (2012). Characterization of *Trichoderma reesei* endoglucanase II expressed heterologously in *Pichia pastoris* for better biofinishing and biostoning. *Microbiology*. 50 (3), 518-524.

Sannigrahi, P., Kim, D.H., Jung, S., Raqauskas, A. (2011). Pseudo-lignin and pretreatment chemistry. *Energy and Environmental Science.* 4, 1306-1310.

Sant'Anna, C. and de Souza, W. (2012). Microscopy as a tool to follow deconstruction of lignocellulosic biomass. *Current Microscopy Contributions to Advances in Science and Technology*. 639-645

Scott, G.M. and Smith, A. (1995). Sludge characteristics and disposal alternatives for the pulp and paper industry. In: Proceedings of the 1995 International Environmental Conference. Tappi Press, 269–279.

Segato, F., Damasio, A.R.L., Gonçalves, T.A., Murakamia, M.T., Squina, F.M., Polizeli, M., Mort, A.J., Prade, R.A. (2012). Two structurally discrete GH7-cellobiohydrolases compete for the same cellulosic substrate fiber. *Biotechnology for Biofuels.* 5 (21).

Selig, M.J., Knoshaug, E.P., Adney, W.S., Himmel, M.E., Decker, S.R. (2008). Synergistic enhancement of cellobiohydrolase performance on pretreated corn stover by addition of xylanase and esterase activities. *Bioresource Technology.* 99, 4997–5005.

Shahbazi, S., Ispareh, K., Karimi, M., Askari, H., Ebrahami, M.A. (2014) Gamma and UV radiation induced mutagenesis in *Trichoderma reesei* to enhance cellulases enzyme activity. *International Journal of Farming and Allied Sciences.* 3 (5), 543-554.

Shahzadi, T., Mehmood, S., Irshad, M., Anwar, Z., Afroz, A., Zeesgan, N., Rashid, U., Sughra, K. (2014). Advances in lignocellulosic biotechnology: A brief review on lignocellulosic biomass and cellulases. *Advances in Bioscience and Biotechnology.* 5, 246-251.

Shallom, D. and Shoham, Y. (2003). Microbial hemicellulases. *Current Opinion in Microbiology*. 6, 219-228.

Sims R.E.H., Mabee W., Saddler J.N., Taylor M. (2010). An overview of second generation biofuel technologies. *Bioresource Technology*. 101, 1570-1580.

Singh, A., Kumar, P.K.R., Shügerl, K. (1991). Adsorption and reuse of cellulases during saccharification of cellulosic materials. *Biotechnology*. 18, 205-212.

Singhania, R.R., Patel, A.K., Sukumaran, R.K., Larroche, C., Pandey, A. (2013). Role and significance of beta-glucosidases in the hydrolysis of cellulose for bioethanol production. *Bioresource Technology*. 127, 500-507.

Sjöde, A., Alriksson, B., Jönsson, L.J., Nilvebrandt, N-O. (2007). The potential in bioethanol production from waste fiber sludges in pulp mill-based biorefineries. *Applied Biochemistry and Biotechnology*. 136-140, 327-337.

Sjögren, E., Svanberg, P., Kanebratt, K.P. (2012). Optimized experimental design for the estimation of enzyme kinetic paramaters: an experimental evaluation. *Drug Metabolism and Disposition.* 40 (12), 2273-2279.

Sluiter, J.B., Ruiz, R.O., Scarlata, C.J., Sluiter, A.D., Templeton, D.W. (2010). Compositional analysis of lignocellulosic feedstocks. *Agricultural and Food Chemistry.* 58 (16), 9043-9053.

Sørensen, A., Lübeck, M., Lübeck, P.S., Ahring, B.K. (2013). Fungal beta-glucosidases: A bottleneck in industrial use of lignocellulosic materials. *Biomolecules.* 3, 612-631.

Stange Jr., R.R., Ralph, J., Peng, J., Sims, J.J., Midland, S.L. and McDonald, R.E. (2001). Acidolysis and hot water extraction provide new insights into the composition of the induced “lignin-like” material from squash fruit. *Phytochemistry.* 57, 1005-1011.

Steiner, W., Sattler, W., Esterbauer, H. (1988). Adsorption of *Trichoderma reesei* cellulase on cellulose: experimental data and their analysis by different equations. *Biotechnology and Bioengineering.* 32, 853-865.

Sun, Y. and Cheng, J. (2002). Hysrolysis of lignocellulosic materials for ethanol production: a review. *Bioresource Technology*. 83, 1–11.

Sunna, A. and Antranikian, G. (1997). Xylanolytic enzymes from fungi and bacteria. *Critical Reviews in Biotechnology*. 17, 39-67.

Sweeney, M.D. and Xu, F. (2012). Biomass converting enzymes as Industrial Biocatalysts for Fuels and Chemicals: Recent Developments. *Catalysts.* 2 (2), 244-263.

Takashima, S., Iikura, H., Nakamura, A., Hidaka, M., Masaki, H., Uozumi, T. (1997). Comparison of gene structures and enzymatic properties between two endoglucanases from *Humicola grisea*. *Biotechnology*. 67 (2), 85–97

Takahashi, M., Takahashi, H., Nakano, Y., Konishi, T., Terauchi, R., Takedu, T. (2010). Characterization of a cellobiohydrolase (MoCel6A) produced by *Magnaporthe oryzae*. *Applied and Environmental Microbiology*. 76 (19), 6583-6590.

Tao, S., Khanizadeh, S., Zhang, H., Zhang, S. (2009). Anatomy, ultrastructure and lignin distribution of stone cells in two Pyrus species. *Plant Science*. 176, 413-419.

Teeri, T.T. (1997). Crystalline cellulose degradation: new insight into the function of cellobiohydrolases. *Trends in Biotechnology*. 15, 160-167.

Teleman A., Drakenberg T., Rouvinen J., Jones T. A., Teeri T. T. (1998). Tryptophan 272: an essential determinant of crystalline cellulose degradation by *Trichoderma reesei* cellobiohydrolase Cel6A. *FEBS Letters*. 429, 341–346.

Thomas, T.M. and Scopes, R.K. (1998). The effects of the kinetics and stability of mesophilic and thermophilic 3-phosphoglycerate kinases. *Biochemical Journal.* 330, 1087-1095.

Tomme, P., Heriban, V., Claeyssens, M. (1990). Adsorption of two cellobiohydrolases from *Trichoderma reesei* to Avicel: evidence for “exo-exo” synergism and possible “loose complex” formation. *Biotechnology Letters.* 12, 525-530.

Tomme, P., Warren, R.A.J., Gilkes, N.R. (1995). Cellulose hydrolysis by bacteria and fungi. *Advances in Microbial Physiology.* 37, 1-8.

Trabucco, G.M., Matos, D.A., Lee, S.J., Saathoff, A.J., Priest, H.D., Mockler, T.C., Sarath, G., Hazen, S. (2013). Functional characterization of cinnamyl alcohol dehydrogenase and caffeic acid *O*-methyltransferase in *Brachypodium distachyon. BMC Biotechnology.* 13 (61).

Trayser. K.A. and Seligson, D. (1969). A new “kinetic” method for enzyme analysis suitable for automation. *Enzyme analyses.* (15) 6.

Tuohy, M.G., Walsh, D.J., Murray, P.G., Claeyssens, M., Cuffe, M.M, Savage, A.V., Coughlan, M.P. (2002). Kinetic parameters and mode of action of cellobiohydrolases produced by *Talaromyces emersonii*. *Protein Structure and Molecular Biology*. 1596 (2), 366-380.

Turon, X., Rojas, O.J., Deinhammer, R.S. (2008). Enzymatic kinetics of cellulose hydrolysis: A QCM-D study. *Langmuir.* 24, 3880-3887.

Väljamäe, P., Sild, V., Pettersson, G., Johansson, G. (1998). The initial kinetics of hydrolysis by cellobiohydrolase 1 and 11 is consistent with a cellulose surface-erosion model. *Biochemistry.* 352, 469-475.

Väljamäe, P., Sild. V., Nutt. A., Pettersson. G., Johansson. G. (1999). Acid hydrolysis of bacterial cellulose reveals different modes of synergistic action between cellobiohydrolase I and endoglucanase. *Biochemistry.* 266 (2), 327-334.

Väljamäe, P., Pettersson, G., Johansson, G. (2001). Mechanism of substrate inhibition in cellulose synergistic interaction. *Biochemistry*. 268 (16), 4520-4526.

Van den Brink, J. and de Vries, R.P. (2011). Fungal enzyme sets for plant polysaccharide degradation. *Applied Microbiology and Biotechnology*. 91 (6), 1477- 1492.

Van Dyk, J.S. and Pletschke, B. (2012). A review of lignocellulose bioconversion using enzymatic hydrolysis and synergistic cooperation between enzymes-Factors affecting enzymes, conversion and synergy. *Biotechnology Advances.* 30 (6), 1458-1480.

Van Hanh, V., Tuan, A.P., Keun, K. (2009). Fungal Improvement for cellulase production using repeated and sequential mutagenesis. *Journal of Mycobiology*. 37 (4), 267-271.

Van Rooyen, R., Hahn-H¨agerdal, B., La Grange, D., van Zyl, W. (2005). Construction of cellobiose-growing and fermenting *Saccharomyces cerevisiae* strains. *Biotechnology*. 120, 284-295.

Van Zyl, W. H., Rose, S. H., Trollope, K., Gorgens J. F. (2010). Fungal β-mannanases: Mannan hydrolysis, heterologous production and biotechnological applications. *Process Biochemistry*. 45, 1203-1213.

Várnai, A., Viikari, L., Marjamaa, K., Siika-Aho, M. (2010). Adsorption of monocomponent enzymes in enzyme mixture analyzed quantitatively during hydrolysis of lignocellulose substrates. *Bioresource Technology.* 102, 1220-1227.

Varrot, A., Schulein, M., Davies, G.J. (1999). Structural changes in the active site tunnel of *Humicola insolens* cellobiohydrolase, Cel6A, upon oligosaccharide binding. *Biochemistry*. 38, 8884-8891.

Vazana, Y., Barak, Y., Unger, T., Peleg, Y., Shamshoum, M., Ben-Yehezkel, T., Mazor, Y., Shapiro, E., Lamed, R., Bayer, E.A. (2013). A synthetic biology approach for evaluating the functional contribution of designer components to deconstruction of cellulosic substrates. *Biotechnology for Biofuels.* 6 (182).

Vivekanand, V., Olsen, E.F., Vincent, G.H., Horn, S.J. (2014). Methane potential and enzyme saccharification of steam exploded bagasse. *Bioresources*. 9 (1), 1311-1324.

Vlasenko, E., Schulein, M; Cherry, J., Xu, F. (2010). Substrate specificity of family 5, 6, 7, 9, 12, and 45 endoglucanases. *Bioresource Technology* 101, 2405–2411.

Voutilainen, S.P., Puranen, T., Siika-Aho, M., Lappalainen, A., Alapuranen, M., Kallio, J., Hooman, S., Viikari, L., Vehmaanpera, J., Koivula, A. (2008). Cloning, expression, and characterization of novel thermostable family 7 cellobiohydrolases. *Biotechnology and Bioengineering*. 101 (23), 515-528.

Voutilainen, S.P., Murray, P.G., Tuohy, M.G., Koivula, A. (2010). Expression of *Talaromyces emersonii* cellobiohydrolase Cel7A in *Saccharomyces cerevisiae* and rational mutagenesis to improve it thermostability and activity. *Protein Engineering, Design and Selection.* 23 (2), 67-79.

Wagschal, K., Heng, C., Lee, C.C., Wong, D.W.S. (2009). Biochemical characterisation of a novel dual-function arabinofuranosidase/xylosidase isolated from a compost started mixture. *Applied Microbiology and Biotechnology*. 81, 855-863.

Warden, A.C., Little, B.A., Haritos, V. (2011). A cellular automaton model of crystalline cellulose hydrolysis by cellulase. *Biotechnology for Biofuels*. 4 (39).

Wei, H., Wang, W., Alahuhta, M., Wall, T.V., O Baker, J., Taylor, L.E., Decker, S.R., Himmel, M.E., Zhang, M. (2014). Engineering towards a complete heterologous cellulase secretome in *Yarrowia lipolytica* reveals its potential for consolidated bioprocessing. *Biotechnology for Biofuels*. 7 (148).

Wong, K.K.Y., Tan, L.U.L., Saddler, J.N. (1988). Multiplicity of β-1, 4-xylanase in microorganisms: Functions and applications. *Microbiological Review*. 52 (3), 305-317.

Wood, T.M. and McCrae, S.I. (1979). Synergism between enzymes involved in the solubilisation of native cellulose. *Advances in Chemistry*. 181: 181-209.

Woodward, J., Lima, M., Lee, N.E. (1988). The role of cellulase concentration in determining the degree of synergism in the hydrolysis of microcrystalline cellulose. *Biochemistry*. 255, 895-899.

Woodward, J. (1991). Synergism in cellulase systems. *Bioresource Technology*. 36, 67–75.

Wu, M., Beckham, GT., Larsson, A. M., Ishida, T., Kim, S., Payne, C.M., Himmel, M.E., Crowley, M.F., Horn, S.J., Westereng, B., Igarashi, K., Samejima, M., Stahlberg, J., Eijsink, V.G., Sandgren, M. (2013). Crystal structure and computational characterization of the lytic polysaccharide monooxygenase GH61D from the Basidiomycota fungus *Phanerochaete chrysosporium*. *Biological Chemistry*. 288, 12828–39.

Wyman, C. (2007). What is (and is not) vital to advancing cellulosic ethanol. *Trends in Biotechnology*. 25 (4), 154-157.

Xiaochun, Yu, Minor, J.L, Atalla, R.H. (1995). Mechanism of action of Simons' stain. *Tappi*. 78 (6).

Xiao-Min, W., Qin, Y., Qu, Y.B. (2010). Molecular Cloning and Characterization of Two Major Endoglucanases from *Penicillium decumbens*. *Microbiology and Biotechnology*. 20 (2), 265-270.

Xiemenes, E., Kim, Y., Mosier, N., Dien, B., Ladisch, M. (2011). Deactivation of cellulases by phenols. *Enzyme and Microbial Technology*. 48, 54-60.

Xu, L., Hou, J., Tang, H., Wang, C., Bao, X. (2014). Promotion of Extracellular Activity of Cellobiohydrolase I from *Trichoderma reesei* by Protein Glycosylation Engineering in *Saccharomyces cerevisiae*. *Current Synthetic and Systems Biology*. 2 (2), 1-6.

Yadav, R.K.P., Timilsina, A., Yadawa, R.K., Pokhrel, C.P. (2014). Potential cellulosic ethanol production from organic residues of agro-based industries in Nepal. *Renewable Energy*. 2014. 1-6.

Yamabhai, M., Sak-Ubol, S., Srila, W., Haltrich, D. (2014). Mannan Biotechnology: from biofuels to health. *Critical Reviews in Biotechnology*. 1 (11).

Yamashita, Y., Sasaki, C., Nakamura, Y. (2010). Development of efficient system for ethanol production from paper sludge pretreated by ball milling and phosphoric acid. *Carbohydrate Polymers*. 79 (2), 250-254.

Yan, Q., Hua, C., Yang, S., Li, Y., Jiang, Z. (2012). High level expression of extracellular secretion of a beta-glucosidase gene (PtBglu3) from *Paecilomyces thermophila* in *Pichia pastoris*. *Protein Expression and Purification.* 8, 64–72.

Yang, B., Dai, Z., Sing, S-Y., Wyman, C.E. (2011). Enzymatic hydrolysis of cellulosic biomass. *Biofuels.* 2 (4), 421-450.

Ye, Z. (2006). The impact of adsorbed cellulase inactivation on enzymatic hydrolysis kinetics. PhD thesis. Fuzhou University. Louisville, Kentucky.

Yoon, J.J., Cha, C.J., Kim, Y.S., Kim, W. (2008). Degradation of cellulose by the major endoglucanase produced from the brown-rot fungus *Fomitopsis pinicola*. *Biotechnology Letters*. 30, 1373-1378.

Zabed, H., Faruq, G., Sahu, J.N., Azirun, M.S., Hashim, R., Boyce, A.N. (2014). Bioethanol production from fermentable sugar juice. *The Scientific World Journal.* 2014. 1-11.

Zha, Y., Westerhuis, J.A., Muilwijk, B., Overkamp, K.M., Nijmeijer, B.M., Coulier, L., Smilde, A.K., Punt, P.J. (2014). Identifying inhibitory compounds in lignocellulosic biomass hydrolysates using an exometabolomics approach. *BMC Biotechnology*. 14 (22).

Zhang, Y.H. and Lynd L.R. (2004). Toward an aggregated understanding of enzymatic hydrolysis of cellulose. Noncomplexed cellulase systems. *Biotechnology and Bioengineering*. 88, 797–82.

Zhang, Y.H. and Lynd, L.R. (2006). A functionally based model for hydrolysis of crystalline cellulose by fungal cellulase. *Biotechnology and Bioengineering.* 94 (5), 888-898.

Zhang, J., Siika-aho, M., Tenkanen, M., Viikari, L. (2011). The role of acetyl xylan esterase in the solubilisation of xylan and enzymatic hydrolysis of wheat straw and giant reed. *Bioresource Technology*. 4 (60).

Zhang, X.Z. and Zhang, Y.H.P. (2013). Cellulases: Characteristics, Sources, Production, and Applications. *Bioprocessing Technologies in Biorefinery for Sustainable Production of Fuels, Chemicals and Polymers*. 131-146.

Zhang, J. and Viikari, V. (2014). Impact of xylan on synergistic effects of xylanases and cellulases in enzymatic hydrolysis of lignovelluloses. *Applied Biochemistry and Biotechnology*. 164 (4), 1393-1402.

Zhao J., Shi, P., Li, Z., Yang, P., Luo, H., Bai, Y., Wang, Y., Yao, B. (2012). Two neutral thermostable cellulases from *Phialophora* sp. G5 act synergistically in the hydrolysis of filter paper. *Bioresource Technology*. 121, 404-410.

Zhao, Z., Zhang, L., Liu, D. (2012). Biomass recalcitrance. Part 1: the chemical compositions and physical structures affecting the enzymatic hydrolysis of lignocellulose. *Biofuels, Bioproducts and Biorefineries*. 6 (4), 465-482.

Zhou, J., Wang, Y.H., Chu, J., Zhuang, Y.P., Zhang, S.L., Yin. P. (2008). Identification and purification of the main components of cellulases from a mutant strain of *Trichoderma viride* T 100-14. *Bioresource Technology*. 99 (15), 6826-6833.

Zhou, J., Wang, Y-H., Chu, J., Luo, L-Z., Zhuang, Y-P., Zhang, S.L. (2009). Optimization of cellulase mixture for efficient hydrolysis of steam-exploded corn stover by statistically designed experiments. *Bioresource Technology*. 100, 819-825.

Internet References

http://web.expasy.org/protparam/. *Bioinformatic Resource Portal*. [Last Accessed 17 November 2014].

http://agrodaily.com/2013/08/01/frost-damages-18-of-brazil-sugar-cane-crop/ *Frost damages 18% of Brazil sugar cane crop*. [Last Accessed 18 December 2014].

http://www.cazy.org/. *Welcome to the Carbohydrate-Active Enzymes Database*. [Last Accessed 10 January 2015].

Appendices

Appendix 1: Reagent list

Table 1A. The name of the reagents/chemicals and the suppliers used

Name of Reagent	**Supplier (Catalogue number)**
Ammonium persulphate	Sigma Aldrich (Cat no A3678)
Acrylamide	Sigma (Cat. No. A8887)
Ammonium persulphate	Sigma Aldrich (Cat. No. A3678)
Avicel PH101	Fluka (11365)
Birchwood xylan	Fluka (Cat. No. 95588)
Bovine serum albumin (BSA)	Sigma (Cat. No. A7906)
Bradford reagent	Sigma (Cat. No. B6916)
Bromophenol blue	Sigma (Cat. No. B8026)
Carboxymethyl cellulose	Calbiochem (Cat. No. 217277)
Calcium carbonate	Merck (Cat. No. 1020660250)
Coomassie Brilliant Blue R250	Merck (Cat. No. 1.12553)
Citric acid	Merck (Cat. No. 1.00244)
3,5-Dinitrosalicylic acid	Sigma (Cat No. D0550)
Ethanol	Merck (Cat. No. 8.18700)
Glacial acetic acid	Merck (Cat. No. 1.00063)
Glycerol	Saarchem (Cat. No. 2676520
Glycine	Merck (Cat. No. 1.04169)
D-Glucose	Saarchem (Cat. No. 2676020)
D-Mannose	Sigma (Cat. No. M2069)
D-Mannose, D-Fructose & D-Glucose kit	Megazyme (Cat. No. K-MANGL)
2-mercaptoethanol	Fluka (Cat. No. 63700)
Methanol	Merck (Cat. No. 8.22283)
N,N-methylenebisacrylamide	Sigma (Cat. No.M7279)
4-Nitrophenyl-β-D-glucopyranoside	Sigma (N1377)
p-Nitrophenol	Sigma (Cat. No. 42,575-3)
PeqGold protein marker II	peqLab (Cat. No. 27-2010)
Phenol	Sigma (Cat.No. P3653)
Phloroglucinol	Sigma (Cat. No. P3502)
Di-potassium hydrogen phosphate	Merck (1.05104.1000)

Di-sodium hydrogen orthophosphate	Saarchem (Cat. No. 5822860)
Potassium sodium tartarate	Merck (1.08087.1000)
Sodium azide	Merck (Cat. No. 8.22335)
Sodium carbonate	Merck (Cat. No. 1.06392.0500)
Sodium dodecyl sulphate (SDS)	BDH biochemicals (Cat. No. 301754)
Sodium hydroxide	Saarchem (Cat. No. 5823200)
Sodium metabisulfite	Sigma-Aldrich (Cat. No. 255556)
Sodium potassium tartrate	Merck (Cat. No. 1.08087)
Sodium sulphate	Saarchem (Cat. No. 5825200)
Sodium sulphite	Saarchem (Cat. No. 5825400)
Sulfuric acid	Merck (Cat. No.1120802500)
N,N,N',N'-tetramethylethylene diamine	Sigma Aldrich (Cat. No. T9281)
Tris (hydroxymethyl) aminomethane	Merck (Cat. No. 1.08382)
Tri-sodium citrate dehydrate	Merck (Cat. No. 1.06448)
D-Xylose	Sigma (Cat. No. K-XYLOSE)

Appendix 2: Standard curves

Appendix 2A: Protein standard curve

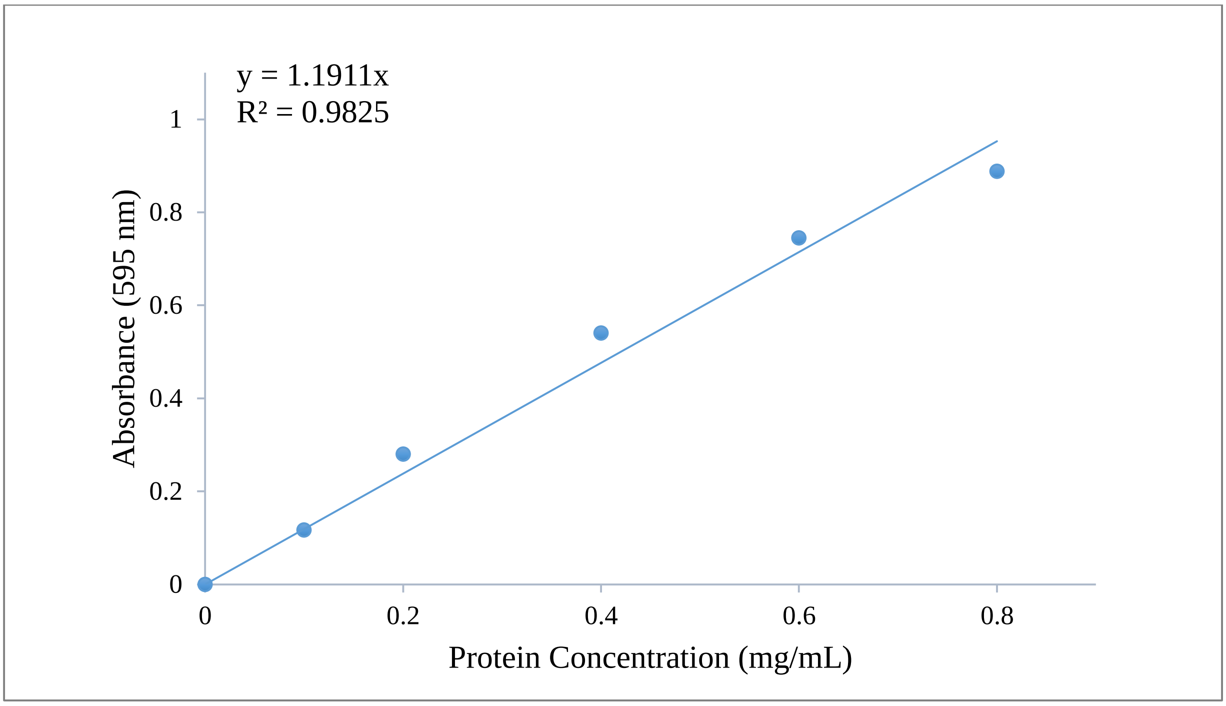

Figure 2A. Protein standard curve. 25 µL of protein sample was added to 230 µL Bradford reagent and incubated for 10 minutes at room temperature. Values are shown as the means (n=3; SD < 5%).

2B: Glucose standard curve

The composition of the DNS reagent were as follows:

2 g sodium hydroxide

2 g 3, 5 dinitrosalicylic acid (DNS)

40 g potassium sodium tartrate (Rochelle salt)

0.4 g phenol

0.1 g sodium metabisulfite

200 mL distilled water

A 2 % sodium hydroxide solution was made before the DNS was added. Once the DNS had dissolved, the other chemicals were added and the volume was made up to 200 mL.

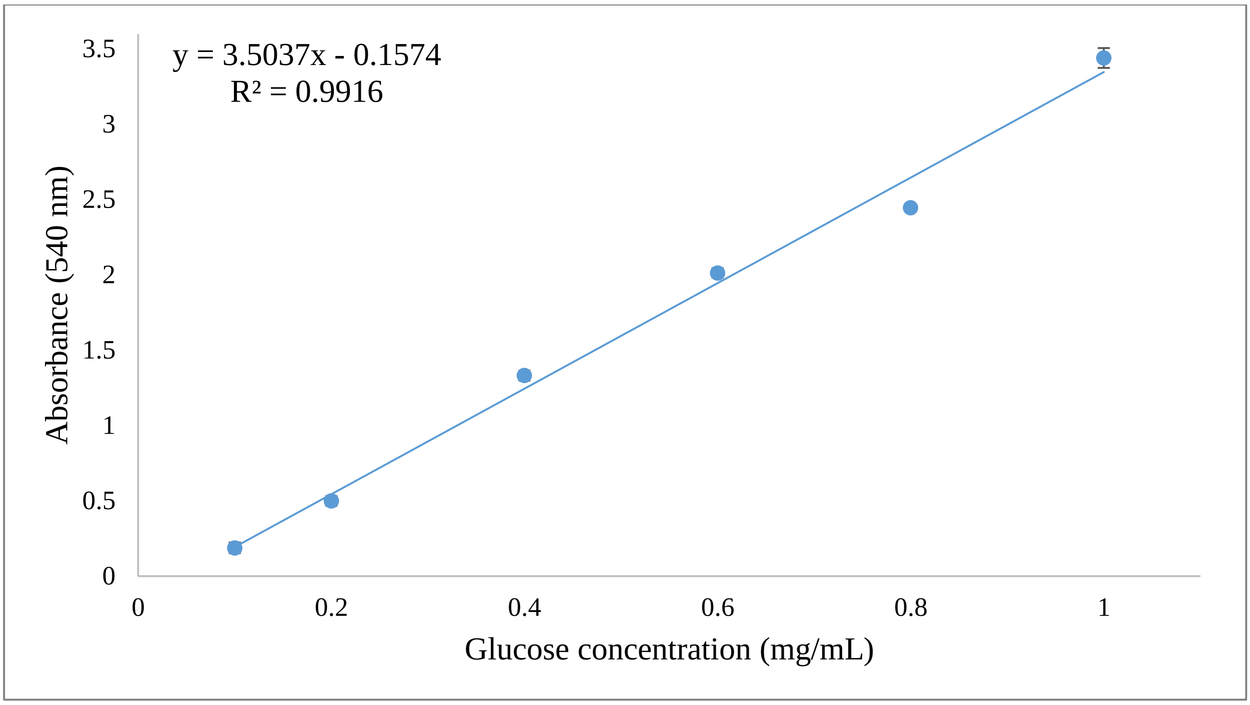

Figure 2B. Glucose standard curve. 150 µL of protein sample was added to 300 µL DNS reagent and incubated for 7 minutes at 100°C. Values are shown as the means (n=3, SD < 5%).

2C. *p*-nitrophenyl standard curve

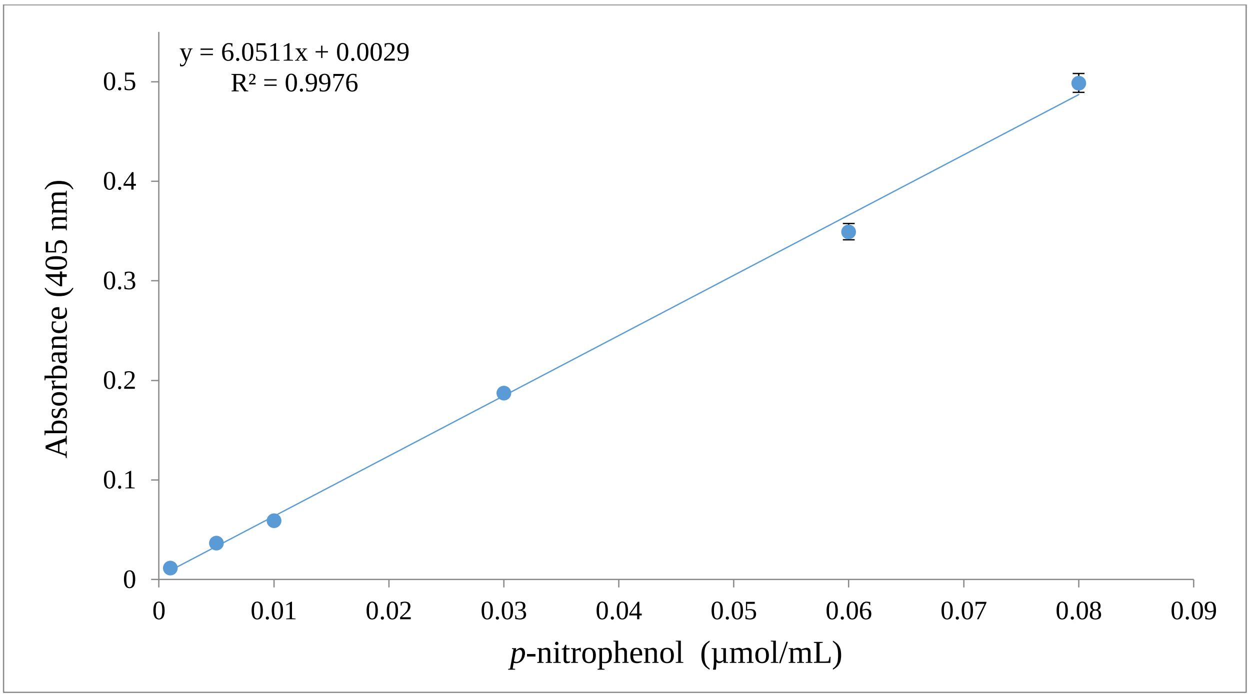

Figure 2C. *p*-nitrophenyl standard curve. Values are shown as the means (n=3, SD < 5%).

Appendix 3: SDS-PAGE

The sizes of the celluloytic enzymes were assessed using sodium dodecyl sulphate polyacrylamide gel electrophoresis (Laemmli, 1970) and modified according to the BioRad® Mini-Protean 3 Cell instruction manual. The solutions were prepared as follows:

1. 30% Acrylamide solution

29.8 g Acyrylamide

0.2 g Bis-Acrylamide

These chemicals were dissolved in 100 mL distilled water, wrapped in aluminium foil and stored at 4^{o}C

2. 10 % (w/v) SDS stock solution

10 g SDS was dissolved in 10 mL distilled water

3. Stacking buffer (0.5 M Tris- HCl; pH 6.8)

6 g Tris (Hydroxymethyl) Aminomethane was dissolved in distilled water and HCl was added to adjust the pH to 6.8 before bringing the volume up to 100 ml. The buffer was stored at 4^{o}C.

4. Resolving gel (1.5 M Tris- HCl; pH 8.8)

18.15g Tris (Hydroxymethyl) Aminomethane was dissolved in distilled water and HCl was added to adjust the pH to 6.8 before bringing the volume up to 100 ml. The buffer was stored at 4 ^{o}C.

5. 10 x SDS running buffer

30.3 g Tris (Hydroxymethyl) Aminomethane

144 g glycine

10 g SDS

These chemicals were dissolved in 1 L distilled water and kept at room temperature.

6. 5 x SDS sample buffer

2.5 mL distilled water

1 mL 0.5 M Tris-HCl buffer (pH 6.8)

1 mL 10% SDS stock solution (w/v)

1 mL 1% bromophenol blue (w.v)

The sample buffer was kept at room temperature. β-mercaptoethanol (5 µl) was added to SDS sample buffer (95 µl), prior to preparing samples for electrophoresis. 3 µl of SDS sample buffer was added to 15 µl of protein samples and boiled for electrophoresis

7. Coomassie Brilliant Blue protein staining solution

0.075% (w/v) Coomassie Brilliant Blue R250 was dissolved in 40% methanol and 0.7% glacial acetic acid.

8. Coomassie destaining solution

45% methanol, 45% distilled water and 10% glacial acetic acid were mixed together.

9. 10% Ammonium persulphate (APS) solution

0.1 g APS was dissolved in 1 ml distilled water. Samples were prepared prior to preparing the gel

10. Preparation of gels

a) 10% resolving gel

4.04 mL distilled water
2.5 mL 1.5 M Tris-HCl buffer (ph 8.8)
3.3 mL 30% acrylamide stock solution
0.1 mL SDS stock solution
0.1 mL 10% APS solution
0.05 mL TEMED

b) 4% stacking gel

6.1 mL distilled water
2.5 mL Tris-HCl buffer (pH 6.8)
1.3 mL 30% acrylamide stock solution
0.1 mL 10% SDS stock solution
0.1 mL 10% APS solution
0.05 mL TEMED

Appendix 4: Synergy enzyme combinations

A) Binary Synergy combinations:

The reaction mixtures for the synergy assays in Chapter 4 were made up to a final volume of 400 µL using 0.5 M sodium citrate buffer (pH 5.0). The total protein concentration was kept constant in all reactins (25 µg). The assays were conducted at 50°C for 24 hours (Avicel) and 72 hours (SEB and PS).

Table 4A. The enzyme combinations and enzyme loading for binary-synergy studies (intra-molecular)

Combination	CBHI (µl)	CBHII (µl)	EGI (µl)	EGII (µl)
C1(100)	100	0	0	0
C2(100)	100	0	0	0
E1(100)	100	0	0	0
E2(100)	100	0	0	0
C1(25):C2(75)	25	75	0	0
C1(50):C2(50)	50	50	0	0
C1(75):C2(25)	75	25	0	0
E1(25):E2(75)	0	0	25	75
E1(50):E2(50)	0	0	50	50
E1(75):E2(25)	0	0	75	25
C1(25):E1(75)	25	0	75	0
C1(50):E1(50)	50	0	50	0
C1(75):E1(25)	75	0	25	0
C1(25):E2(75)	25	0	0	75
C1(50):E2(50)	50	0	0	50
C1(75):E2(25)	75	0	0	25
C2(25):E1(75)	0	25	75	0
C2(50):E1(50)	0	50	50	0
C2(75):E1(25)	0	75	25	0
C2(25):E2(75)	0	25	0	75
C2(50):E2(50)	0	50	0	50
C2(75):E2(25)	0	75	0	25

B) Temporal studies

The reaction mixtures for the temporal synergy assays in Chapter 4 were made up to a final volume of 1200 µL using 0.5 M sodium citrate buffer (pH 5.0). The total protein concentration was kept constant in all reactins (25 µg). The assays were conducted at 50°C for 120 hours

Table 4B. The enzyme combinations and enzyme loading for temporal-synergy studies

Substrate	Combination	CBHI (µl)	EGI (µl)	EGII (µl)
Avicel and PS	C1(100)	300	0	0
	E2(100)	0	0	300
	C1(75):E2(25)	225	0	75
SEB	C1(100)	300	0	0
	E1(100)	0	300	0
	C1(75):E2(25)	225	75	0

C) Ternary Synergy studies

The reaction mixtures for the temporal synergy assays in Chapter 4 were made up to a final volume of 400 µL using 0.5 M sodium citrate buffer (pH 5.0). The total protein concentration was kept constant in all reactins (25 µg). The assays were conducted at 50°C for 24 hours (Avicel) and 72 hours (SEB and PS)

Table 4C. The enzyme combinations and enzyme loading for ternary-synergy studies (inter-molecular)

Substrate	Combination	CBHI (µl)	EGI (µl)	EGII (µl)	X
Avicel and PS	C(100):X(0)	75	0	25	0
	C(75):X(25)	56.25	0	18.75	25
	C(50):X(50)	37.5	0	12.5	50
	C(25):X(75)	18.75	0	6.25	75
	C(0):X(100)	0	0	0	100
SEB	C(100):X(0)	75	25	0	0
	C(75):X(25)	56.25	18.75	0	25
	C(50):X(50)	37.5	12..5	0	50
	C(25):X(75)	18.75	6.25	0	75
	C(0):X(100)	0	0	0	100